Identification of mycolic acid class ratios

from *Mycobacterium* species using

liquid chromatography-mass spectrometry

Dissertation submitted in fulfilment of the requirements for the degree,

MSc in Department of Pharmacology, at the Faculty of Health Sciences,

University of Pretoria

2019

Candidate

Name: Brendon Naicker

Student number: 98286138

Department: Pharmacology

Faculty of Health Sciences

University of Pretoria

Abstract

Alongside the recent technology advancements in liquid chromatography (LC) and mass spectrometry (MS) instrumentation there has also been steady progress made with respect to the systematic lipidomic studies of *Mycobacterium tuberculosis* (*M. tb*) where hyphenated LC and MS instrumentation were the main analytical technique employed. Although many reports have shown low limits of detection and high precision in analysing mycolic acids (MAs) and other *M. tb* lipids, few have reported efficient LC selectivity, even when employing high resolution mass spectrometry (HRMS) to determine the accurate mass of a lipid molecule for identification purposes. MAs are one of the most widely reported lipid classes that are found in the cell wall of *M. tb* and consist of a diversity of high mass branched chain of fatty acids that could potentially be used as diagnostic biomarkers for determining active *M. tb* infections. The chemical diversity of MAs can be used for taxonomic identification of mycobacterial species, but their analysis is complicated due to their extreme hydrophobic properties and homologous chemistry.

Three dominant subclasses of MA molecules are found in mycobacteria: alpha-(α-), keto- and methoxy-MAs. When analysing MAs using MS, the product ions obtained from the infusion of a purified mixture of MAs, extracted from *M. tb* H37Rv strain, on a tandem mass spectrometer (MS/MS) are m/z 367.3 and 395.4, which correlate with published data but are not unique to single MA classes and therefore cannot be used for the identification of a specific MA subclass molecule. The ratios of the diverse MA class precursor ions can however be used to predict the identity of *M. tb* strains. Further genetic assays are however required to confirm the taxonomic identification. In this study, self-extracted MAs (*M. tb* H37Rv strain) were compared to that of commercially available MAs (*M. bovis* strain) and by integrating the chromatographic peak area of each dominant precursor ion within a MA class, a peak area ratio between the α-, keto- and methoxy- MAs were determined. The resulting percentage ratios between α-, keto- and methoxy- MA classes were found to be 53:8:38 for *M. tb* H37Rv and 53:15:32 for *M. bovis* respectively. The LC data dependent acquisition (DDA) precursor ion method, developed here specifically for the MA ratio comparison, has also shown the ability to resolve isomers within a MA class that has not previously been reported. Two other classes of mycobacterial lipids, phthiocerol

dimycocerosates (DIMa) and phthiodiolone dimycocerosates (DIMb), collectively called PDIMs, have recently emerged as lipids which play a significant role in the virulence of drug resistant *M. tb*. Hence, a robust LC-HRMS method was developed for the analysis of extractable non-polar lipids extracted from three different drug resistant phenotypes of *M. tb* from clinical isolates and compared to a drug susceptible *M. tb* H37Rv clinical isolate.

The results obtained from using LC-HRMS showed that organic phase extraction and analysis of drug resistant and drug susceptible *M. tb* clinical isolates grown on solid culture media have lipid class differences that can potentially be interpreted by way of calculated mass defect analysis (Kendrick mass defect analysis) or organic content ratio analysis (Van Krevelen graphs). In comparison to matrix assisted laser desorption ionization (MALDI)-MS methods, which are mainly used to analyse intact large molecules, and can be used to identify mycobacteria to species level by analysing a crude lipid extract, the LC-HRMS method employed in this study has shown the potential to further classify *M. tb* species according to their strain. Apart from the possible diagnostic application, there is also the collection and processing of large amounts of high resolution m/z data points which, when combined with reproducible LC methodology, is searchable using available online databases for the accurate identification and classification of analysed lipids. This approach depends strongly on the mass resolution of the mass spectrometer used, but unavoidably and especially in lipidomics studies, because of the presence of stereoisomers and the overlapping isotope distributions between related but different lipid classes, highly selective chromatographic peak resolution needs to be achieved when developing and optimizing the hyphenated LC method.

In future, the feasibility of using LC-HRMS as a routine technique to phenotype *M. tb* drug resistant strains may require a mass analyser with a mass resolution in excess of 100 000, as well as chromatographic technologies that are capable of resolving non-derivatized complex mixtures of large (C_{60}-C_{100}) nonpolar and/or polar lipid molecules.

Declaration of Originality and Plagiarism

University of Pretoria
Faculty of Health Sciences
Department of Pharmacology

I, Brendon Naicker

Student number: 98286138

Subject of work: Identification of mycolic acid class ratios from *Mycobacterium* species using liquid chromatography-mass spectrometry

Declaration

1. I understand what plagiarism is and am aware of the University's policy in this regard.
2. I declare that this dissertation is my own original work. Where other people's work has been used (either from a printed source, internet or any other source), this has been properly acknowledged and referenced in accordance with departmental requirements.
3. I have not used work previously produced by another student or any other person to hand in as my own
4. I have not allowed and will not allow anyone to copy my work with the intention of passing it off as his or her own work.

Signature

Acknowledgments

I dedicate this dissertation to my wife, my two children, our parents,

close friends, close colleagues and my study supervisor

who have all played a crucial role in me achieving this important milestone in life.

Table of Contents

List of Figures

List of Tables

Abbreviations

APCI	atmospheric pressure chemical ionization
CID	collision induced dissociation
ESI	electrospray ionization
GC	gas chromatography
HIV	human immunodeficiency virus
HPLC	high-performance liquid chromatography
HRMS	high resolution mass spectrometry
INH	isoniazid
IRS-TB	*M. tb* susceptible to both INH and RIF
IR-TB	*M. tb* resistant to INH but sensitive to RIF
LC	liquid chromatography
M. tb	*Mycobacterium tuberculosis*
m/z	mass-to-charge ratio
MA	mycolic acid
MAs	mycolic acids
MDR-MTB	*M. tb* resistant to both INH and RIF
MDR-TB	multidrug-resistant tuberculosis
MRM	multiple reaction monitoring
MS	mass spectrometry
MS/MS	tandem mass spectrometry
NAATs	nucleic acid amplification techniques
PCR	polymerase chain reaction
PDIMs	phthioceroldimycolates
q- TOF-MS	quadrupole time-of-flight mass spectrometry
RFLP	restriction fragment length polymorphism
RIF	rifampicin
RR-TB	*M. tb* resistant to RIF but sensitive to INH
TB	tuberculosis
UV	ultraviolet
WHO	World Health Organization

1 Introduction

The United Nations General Assembly held the first-ever high-level meeting on the fight against tuberculosis (TB) on 26 September 2018 (UNGA HLM Ending TB) [1]. It was 25 years previous to this that TB was declared a global emergency by the World Health Organization (WHO) [2]. Since then at least ten more declarations have stressed the burden of TB and the need to develop new means to prevent, diagnose and cure TB [3].

The ultimate message conveyed at the UNGA HLM Ending TB meeting in September 2018 was that TB is a cruel epidemic that is grossly underfunded. According to the U.N. deputy secretary-general the TB epidemic is fuelled by impoverishment, discrimination, migration and conflicts, and that approximately $13 billion per year is required to bring the global status of TB under control. The conference recognized that the cost of new TB medications like delaminid and bedaquiline are exorbitant and the stigma that is frequently associated with TB interferes with the screening and treating of people.

The WHO's most recent annual statistics reported TB cases in every country around the world and among almost all age groups. Two-thirds of the reported cases were in eight countries - India, Pakistan, Bangladesh, China, Indonesia, the Philippines, Nigeria and South Africa (FIGURE 1.1). Over 1.3 million people were reported to have died from TB in 2017 - more people than any other communicable disease. The recent WHO TB reports have shown that the almost 10 million people per year who are newly infected with the disease occur in poor countries where health care access and provision is severely limited.

Research into the development of better TB diagnostic technologies and more effective anti-TB therapies continue to take place, but after 48 years rifampicin (RIF) and isoniazid (INH) are still the first line drugs of choice for treating positively diagnosed TB infections [4]. The emergence of multi-drug resistant forms of the disease has increased reliance on more expensive and toxic second line drugs [5].

South Africa, as listed above, bears an enormous burden of the disease. The high incidence rate of TB in South Africa has been particularly propelled by a correspondingly high

prevalence of HIV infections. TB-HIV co-infection poses a diagnostic and therapeutic challenge for the country's health care system [6].

Estimated TB incidence rates, 2017
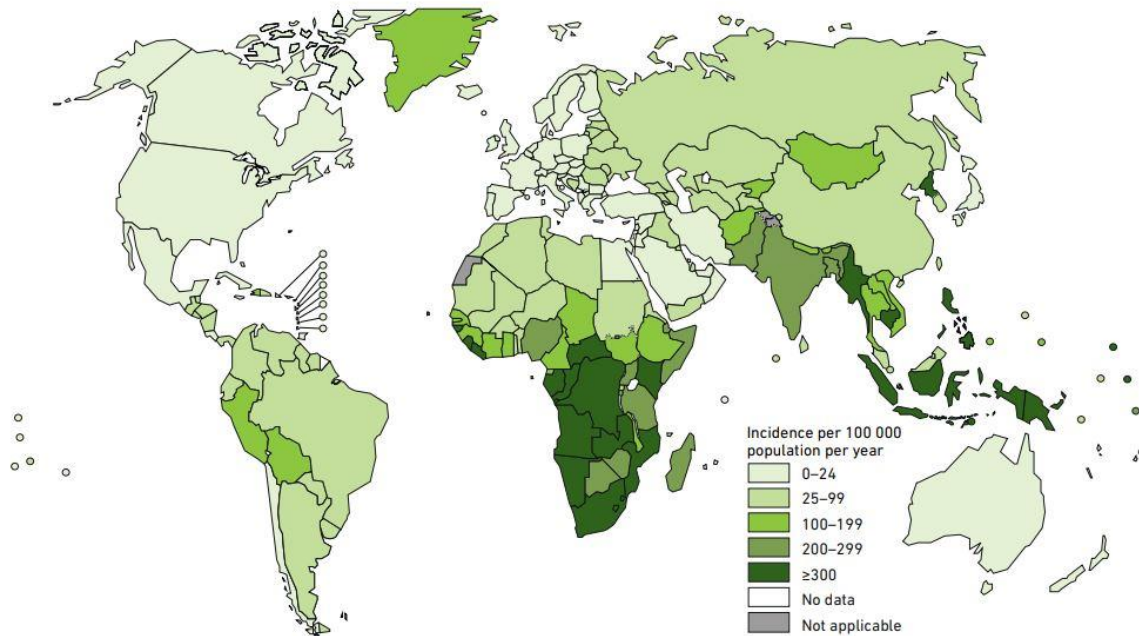
Figure 1.1: Estimated global TB incidence rate for 2017, showing Sub-Saharan Africa with the highest infection rate [7, 8].

1.1   The Disease TB

TB is one of the oldest infectious diseases of mankind with evidence of infections occurring in pre-historic settlements [9]. It primarily infects the lungs but can also cause infection of other organs and tissues such as the abdomen, genitourinary tract, skin, joints and bones [10]. Pulmonary TB presents with chest pains, persistent coughs and bloody sputum whilst extrapulmonary TB may manifest as fever, anorexia, weight loss, malaise and fatigue [11].

Primary infection is in many cases missed because the symptoms are mild, non-specific and usually self-resolving. It is diagnosed by performing a tuberculin skin test or interferon-gamma release assay which reflects a delayed-type hypersensitivity reaction to specific proteins of *Mycobacterium tuberculosis* (*M. tb*). A primary complex, called a Ghon complex, is formed which consists of a granuloma, typically in the middle or lower zones of the lung.

The Ghon complex usually resolves within a few weeks or sometimes months, leaving signs of fibrosis and calcification that is detectable on chest X-rays. The risk of disease progression following a primary infection is low, but young children and immunocompromised patients are at an increased risk. Re-infection can frequently occur in TB endemic areas and triggers similar responses to those observed with a primary infection. Re-infection is however likely to occur multiple times during the lifetime of an individual living in a TB-endemic area [12].

TB symptoms have a gradual onset and duration varies from a few weeks to months. Acute onset can occur in young children or immunocompromised individuals. Fever, night sweats and weight loss present in approximately 75, 45 and 55% of patients respectively, while a persistent non-remitting cough is the most frequently reported symptom at 95% [12, 13].

1.2   TB transmission and pathogenesis

TB is an airborne disease. Individuals with active TB may transmit the infection through coughing, sneezing or speaking when aerosolized saliva droplets containing the pathogen are expelled (FIGURE 1.2). These droplets remain suspended in the air for several minutes. The likelihood of actual infection depends upon several factors, including the number of infectious droplets expelled by the infected individual, the effectiveness of ventilation, the period of exposure, the virulence of the pathogen as well as the level of immunity of the uninfected person. If droplets containing the TB pathogen are inhaled by a susceptible individual and deposit in an appropriate location in the respiratory tract, infection and disease can develop. Frequent and prolonged close contact with individuals having active TB increases the risk of contracting the disease [14].
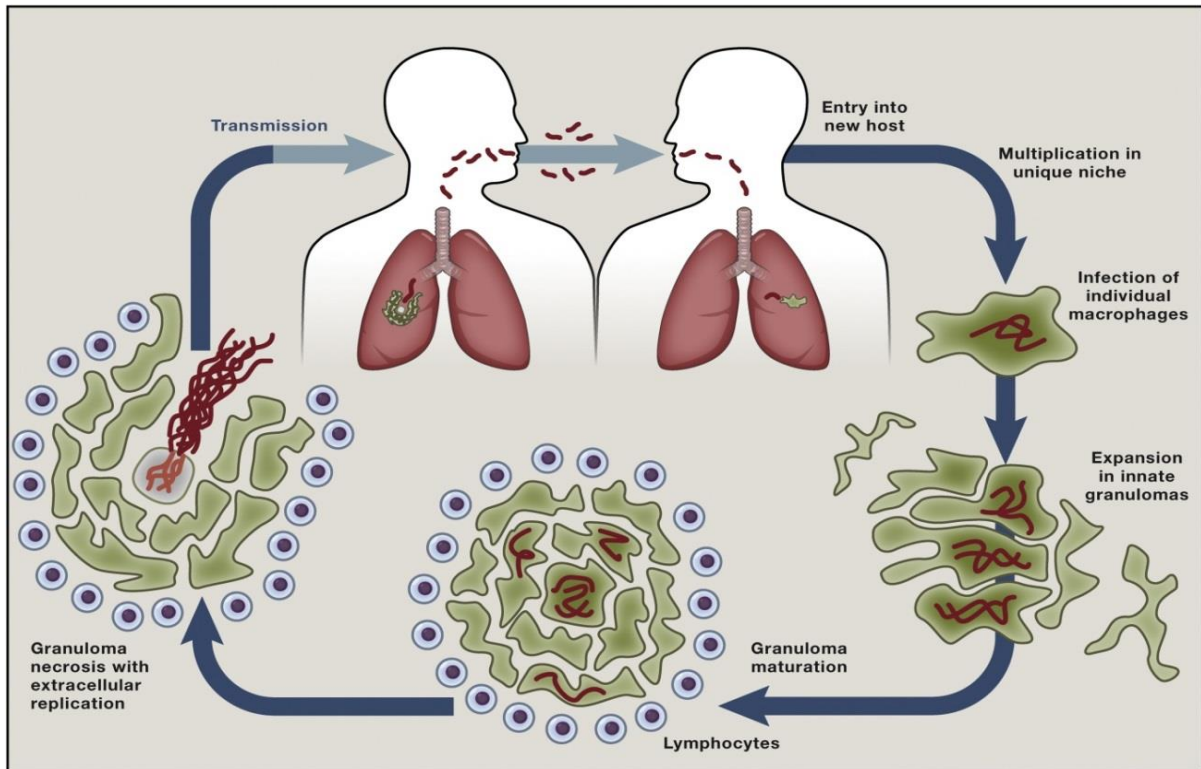
Figure 1.2: Pathogenic life cycle of *M. tb* [13].

M. tb has evolved an efficient means of aerosol transmission that exploits the immune system-mediated response to damage the pulmonary tissues in individuals with active TB. It is estimated that almost one out of every ten individuals that are infected with *M. tb* eventually develops active TB within a few years after exposure. The risk of developing active TB is significantly increased by suppression of immune response mechanisms, diabetes and prolonged preventative therapy with isoniazid. Current strategies for controlling TB infection focus mainly on reduction of transmission by rapid characterisation of the actual causative agent, be it *M. tb* or any other mycobacterial species, and prompt treatment of infected individuals [15].

1.3   The causative agent – *M. tuberculosis*

TB is caused by the bacterial pathogen *M. tuberculosis* (*M. tb*) which is reported to have survived over 70,000 years [16, 17]. It is a large, non-motile bacillus ranging from 2-4 μ m in length and 0.2-0.5 μ m in width (FIGURE 1.3). *M. tb* is an aerobic organism and is often found

infecting the well-aerated upper lobes of the lungs. Although it contains peptidoglycans in its cell wall, *M. tb* is neither classified as Gram-negative nor Gram-positive [18]. It reproduces at a very slow rate of one cell cycle every 15 to 20 hours compared to that of other bacteria which typically reproduce in less than an hour [19, 20]. *M. tb* is capable of remaining dormant throughout the lifespan of a host individual.

Apart from upper and lower respiratory infections, *M. tb* also infects fatty tissues surrounding the kidneys, the lymph nodes, heart and skin [21]. The bacilli are able to enter fat cells of adipose tissues where they accumulate within intra-cytoplasmic lipid inclusions and remain dormant in a non-replicating state [22].
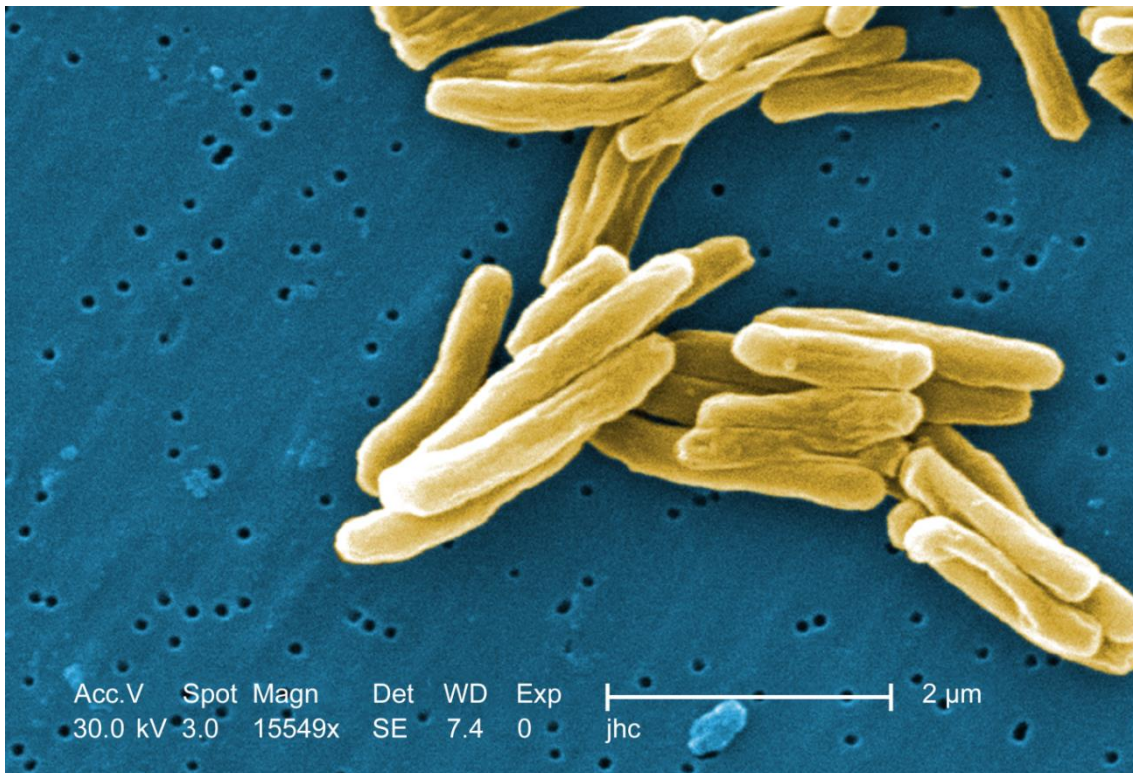
Figure 1.3: Digitally-colourized scanning electron micrograph (SEM) of *M. tb* **bacteria under high magnification (15549 x). Image provided courtesy of CDC/Ray Butler MS.**
https://phil.cdc.gov/details.aspx?pid=9997

1.4   TB Diagnosis

Direct microscopy of a concentrated specimen is the most commonly used diagnostic method for TB (FIGURE 1.4). However, the culturing of *M. tb* from clinical specimens is considerably more sensitive than either direct or indirect smear microscopy. Culturing can

be performed using solid media, for example Lowenstein-Jensen, or liquid media, such as that used in automated culture systems. The disadvantage of culturing is the time required to obtain results - approximately two weeks for liquid culture and up to four weeks for solid media culture. This is a consequence of the slow doubling time of *M. tb*. Until the recent development of molecular biology testing for drug resistance, the isolation of *M. tb* followed by culturing was a prerequisite for subsequent phenotypic drug-susceptibility testing [23, 24].

There have been few advances in TB diagnostic methods in the last century and the development of new diagnostic tools has become a crucial part of global TB research in recent years [25]. Many establishments acknowledge the urgent need for improved TB diagnosis and have encouraged additional research in this area. Several promising TB diagnostic tests are currently under development and some have already been implemented in many countries. New diagnostic tests that increase the sensitivity or simplicity of diagnosing active disease are also in the late stages of development. Rapid implementation of proven new TB diagnostic technologies is critical in meeting current and future public health needs.

Molecular tests, one of the few advancements that were made in the last century, are currently used to identify mycobacterial species. These tests make use of nucleic acid amplification techniques (NAATs) such as the polymerase chain reaction (PCR), transcription mediated amplification or strand displacement amplification [26, 27]. Identification using these molecular methods involves targeting and amplifying a unique and specific nucleic acid sequence of the mycobacterial genome. Identification of drug susceptible *M. tb* strains using NAATs is usually performed using either the GeneXpert® assay from Cepheid [28, 29] or more commonly the GenoType MTBDRplus® assay (FIGURE 1.4) from HAIN Life Sciences [30-33]. Both test systems enable the simultaneous detection of *M. tb* and relevant mutations in the *rpoB* gene that are associated with drug resistance to RIF. In addition, the most important mutations in the genes *katG* and *inhA,* that are associated with the resistance to isoniazid, are detected. A key disadvantage of using molecular techniques alone to determine *M. tb* drug resistance is that it does not directly confirm the phenotype of the mycobacteria's drug susceptibility. For confirmation of drug resistance, the gold

standard for testing drug susceptibility still involves the use of solid media culture as it confirms the phenotype of the infectious organism [34].
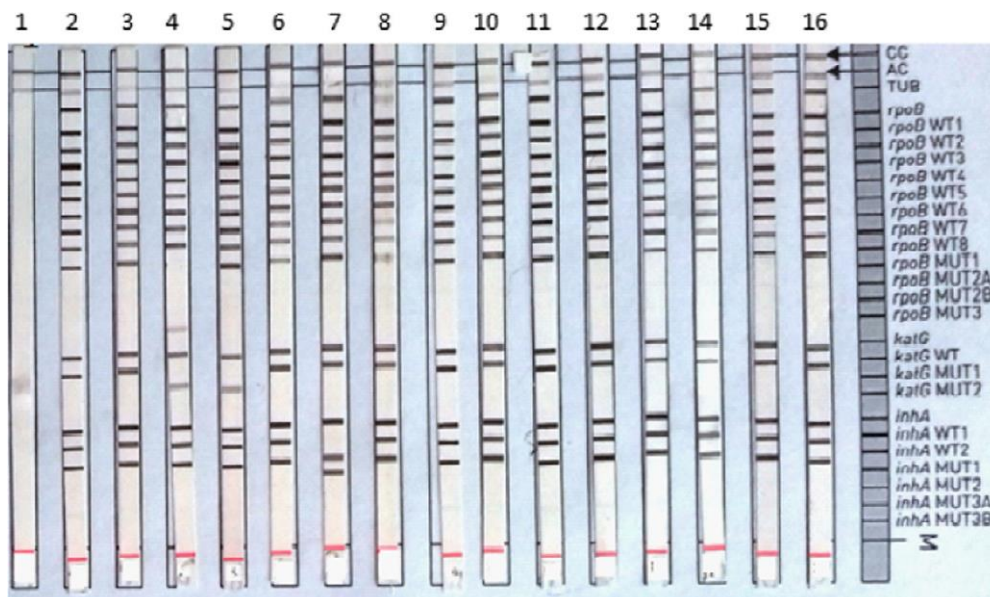
Figure 1.4: Representative DNA patterns obtained by the GenoType MTBDRplus® assay. Lane 1, water as a negative control, Lanes 2, 3, 6, 8, 9, 10, 11, 12, 13, 14, and 15 all are examples of a pattern of RIF^s and INH^s; Lane 4, example of a pattern of RIF^r and resistant INH^r; Lane 5, example of a pattern of RIF^s and INH^r with *katG* mutation; Lane 7 is an example of pattern of RIF^s and INH^r with *inhA* mutation; Lane 16, H37Rv as a positive control. Note: The superscript 'r' represent resistance and 's' represent sensitive [33].

1.5 TB treatment

Patients with active TB infection require an extended drug combination regimen of oral first-line drugs which is comprised of:

a) an initial phase of RIF, INH, pyrazinamide, and ethambutol daily for two months
b) a continuation phase of RIF and INH for a further four months, either daily or three times per week

TB patients undergoing first-line chemotherapy are vulnerable to side effects such as hepatotoxicity, hyperuricemia, ototoxicity, psychiatric effects and a skin rash [35-40]. These effects, along with the prolonged treatment period, results in many patients' non-compliance to completing the treatment. The most critical consequence of this non-compliance is the emergence of multidrug-resistant TB (MDR-TB). As soon as resistance to

the first-line drugs is detected, treatment is frequently escalated to second-line drugs that have more adverse side effects, and that need to be administered for a much longer period. Second-line multi-drug therapy currently consists of: [41, 42]

a) injectable aminoglycosides: streptomycin, kanamycin, amikacin

b) injectable polypeptides: capreomycin, viomycin

c) oral and injectable fluoroquinolones: ciprofloxacin, levofloxacin, moxifloxacin, ofloxacin, gatifloxacin

d) oral: *para*-aminosalicylic acid, cycloserine, terizidone, ethionamide, prothionamide, thioacetazone, linezolid

Bedaquiline, which has been registered specifically for the treatment of MDR-TB, belongs to a new class of antibiotics called diarylquinolines [43]. Bedaquiline was approved by the Food and Drug Administration (FDA) of the United States of America at the end of 2012 for the treatment of adults with MDR-TB for whom an effective treatment regimen is not otherwise available [44].

Delamanid, a nitro-dihydro-imidazooxazole derivative, received its first global approval for the treatment of MDR-TB in 2014 [45]. Treatment with delamanid for six months in combination with a background regimen can improve outcomes and reduce mortality among patients with MDR-TB [46].

1.6 *M. tb*'s cellular envelope

The development of drug resistance is intrinsic to nearly all microorganisms. In *M. tb* resistance has mainly been attributed to the thick lipid-rich cell wall. This hydrophobic cell wall provides the mycobacteria with an effective structural barrier against many chemotherapeutic agents, which for *M. tb* are mostly hydrophilic molecules [47, 48]. The cell wall is rich in mycolic acid (MA) type lipids along with regular peptidoglycan, phospholipids and glycolipids.

M. tb's cellular envelope consists of a phospholipid plasma membrane surrounded by a cell wall. The latter contains mainly long-chain lipids on the outer layers of the cell wall (FIGURE 1.5) [49]. The components of the outer cellular envelope provide mechanical support,

osmotic protection and inhibit the exchange of ions with the micro-environment [50]. The cellular envelope also contributes to the microbe's survival inside the macrophages by modulating the macrophage endolysosomal degradation pathway [51, 52].
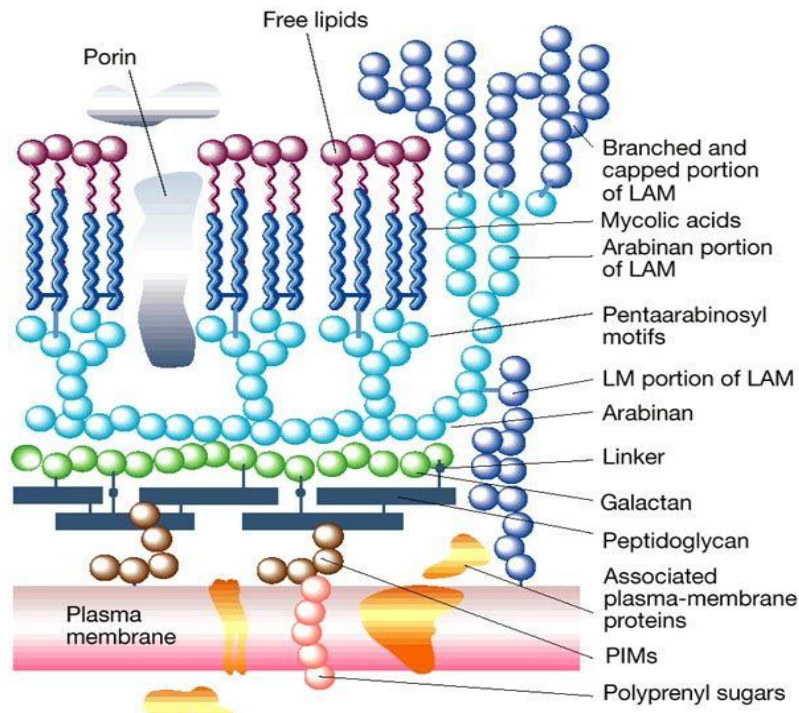
Figure 1.5: A cross-sectional diagram of the cellular envelope of *M. tb* showing a large amount of glycolipids and MAs in the outer membrane. LAM, lipoarabinomannans; LM, lipomannans; PIM, phosphatidylinositol mannosides [47].

M. tb membrane lipids are divided into 9 major classes with sub-divisions into subclasses based on the number of sugar moieties present. Fig. 1.6 shows the basic structures of major lipid classes that are found in most mycobacteria [53]. The acyl lipids are divided into two subclasses, mycolic acids (MAs) and phthioceroldimycolates (PDIMs), which together are the most abundant constituents, by mass, of *M. tb*'s outer cell wall and are unique to mycobacteria.
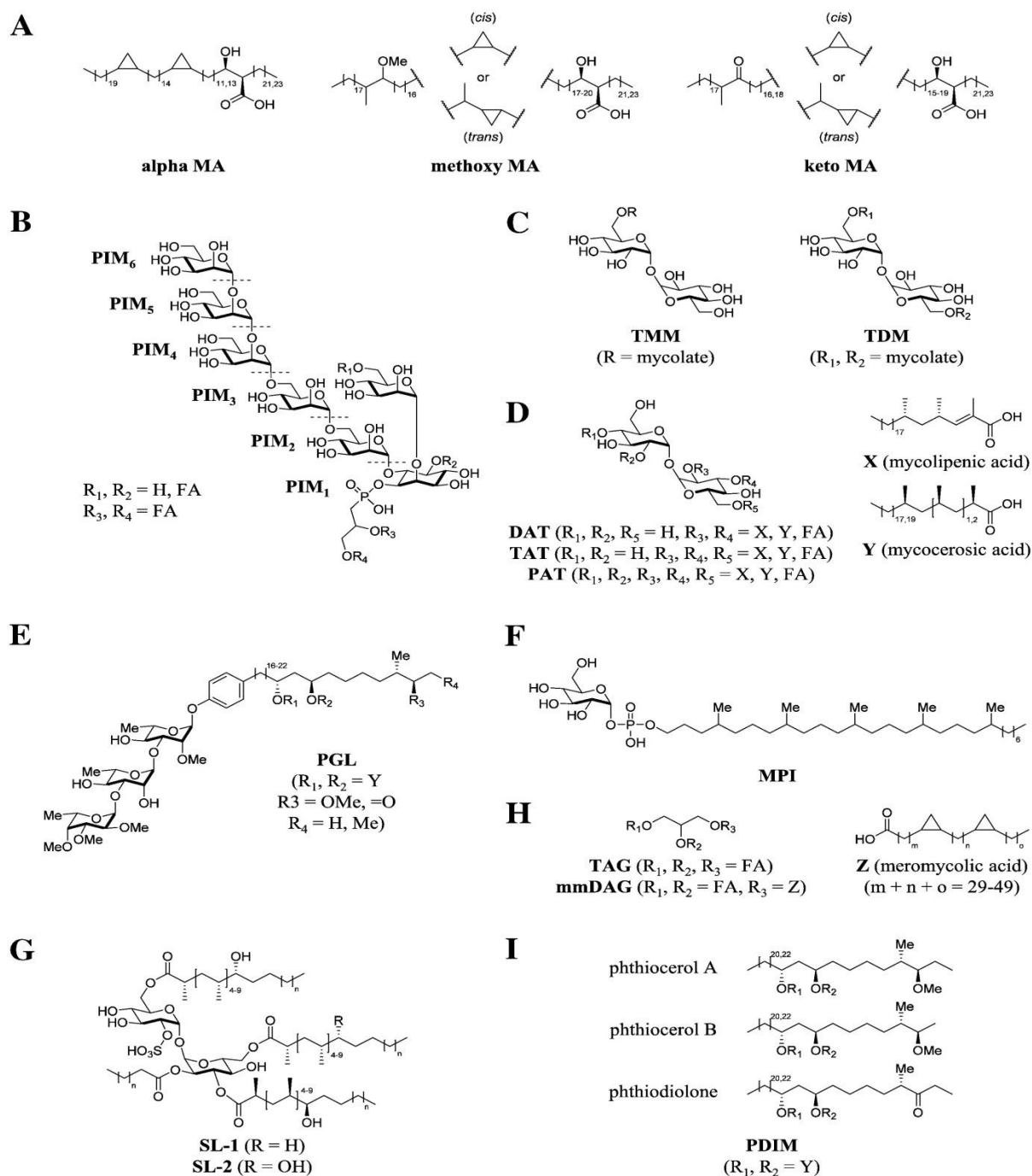
Figure 1.6: Representative structures of major α, methoxy and keto MAs of *M. tb*. (B) Structure of PIMs. Dotted lines show the position of attachment of each mannose unit. (C) Structure of TMMs and TDMs. The mycolate substituents are those shown in Fig. 1A. (D) Structure of DATs, TATs and PATs long with the major mycolipenic and mycocerosic acids that are bound to the trehalose core. (E) Structure of PGLs. (F) Structure ofMPI. (G) Structure of SL-1 and SL-2. (H) Structure of TAGs and mmDAGs along with the major meromycolic acids that are bound to position R3 of mmDAGs. (I) Structure of PDIMs showing the major phthiocerols and phthiodiolones that make up the core of this lipid class. Abbreviations: DAT, diacyl trehalose; FA, fatty acid; MA, MA; mmDAG,monomeromycolyl diacylglycerol; MPI, mannosyl -1-phosphoisoprenoid; PAT, polyacyl trehalose; PDIM, phthiocerol dimycoceroserate; PGL, phenolic glycolipid; PIM, phosphatidyl-myo-inositol mannoside; TDM, trehalose dimycolate; TMM, trehalose monomycolate; SL, sulfolipid; TAG, triacylglycerol; TAT, triacyl trehalose.

1.7   Mycolic Acids (MAs)

Mycolic acids (MAs) are long-chain 2-alkyl, 3-hydroxy fatty acids where the main carbon chain is referred to as the meromycolate branch or chain where the functionality can vary. Mycolic acids are a key characteristic feature in the cell wall layer of all mycobacterial species discovered so far [54]. These long-chain fatty acids are largely found covalently attached to the peptidoglycan–arabinogalactan complex of the mycobacterial cell wall where they are involved in mycobacterial target recognition and contribute to the pathogen's survival inside macrophages [55].

The first report of MAs in tubercle bacilli was published by Robert Koch in 1889 [56]. MAs occur in a distinct group of bacteria, specifically the genera *Mycobacterium*, *Nocardia*, *Rhodococcus* and *Corynebacterium*, that are all classified within the suborder of the family *Corynebacterineae* [57]. In the genus *Corynebacterium* the MAs are C_{28}–C_{40} in length and provide a partial permeability barrier for the exchange of nutrients and antibiotics via the cell wall [58]. In the genus *Rhodococcus* MAs are C_{30}–C_{54} range and in the genus *Nocardia* they are even longer with a C_{42}–C_{66} range. Interestingly, in both *Rhodococcus* and *Nocardia*, MAs occur without functional groups in the meromycolate chain but there is the possibility of one or more double bonds being present in the meromycolate chain [59-61]. Mycobacterial species on the other hand are fully dependent on their cell wall MAs for growth and survival. In mycobacteria, MAs are found to be some of the largest that occur in nature, in the range of C_{60}-C_{90} [62, 63].

There are three major classes of MAs in mycobacteria: alpha- (α-), keto- and methoxy-MAs (FIGURE 1.7). The α-MAs have a cis,cis-dicyclopropyl configuration in its meromycolate chain while the methoxy- and keto-MAs both have sub-classes characterized by the presence of cis-cyclopropane or a trans-cyclopropane group with an adjacent methyl branch, the former predominating in methoxy-MAs and the latter in keto- MAs [64]. The chemical diversity of MAs can be used for taxonomic identification of mycobacterial species, but their analysis is complicated due to their extreme hydrophobic properties and very similar chemistry. MAs are attractive diagnostic markers for mycobacterial infections as they are: (1) not synthesized by humans, (2) their chemical diversity can be used for taxonomy and (3) they represent a substantial mass fraction of the cell wall in mycobacteria [65].

α-Mycolic acid

Keto-Mycolic acid

Methoxy-Mycolic acid
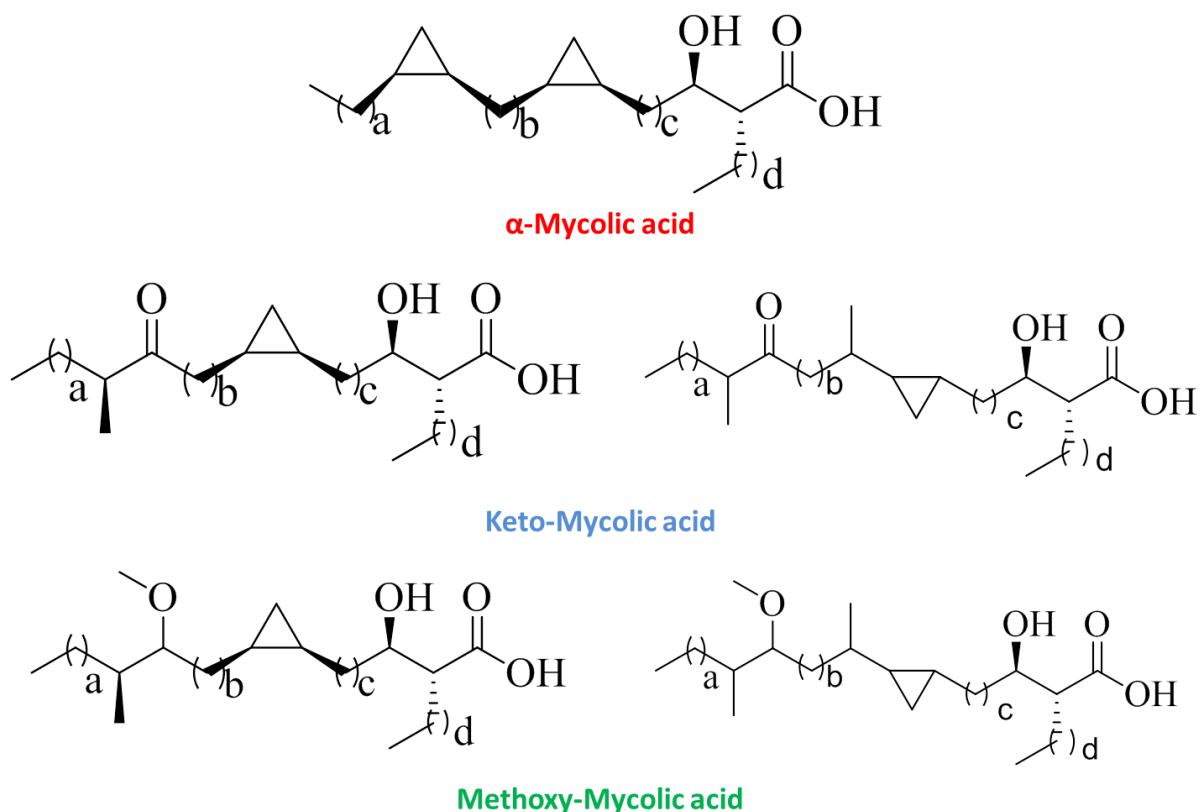
Figure 1.7: The three major classes of MAs in mycobacteria: α, keto and methoxy MAs. The α-MAs have a cis,cis-dicyclopropyl configuration in the meromycolate moiety while the methoxy- and keto-MAs both have sub-classes, characterized by a single cis-cyclopropane ring or a trans-cyclopropane ring with an adjacent methyl branch.

1.8 Phthiocerol dimycocerosates (PDIMs)

Although MAs have been studied in detail, the presence of larger lipids in the cellular envelope of *M. tb* cannot be ignored. One such class of large lipids are the PDIMs (FIGURE 1.8). PDIMs are major virulence factors of *M. tb*, especially in the initial stages of infection when tubercle bacilli come into contact with host macrophages. The precise molecular mechanisms of action of these large lipids remain unclear. By making use of *M. tb* mutants lacking the genes responsible for PDIM biosynthesis, Astarie-Dequeker *et al*. demonstrated that PDIMs take part both in the receptor-dependent phagocytosis of *M. tb* as well as the prevention of acidification within the phagosome [66]. These researchers also proposed that the PDIMs may be controlling *M. tb* invasion into macrophages by targeting certain lipids in the host's macrophage membrane and could also be modifying the membrane's biological

and physical properties. These changes in the macrophage's lipid membrane could be playing a vital role in the high efficiency of *M. tb* receptor-mediated phagocytosis.

The precise role of PDIMs during the course of TB infection also remains to be determined. Rosseau *et al*. showed in mice that the attenuation of PDIM-deficient *M. tb* strains takes place during the acute phase of TB infection [67]. Although purified PDIM molecules had no effect on the activation of macrophages *in vitro*, Rosseau *et al*. found that the localization of PDIMs in *M. tb*'s cell wall plays a key role in eliciting the pathogen's biological effect. Their findings suggested that the production of PDIMs contributes to the initial growth phase of pathogen by protecting it from macrophages and also modulating an early immune response to TB infection.
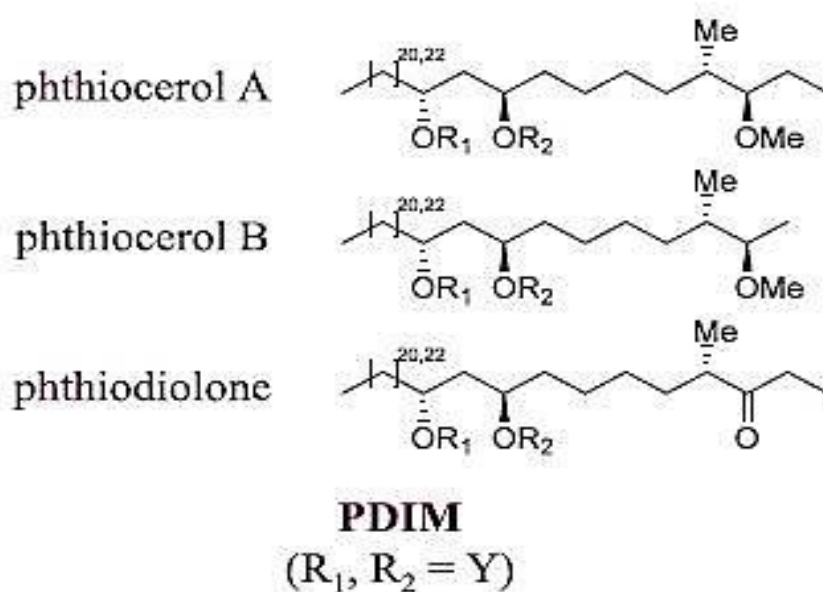
Figure 1.8: The generalised structures of PDIMs showing the differences between major phthiocerols and phthiodiolones [65].

The molecular role that PDIMs play in *M. tb* acquiring drug resistance has gained increasing interest over the last century. As shown by Bisson *et al*., mutations in the *rpoB* gene of drug-susceptible wild type *M. tb* have resulted in the upregulation of specific secondary metabolites [68]. They compared the expressed proteomes and metabolomes of two drug-susceptible wild type *M. tb* strains to rifampin-resistant *rpoB* mutant *M. tb* strains. The *rpoB*

mutants showed upregulation of specific polyketide synthase genes, which are responsible for the operon which encodes the initial formation of multifunctional enzymes that are involved in PDIM biosynthesis and other *M. tb* lipids. The metabolomic analysis identified a greater abundance of PDIM precursors in the *rpoB* mutant isolates.

MAs have been extensively studied in terms of their biosynthesis and the role that it plays in *M. tb* virulence but recently greater attention has been paid the function of PDIMs. The precise role of PDIMs in *M. tb* was recognized by studies which identified that mutants of *M. tb* were unable to produce or localize PDIMs into the cell membrane [67, 69-73]. *M. tb* and its close pathogenic relative *M. marinum* were also reported to elicit changes in macrophage lipid order through the coordinated use of PDIMs and phenolglycolipids to initiate TB infection [74]. The role of PDIMs in mycobacterial reproduction and multiplication in organs other than the lungs remains unclear [75].

Interestingly, it has been reported that PDIMs bind to MAs to form the outer layer of the *M. tb* cell envelope along with other branched lipids [76]. In addition to their important biological roles, PDIMs alone have shown the potential to be biomarkers of mycobacterial detection as well as species identification. As far as MAs are concerned, a GC-MS method was previously developed and showed that it could diagnose *M. tb* infection from sputum samples with 65% sensitivity and 76% specificity [77]. In principle, a combination of various lipidomics analytical MS techniques may lead to a powerful TB diagnostic tool kit.

As an example of the effectiveness of MS as a tool in TB biomarker detection, both PDIMs and MAs have been detected in ancient skeletal samples. MAs were detected in two samples from a 17,000 year old bison skeleton, but due to degradation, they could not conclusively be linked to *M. tb*. However, both the mycocerosate and phthiocerol components of PDIMs were identified by a GC-MS method and this provided sufficient evidence of there being a TB infection in these animals [77].

1.9 TB Lipidomics

The wax lipid-rich cell wall of mycobacteria is much thicker than that found in most other bacteria. These lipids make up 30 – 60% of the cell wall dry weight and are thought to play important biological roles, notably in determining virulence and drug resistance [78]. There has been a recent surge in the study of mycobacterial lipids which can be partially attributed to the emergence of the field of lipidomics which in turn has been driven by technical advances in mass spectrometry (MS) instrumentation. Making use of atmospheric pressure chemical ionization (APCI), electrospray ionization (ESI) and coupling liquid chromatography (LC) to mass spectrometers have allowed the identification and quantitation of several lipid species [53].

Lipidomics is a rapidly progressing field that deals with the study of all existing lipid molecules within a biological system. The vast amount of detailed information obtained from a lipidomics study can potentially be used to propose or even confirm specific metabolic pathways within a particular organism. The ultimate aim of all currently explored "omics" areas, viz. metabolomics, proteomics, transcriptomics, genomics, lipidomics and more recently metal-omics, is to fully characterize the full complement of specific biological molecules to their structural chemical level and to confirm their proposed function within a biological system. Examples of this can be (1) a protein molecule that is expressed in a cell, (2) a gene that is required for regulating specific metabolic expression or (3) a lipid molecule that is expressed on the outer cellular membrane.

Although lipidomics is widely viewed as an emerging "omics" field, the modern techniques and advanced tools that are utilized to perform these types of studies provide powerful new analytical approaches to comprehensively understand the biological system in question. Lipidomics has recently gained considerable attention in published scientific literature and currently appears to be an essential part of any biologist's arsenal in order to effectively perform both basic and translational biological research.

Lipids play a significant role in various metabolic pathways in many biological systems. They are essentially the main structural components of cellular membranes where ion channels, receptors, and other protein complexes are embedded. Together with the analysis of all other components within a cellular membrane, the data acquired from lipid analysis is

crucial in determining cellular function at a molecular level in order to phenotypically define a cell or a tissue in response to environmental conditions or genetic modifications. Lipids participate in several types of biochemical reactions, integrating across different metabolic pathways where any alteration of the lipids involved in a particular biochemical reaction will affect the resulting or required metabolites in that biochemical pathway [79].

Lipid molecules are the fundamental components of most cellular membranes where diverse lipid classes can reside in close proximity to each other. Biosynthesis of lipids is almost always initiated from two precursor units: isoprene and ketoacyl groups (FIGURE 1.9).
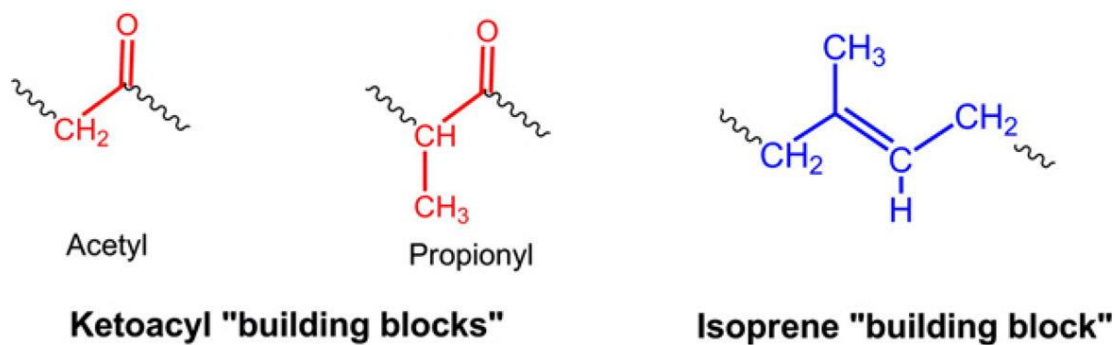
Figure 1.9: Ketoacyl and isoprene building blocks for different lipids. The universal LIPID MAPS classification system is based on the concept of these two fundamental biosynthetic "building blocks": ketoacyl groups and isoprene groups [79]. http://www.lipidmaps.org/resources/tutorials/

Lipids can be divided into eight categories: fatty acids, glycerolipids, sphingolipids, glycerophospholipids, saccharolipids, sterol lipids, prenol lipids, and polyketides (FIGURE 1.10). The large number of categories and diverse structures of lipids can present an analytical challenge. Currently there are two strategies employed in molecular lipid analysis: (1) targeted and (2) non-targeted lipid analysis. Targeted lipid analysis involves the development and optimisation of specific methods that have a sufficiently high sensitivity to identify and quantify selected lipids. The latter approach is typically performed using nominal mass resolution spectrometers that have a mass-to-charge ratio (m/z) accuracy of one decimal place (e.g. 1,500.2 m/z). Non-targeted lipid analysis approaches involve the examination of all lipid species within a particular biological system with the ultimate aim of

identification and classification of the full complement of lipid molecules. HRMS instruments are almost exclusively used to perform non-targeted lipid analysis because of their ability to obtain accurate m/z values of analysed molecules. The accurate mass data can then be used to search known chemical databases to propose or confirm the identity and class of any lipid molecule detected.

(a) Fatty Acyls: hexadecanoic acid

(b) Glycerolipids: 1-hexadecanoyl-2-(9Z-octadecenoyl)-*sn*-glycerol

(c) Glycerophospholipids: 1-hexadecanoyl-2-(9Z-octadecenoyl)-*sn*-glycero-3-phosphocholine

(d) Sphingolipids: N-(tetradecanoyl)-sphing-4-enine

(e) Sterol Lipids: cholest-5-en-3β-ol

(f) Prenol Lipids: 2E,6E-farnesol

(g) Saccharolipids: UDP-3-O-(3R-hydroxy-tetradecanoyl)-αD-N-acetylglucosamine

(h) Polyketides: aflatoxin B1

Figure 1.10: Representative structures of each lipid category [79].

In order to successfully achieve qualitative and quantitative lipid analysis from biological samples many analytical techniques have been employed, including thin-layer chromatography, gas chromatography-MS and LC-MS/MS. The use of LC-MS/MS for lipidomics was accelerated by the development of electrospray ionization (ESI) and the availability of accurate mass resolution coupled to soft ionisation techniques, resulting in the use of HRMS systems [80].

Until recently, the study of mycobacterial diseases was confined to microbe culture-based technologies that are over a century old. The use of nucleic acid amplification techniques changed this with powerful new technologies currently being implemented in routine TB diagnostic settings. "Omics" studies are also currently being used, mainly in research environments, to clarify mechanisms of the disease and identify biomarkers which may lead to improved diagnosis and treatment. The validation of any "omics" biomarker is however complicated by challenges in determining and defining the limitation of the analytical techniques with respect to accuracy, selectivity, linearity, reproducibility, robustness, and limits of detection of a potential method, but also the normal biological variability. The statistical challenges with any identified "omics" biomarker(s) includes analysis and interpretation of large data sets generated. Despite some of these drawbacks, "omics" studies provide the potential to further understand and to manage mycobacterial diseases [81].

"Omics" sub-disciplines can be viewed as fields that broadly analyse an organism's molecular assembly to provide a representation of that organism at any instant in time or a series of representations that can describe an organism's response to a chemical agent. Downstream from genes and enzymes, metabolites are also important components of the biomass of the cell. Transcriptomics and proteomics essentially study linear polymers and the key information obtained from these studies is the sequence of building blocks comprised of nucleotides or amino acids. Proteins and nucleic acids can principally be studied by applying one detection method to one type of molecule to determine its sequence. In contrast, metabolites are small molecules that show extreme diversity in their atomic composition and are composed of aliphatic hydrocarbons, peptides, sugars, purines, pyrimidines, and other constituents in which individual molecules vary in mass. A frequent challenge in planning metabolomics platforms is that chemical metabolites are not often obvious or self-defining and therefore the reporting of metabolic profiles requires that all investigators in the field agree on organizational systems for grouping metabolites together.

Cellular metabolites can be organized based on the similarity of their chemical structures, as seen in the Lipid Maps initiative, or by laying out the sequential relationships of substrates, enzymes, and products into biosynthetic pathways. A further practical challenge in building effective metabolomics platforms relates to the chemical diversity of metabolites, which

require different solvents and separation techniques for individual subclasses of metabolites, such as nucleotides, peptides and lipids. In recent times these basic problems in organizing and detecting metabolites in high throughput analysis have been largely solved, giving rise to functioning experimental platforms for metabolomics, which represent the youngest of the major systems biology disciplines. Metabolomics platforms take advantage of nuclear magnetic resonance (NMR) spectroscopy as well as MS as nearly universal detection methods. Based on the implementation of increasingly comprehensive metabolite databases, it is now possible to rapidly profile thousands of metabolites in a single experiment to generate an organism's or a cell's metabolome.

Metabolomics assumes a practical definition as the high throughput study of non-protein, non-DNA, non-RNA cellular intermediates, which emphasizes small molecules with atomic masses lower than 3,000 g/mole. Lipidomics on the other hand has emerged as a distinct subspecialty of metabolomics which recognizes that conventional metabolites and lipids differ in one essential property: solubility in aqueous solutions. Conventional metabolomics focuses on molecules that are soluble in the cytosol, whereas lipidomics is mainly concerned with water-insoluble molecules that form part of cellular membranes and other functional activity such as signalling. Practical issues related to differences in sample preparation methods needed to recover cytosolic metabolites and membrane lipids increasingly lead to the divergence of metabolomics and lipidomics into meaningful different subfields with different biological emphases. As contrasted with cytosolic metabolites, lipids tend to have more aliphatic hydrocarbons, larger size and low polarity. These differences translated into a need for hydrophobic solvents, distinct ion-pairing reagents, and chromatographic and mass spectrometric ionization methods that are matched to the chemical properties of lipids. Lipids can generally be described as molecules composed of a polar region which varies in size and that is linked to aliphatic hydrocarbon chains or ring structures. Each lipid subclass is comprised of different acyl forms or alkyl forms that contain the same core structure but differ in the length, saturation status, or substitutions on the aliphatic chains. Thus, the lipidome of a single organism might contain up to 100,000 individual molecular lipid species [82].

1.10 LC-MS in TB Lipidomics Research

There are several types of LC and MS system combinations. In this study the focus was on using two of the commonly available commercial instrumentation, i.e. LC combined with tandem MS (LC-MS/MS) and LC hyphenated to quadrupole time-of-flight MS (q-TOF-MS).

An LC-tandem-MS (LC-MS/MS) instrument consists of a LC system coupled to three quadrupole mass spectrometers in series and is able to obtain the m/z of an ionized chemical compound at nominal mass resolution [83]. A time-of-flight mass spectrometer (TOF-MS), which can also be hyphenated to an LC system, can very accurately measure the m/z ratio of ions based on a time measurement [84].

The homologous chemistry of the three main classes of MAs found in all mycobacteria found to date has challenged chemists since the early 1900s to seek novel and unique methods with which to separate, isolate, identify and quantitate each class [85-87]. The combination of the three MA subclasses elicits a measurable immunogenic effect *in vivo* [88], and detection of MAs in human clinical samples has been used as sufficient evidence of TB infection in patients [65].

The long carbon chain (C_{60}-C_{90}) of MAs contributes to the extreme hydrophobicity of the molecule making these compounds a challenge to separate using commercially available normal or reverse phase analytical LC columns (silica, C_{18} or C_8 stationary phases). When using reverse phase LC conditions, a major challenge is to achieve efficient separation between each of the lipids in the homologous series of MAs eluting from the column, which is further complicated by the co-elution of the homologous series of the other subclasses of these lipids in order to accurately identify and quantitate each of them individually. The large molecular mass, high boiling points and extreme hydrophobic nature of the MAs and other non-volatile lipids has prevented earlier studies from being performed on commercial GC-MS and LC-MS instruments [89] mainly due to the need to derivatize these molecules for GC-MS analysis [90] or in the use of highly non-polar organic solvents such as chloroform or dichloromethane for LC-MS analysis. [91].

The study of different subclasses of MAs can be viewed as a niche research area within the growing field of lipidomics. Lipidomics itself is a rapidly expanding research field and is

driven by recent advances in the soft ionisation electrospray ionization MS (ESI-MS). Lipidomics is concerned with the identification and quantitation of all the cellular lipids and lipid alterations that occur during cellular growth, movement, metabolism and proliferation. Lipidomics is closely related to that of metabolomics which is mainly concerned with the study of the more polar cellular metabolites. Lipidomics research utilizes multiple techniques and incorporates vast amounts of data in order to identify and possibly quantify the chemical constituents of a cell's lipidome. Lipidomics includes the study of both intra- and extracellular lipids by identification of all lipid molecules according to their specific class and subclass. Lipid metabolism and the interactions of lipids with cellular proteins can provide novel insights into current health and disease challenges [92].

As a result of advances in MS, lipidomics has emerged as a promising research field within biological science. Initially, direct infusion techniques were prevalent due to [i] the ease and simplicity of using a syringe pump to introduce the sample into the ion source of the mass spectrometer, [ii] fast analysis time and [iii] the possibility of detecting various different lipid classes in a single injection. The identification of any particular lipid within different subclasses was extremely difficult due to the isobaric masses of several different lipid isomers and the fact that saturated and mono-unsaturated lipids of the same lipid class showed overlapping isotopic distribution in the mass spectra [93].

To circumvent this overlap of mass spectral peaks due to isotopic distribution in the spectral data from different isomers, it would be necessary to separate the compounds prior to mass spectral analysis. This would require chromatographic separation which has several advantages over direct infusion techniques, such as [i] more reliable identification of individual lipid species, [ii] the potential separation of isomers and [iii] the reduction of competing ion-suppression effects. Lipidomic analyses using LC-MS-based techniques involve the initial selective extraction of lipids from a biological sample followed directly by LC separation without any hydrolysis or derivatisation steps. The lipid molecules are chromatographically separated on the analytical LC column and are introduced into the ESI source where ionization occurs followed by the mass separation of the different ions according to the m/z of each specific ion in the MS. When using a tandem mass spectrometer the mass analyser that can either detect precursor ions or product ions of

particular selected masses when product ions (formed after collision induced dissociation (CID) of selected precursor ions) [93] are analysed.

A chromatographic method has previously been standardized for use in clinical settings to separate the different classes of MAs for mycobacterial identification [94-96]. MAs were examined as *p*-bromophenacyl esters by high-performance LC (HPLC) combined with fluorescence detection. Standard HPLC patterns were developed for different species of *Mycobacteria* by examination of different strains from culture collections and other well-characterized isolates. Relative retention times of peaks and peak height comparisons were used to identify mycobacterial species.   Unfortunately the laboriousness of sample preparation and high technical expertise required to operate the analytical instrument and interpret results lead to the assay being gradually phased out in many TB diagnostic laboratories.

With advances in LC and in particular MS, MA and total mycobacterial lipid analysis via LC-MS has been in the forefront of TB research recently with several authors having used LC-MS to analyse MAs. Although some of these studies show low limits of detection and high precision only Layre *et al*. [97] and Sartain *et al*. [98] could show analyte selectivity using high resolution MS (HRMS) to analyse not just MAs but total mycobacterial lipid extracts.

Although accurate mass measurements of MAs and PDIMs have been obtained and reported by both Layre *et al*. and Sartain *et al*., no reports have yet been published which make use of accurate mass defect analyses to characterise these high molecular weight lipid compounds. Pal *et al*. [99] have recently compared major lipid class compositions between drug sensitive and drug resistant *M. tb* but did not identify any unique biomarkers that could be used to differentiate between drug resistant and drug susceptible *M. tb* strains. It should also be noted though that Pal *et al*. employed a targeted approach using a nominal MS technique.

The ability to conduct a comprehensive analysis on the full complement of *M. tb* lipids using available analytical techniques and tools has been elusive. Sartain *et al*. developed and optimized an LC-MS method to detect and identify lipids from all major *M. tb* lipid classes. Their methodology was based on efficient chromatographic separation and automated ion identification using an accurate mass spectrometer. They demonstrated the sensitive

detection of molecules representing all known classes of *M. tb* lipids from a single crude extract. They also demonstrated the ability of their methodology to identify changes in lipid content in response to cellular growth phases [98].

1.11   Summary of the research undertaken

With the cell wall lipids of *M. tb* playing a major role in TB speciation, pathology, survival and proposed role in diagnostic and treatment research, this study was undertaken in a sequence of developing more advanced analytical capability with the intent of establishing either a nominal mass LC-MS/MS method on a triple quadrupole mass spectrometer system or an accurate mass LC-q-TOF-MS technique that can be used to analyse partially purified membrane lipid extracts or crude lipid extracts from culture-grown *M. tb* strains. Although the initial methods were aimed at analysing the different classes of MAs in semi-purified form, each of the methods developed thereafter included all the steps from mycobacterial culturing using established standard operating procedures in a microbiology laboratory, sample collection, sample processing and preparation, sample analysis and data collection, conversion and interpretation.

The standard methods used to date for mycobacterial lipid analysis use saponified mycobacterial membrane samples where the MAs are released from the conjugating molecules and where the classical class separations of either derivatised or underivatised MAs are further analysed. These analyses generally use chromatographic separation followed by colorimetric or fluorescent analysis where lipid chain length or total carbon number cannot be confirmed. Many of the MAs with different chain lengths co-elute from the short chromatographic run times used which means that valuable data is being lost during these analyses.

The assays developed and performed during this study were initially established with the aim of determining the ratio of the different classes of the MAs to be able to support a study relating to the hypothesis that the methoxy- and keto- MAs are more immunogenic than the α- MAs, which linked into an immunity based study investigating detection of active TB infections.

During these initial assays it became apparent that MA chain length and the molecular origins of the MAs were in fact important in the determination of the drug resistance and virulence of the mycobacterial species. To address the analytical requirements to determine these parameters, further method development was performed on MAs that were both saponified, to link to the generally used methods, but also on unsaponified lipid extracts to determine the possibility of using the fingerprints of these fully-conjugated molecules from which the MAs originated, as indicators of the mycobacterial phenotype.

During the LC-MS/MS method development for MA class ratio determination it was shown that the product ion scans that resulted after collision induced dissociation (CID) of selected major precursor ions (i.e. m/z 1136, 1264 and 1252 for the major α-, keto- and methoxy-MAs respectively) were the product ions m/z 367 and 395. These two product ions were found to be the same for all MA precursor ions used to create the final multiple precursor ion scan method. The same product ion fragmentation was also found whilst setting up the LC-qTOF-MS method. It was consequently found that the precursor ion scan of either m/z 367 or 395 produced a mass spectrum that correlated to the initial precursor ion scan. This result proved that both these product ions, m/z 367 or 395, were not unique to any particular precursor ion but were common product ions from all three different classes of MA molecules irrespective of the precursor ion that was selected for CID. Either or both m/z 367 and 395 could therefore not be used as unique fragmentation ions to setup a MRM based LC-MS/MS method. Hence, a multiple precursor ion scan method containing 19 precursor ions was created on the LC-MS/MS and a scan method in the m/z range 50-3000 was used on the LC-qTOF-MS.

The use of the Kendrick mass defect and the van Krevelen plots were investigated as a simplified means to determine the different classes of the MAs using a mass spectrometer with mass resolution of 30 000.

1.11.1 Research questions

1. Can LC-MS/MS be used to efficiently separate the homologous series of the different classes of mycobacterial membrane derived mycolic acids?

2. *Can drug resistant phenotypes of M. tb. be distinguished from sensitive phenotypes using mass spectrometric lipid profiles?*

3. Can mass defect data of high molecular mass *M. tb* lipids be used to assign lipid classes to these molecules?

1.11.2 Aim

The aim of this project was to develop selective and sensitive LC-MS/MS methods to identify and determine the relative quantities of the α-, keto- and methoxy- mycolic acids classes, which can be used to differentiate between different *Mycobacterium* phenotypes.

1.11.3 Objectives

The specific objectives of this research study were:

- To separate the MAs and identify the class of each MA using LC-MS/MS of the lipid fraction of extracts from cultured *Mycobacterium tuberculosis*.

- To determine the ratio between the three main classes of MAs in isolated MA's and commercially available MA preparations.

- To assess the feasibility of using accurate mass data from a q-TOF-MS to classify MA using measured mass defects.

- To assess whether *Mycobacterium tuberculosis* lipid fraction profiles determined by LC-MS/MS can be used to identify drug resistant phenotypes as confirmed by genotypic data.

2 Development of a LC-MS/MS method for analysing purified natural mixed MAs

2.1 Introduction

The first report of MAs present in tubercle bacilli was published in 1889 [56]. These unusual fatty acids occur in the families *Mycobacteriaceae*, *Nocardiaceae*, *Corynebacteriaceae, Dietzaceae, Gordaniaceae* and *Tsukamerallaceaae* which fall under the suborder *Corynebacteriaea* (FIGURE 2.1) [100, 101]. Mycobacterial species are fully dependent on their cell wall MAs for growth and survival. MAs of the *Mycobacterium spp.* are among the longest that occur in nature, with a total number of carbon atoms varying between 60 and 90, whilst the meromycolate chain varies between 42 and 62 carbons in length [62, 63]. TABLE 2.1 shows the range of total number of carbon atoms that are present in MAs within *Mycobacterium spp.*, *Corynebacterium spp.* and *Nocardia spp.* as well as the range of carbon atoms present in the meromycolate chain of MAs of a few species. The number of carbon atoms present in the meromycolate chain (FIGURE 2.2) of MAs is indicative of its hydrophobicity.
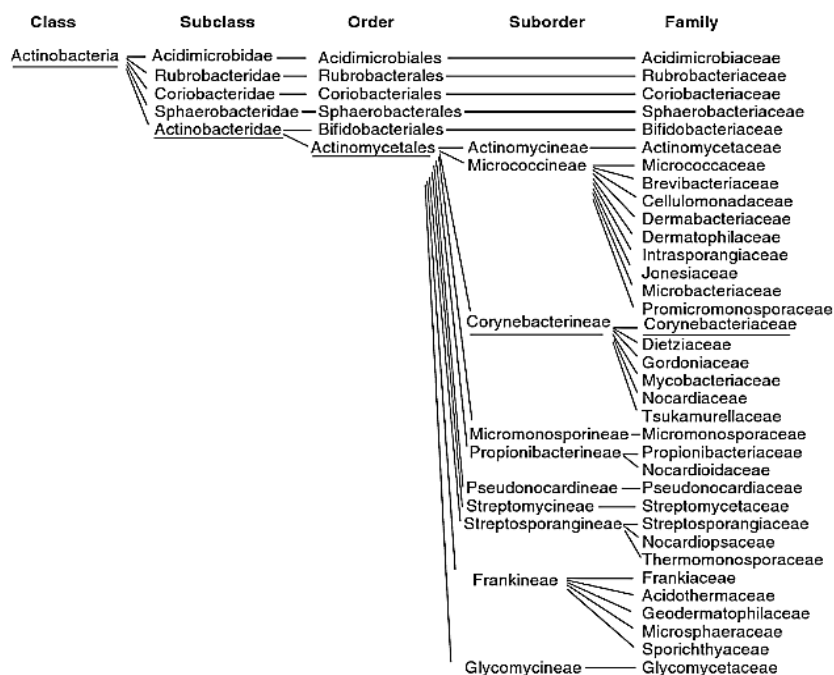
Figure 2.1: Heirarchal classification system of the class Actinobacteria according to Stackebrandt *et al.* [97] and Eggeling *et al.* [98].

Table 2.1: Total carbon in MAs and number of carbons in the meromycolate chain of MAs of a few species within the suborder Corynebacteriaea.

Species Name	Total Carbon in MAs	Number of Carbons in the Meromycolate Moiety	Reference
Mycobacterium spp.	60-90	42-62	[102]
Corynebacterium spp.	22-36	8-18	[103]
Nocardia spp.	46-60	32-40	[60]
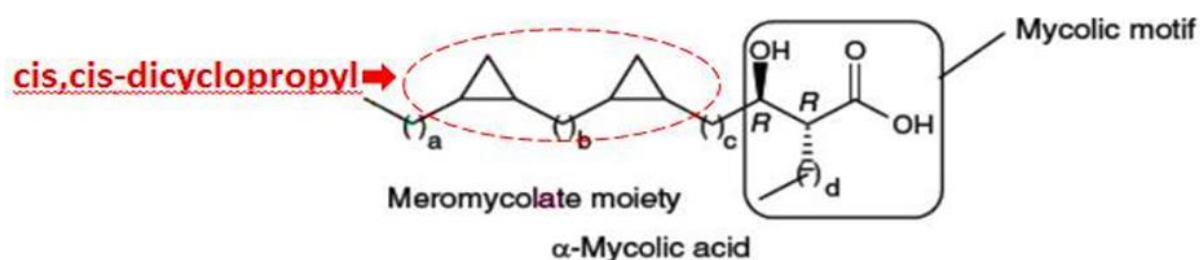
Figure 2.2: Basic structure of α-MA, depicting the meromycolate moiety, the cis,cis-dicyclopropyl configuration and the mycolic motif [101].

MAs have intrigued scientists with their long meromycolate carbon chains, [102, 103] but their analysis has been a challenge for decades [85, 86, 104, 105]. The chemistry of the meromycolate chains of the different types of MAs that are found in nature has also been the subject of significant interest amongst the scientific community [106]. The large size, extreme hydrophobicity, similar chemistry and lack of -chromophor of MAs have made them analytically challenging to separate and detect (or even collect) using normal or reverse phase LC techniques [107-110]. It is for these reasons that LC-MS has been widely explored in recent times as a hyphenated analytical technique with which to separate and detect each of the naturally occurring MA molecules [65, 97, 98, 111].

Chromatographic separation and quantitative mass spectrometric detection of each of the MA molecules to identify, classify and quantitate them provides a phenotypic profile that

appears to be characteristic for each of the species of mycobacteria. All known mycobacterial species express their phenotype according to their inherent genotype. This link between genotype and phenotype through the MA profile has resulted in newly discovered mycobacterial species requiring MS profiling of MA as a prerequisite for the phylogenetic speciation of mycobacteria [112]. Mass spectra of the MA composition of an isolated mycobacterial species combined with currently used genotypic techniques, can conclusively confirm an active TB infection. Genotypic techniques alone cannot be used to confirm drug resistance of a mycobacterial strain [113, 114] since the genotype of an organism infers its phenotype, but it is the phenotypic expression of a protein, enzyme, metabolite or lipid, (which are the main targets of currently used therapeutic agents) that needs to be confirmed [115, 116].

Standardized analytical methods for determining the phenotypic profile of mycobacteria may still have an important role to play in clinical microbiology settings. An MS analysis alone may not be able to achieve an acceptable level of specificity but if hyphenated to a chromatography system, a standardized phenotyping method could be developed. The results of such a standardised method could provide much needed information with which to treat TB infections.

The identification of mycobacterial species can be performed by testing for mutations in the genetic material [117-121]. Recent reports have shown that the long chain MAs are in fact unique to *Mycobacterium spp.* [55, 57] and that LC-MS techniques are being thoroughly investigated for the ability to differentiate mycobacterial species based on their MA composition [65]. LC-MS methods have yet to be standardized in clinical settings though, partly because of the unavailability of certified reference MA standards.

Long hydrocarbon molecules are challenging to resolve chromatographically using either normal or reverse phase analytical columns. One of the challenges of using reverse phase analytical columns is to completely separate a mixture of MAs without employing derivatization techniques.

In order to identify and quantify each of the many different MAs present in a natural extract there needs to be clear separation of the MA subclasses (α -, methoxy- and keto-) as well as

separation of the homologous series of MAs within each subclass (e.g. a methoxy-MA molecule, which can occur in up to four different stereoisomeric configurations).

The extreme hydrophobicity of MAs has limited many earlier studies performed on both GC-MS and LC-MS instruments [89]. Derivatization procedures are required for GC-MS analysis [90] while highly non-polar organic solvents such as chloroform or dichloromethane need to be used for LC-MS analysis [91].

This chapter focusses on the development of a triple quadrupole LC-MS/MS method that efficiently separates and detects non-derivatized MA molecules. MAs from two sources were used: a commercially available *M. bovis* MA extract and semi-purified extracts from laboratory-grown *M. tb* H37Rv strain.

2.2   MA analysis using LC-ESI-MS/MS: a targeted lipidomics approach

The analysis of MAs using LC combined with single quadrupole (MS) or tandem MS (MS/MS) in order to identify and quantify each of the MA classes using precursor mass or precursor mass/product ion mass combinations are considered targeted lipidomics. Lipidomics is a rapidly expanding research field that is driven by recent advances in and novel applications of soft LC-ESI-MS/MS [92]. The term lipidomics describes a diverse research area within which the spectrum of lipids in a biological system are mapped to describe the function and metabolism of individual lipids [122]. Whilst lipidomics is mainly concerned with the identification and quantitation of the full complement of tissue or cellular lipids and does include the study of both intra- and extracellular lipids, it also investigates lipid changes that occur during metabolism, remaining closely related to metabolomics, which in turn is widely viewed as studies interrogating cellular metabolites.

Lipidomics utilizes a variety of analytical techniques and incorporates the collection of large data sets in order to identify and quantify the chemical constituents of a cell's lipidome. Lipids can be identified per class and even a specific subclass fairly easily from mass spectral data and allows analysis of lipid metabolism and interactions of lipids with other cellular components such as proteins that can provide insight into health and disease challenges [92].

Direct MS infusion techniques were initially employed for earlier lipidomic studies. This was mainly due to: (1) the ease and simplicity of using an internal or external syringe pump to introduce the sample directly into the ion source of the mass spectrometer, (2) the relatively quick analysis time and (3) the possibility of detecting different lipid classes in a single injection analysis. However, the identification of specific lipid molecules was not possible due to the m/z of many isomeric lipids overlapping when preforming an infusion analysis. Furthermore, saturated and unsaturated lipids within a lipid class showed overlap within the isotopic distribution pattern in the combined mass spectrum [93].

To circumvent the spectral data overlap from different compounds it was necessary to separate individual lipid molecules prior to ionization and mass spectral analysis. In the case of extracted natural mixtures of MAs this required LC separation that provides several advantages over direct infusion. This resulted in: (1) a more reliable identification of individual lipid species, (2) possible separation of the *cis-* and *trans-*isomers of the oxygenated MA subclasses and (3) the reduction of in-source ion-suppression effects.

Lipidomic studies that are performed using MS instruments require an initial sample preparation protocol that involves the extraction of all lipids from a biological sample, with or without any hydrolysis or derivatization steps, followed by LC separation. The lipid extract is chromatographically separated on an analytical LC column, eluted as separate lipid molecules at specific retention times into an ESI-MS source where ionization of each lipid molecule occurs. Ionization is followed by the MS detection of each of the different ions that are formed in the source. When making use of MS/MS, the mass analyzer can detect both the precursor ion (primary ion) as well as the fragments of the precursor ion - product ions, which are formed after collision induced dissociation (CID) of selected precursor ions (FIGURE 2.3) [93, 123].
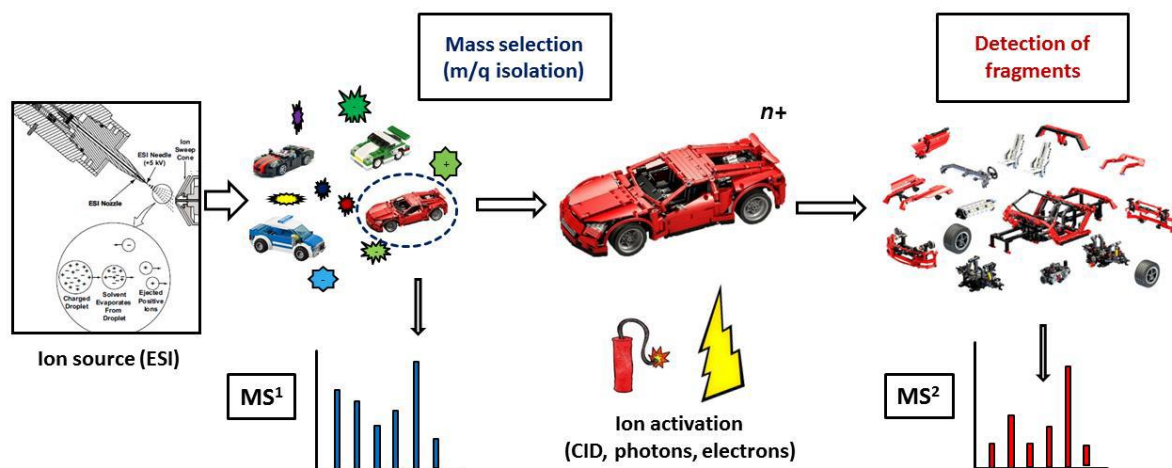
Figure 2.3: Schematic cartoon representation of the steps taking place in a tandem MS system [121].

In the late 1980s a HPLC method was developed, standardized and implemented in clinical laboratory settings worldwide to confirm the identity of isolated mycobacterial species [94-96]. In this assay, MAs were hydrolysed, isolated and derivatized to form *p*-bromophenacyl esters that were analysed by HPLC hyphenated with an UV detector (FIGURE 2.4). HPLC "patterns" were created for different mycobacterial species. The relative retention times of eluting peaks and peak height comparisons were used to identify and speciate isolates of mycobacteria (FIGURE 2.5).
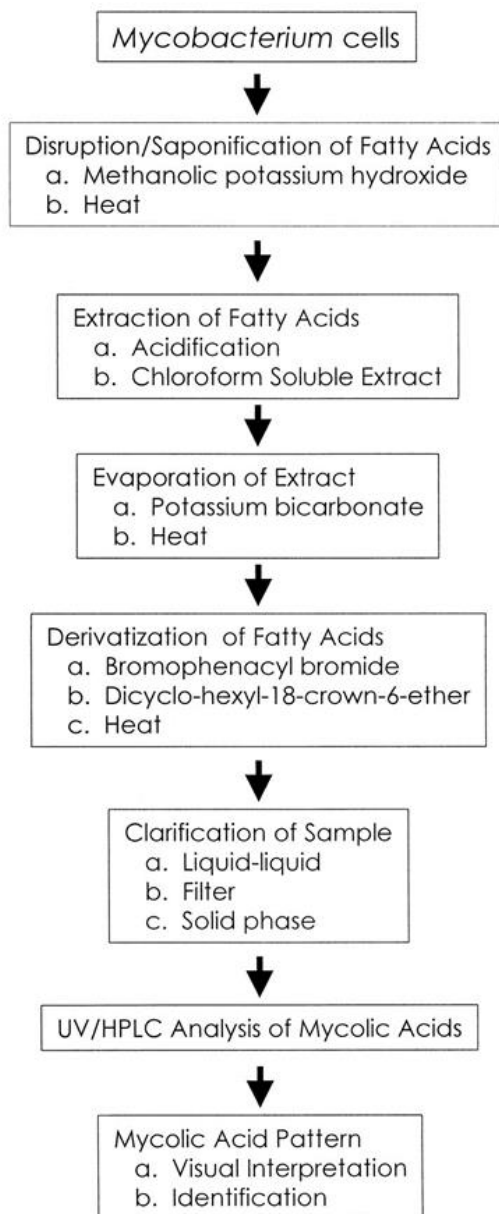
Figure 2.4: General flowchart for the sample preparation, lipid extraction, derivatization and clarification to analyse MAs using HPLC-UV [94].
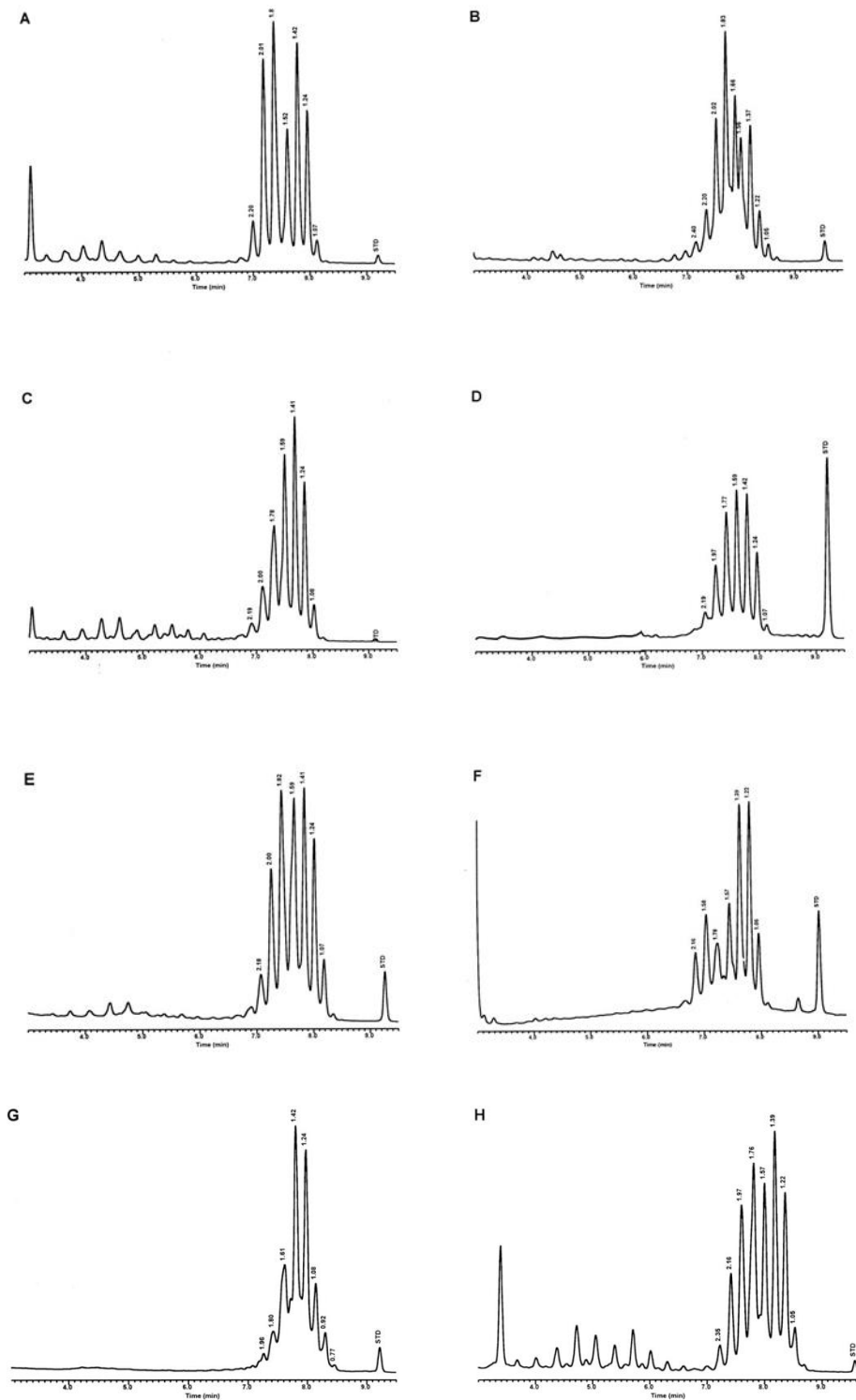
Figure 2.5: Characteristic HPLC-UV chromatograms of bromophenacyl derivatised mycolic acids from different _Mycobacterium spp_. showing the extended retention time, simple envelope, single-cluster and peak patterns. (A) _M. asiaticum_ **ATCC 25276T; (B) M. bovis BCG Pasteur; (C)** _M. gastri_ **ATCC 15754T; (D) M. gordonae ATCC 14470T, UV-HPLC chromotype I; (E)** _M. kansasii_**, ATCC 12478T; (F)** _M. leprae_**, 'armadillo'; (G)** _M. tb_ **complex (includes** _M. africanum_ **ATCC 25420T, M. bovis ATCC 19210T, "**_M. canettii_**" NZM 217/94,** _M. caprae_ **CIP 105776T,** _M. microti_ **ATCC 19422T, and** _M. tb_ **ATCC7294T); (H)** _M. szulgai_ **ATCC 35799T [95].**

Although the HPLC-UV technique was successfully implemented for mycobacterial species identification, the laborious sample preparation and high technical expertise required to operate an HPLC instrument as well as interpret the chromatographic results led to this assay gradually being phased out in many TB diagnostic laboratories.

From the late 1990s onwards, with the increasing availability of LC-MS instruments, the analysis of MAs using LC-MS techniques gained ground as being a useful tool for diagnosing TB from relatively small clinical samples [65, 111, 124]. The increased sensitivity and specificity of the MS system contributed to the LC-MS technique becoming the preferred analytical method for detecting MAs in clinical samples.

For example, Shui *et al*. [65] studied the specific precursor fragment ion transitions of approximately 2000 individual MAs. MAs were extracted from 200 µL of liquefied sputum and analysed without the requirement for derivatization. These results demonstrated for the first time the feasibility and clinical relevance of using LC-MS technology for the direct detection of MAs as biomarkers of TB infection (FIGURE 2.6).
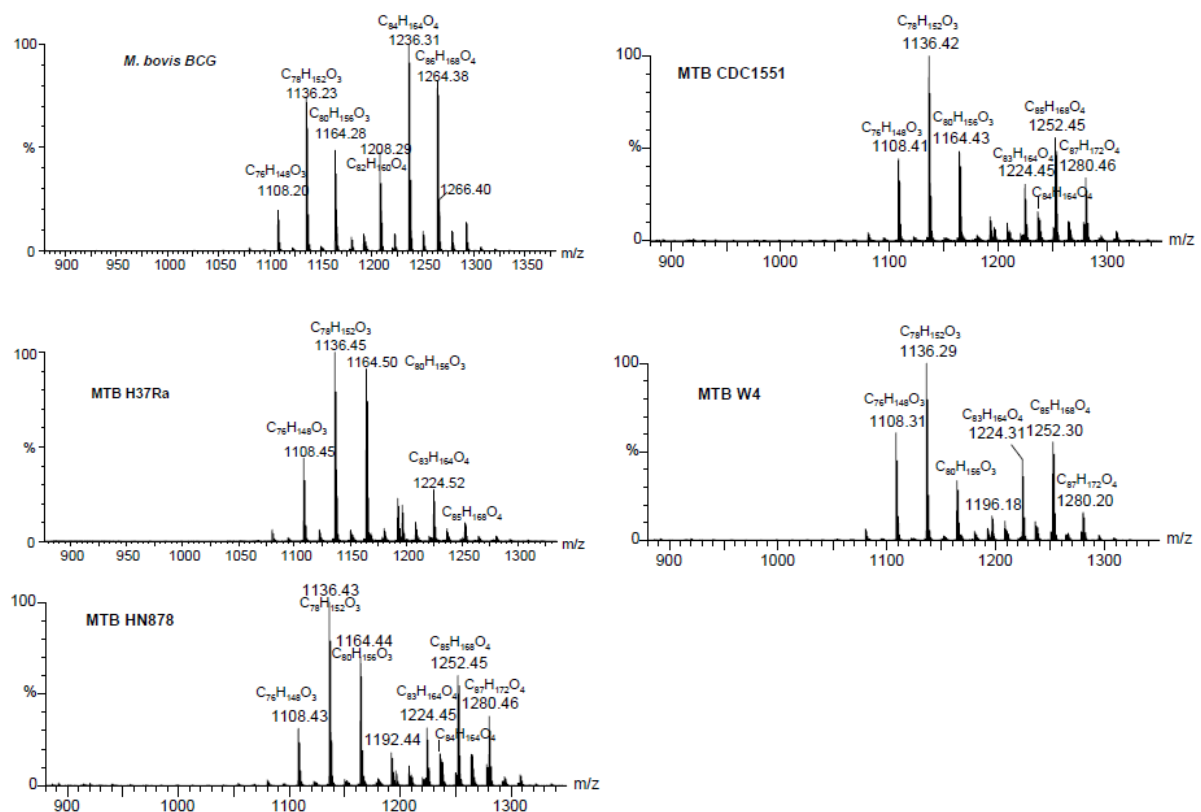
Figure 2.6: Mass spectral profiles of MAs from various *M. tb* strains [62].

A targeted analytical approach based on the ten most abundant and characteristic multiple reaction monitoring (MRM) pairs to profile the crude fatty acid mixtures from *M. tb* and several nontuberculous mycobacterial strains was developed by Szewczyk *et al*. [111]. They performed comparative analyses and obtained unique MA profiles which enabled the identification of mycobacterial species. In a case-control study of Polish TB and non-TB patients, it was demonstrated that the approach could rapidly diagnose active TB with high sensitivity and specificity. Their method identified TB-positive patients after 2 hours of sample preparation in the case of direct sputum analysis or ten days of culturing. Szewczyk *et al*. however did not make use of LC separation prior to MS detection but performed a 1 min direct infusion of a clarified lipid extract on an LC-MS/MS instrument. They analysed for the product ions of a mixture of MA molecules. Their approach remains somewhat unclear since there is a known non-unique fragmentation pattern that is obtained from fragmenting any MA precursor ion.

Song *et al*. investigated whether electrospray ionization-tandem MS (ESI-MS/MS) could be used to correctly identify mycobacterial species based on their MA profiles [124]. In their study, *M. tb* clinical isolates and 18 non-tuberculous (NTM) mycobacterial species previously identified by PCR-restriction fragment length polymorphism (PCR-RFLP) and real-time PCR analyses were examined. In their sample preparation, crude lipid extracts were prepared by the saponification of 1–2 colonies of individual bacterial isolates followed by a chloroform/methanol (2:1, v/v) extraction. The ESI-MS/MS instrument was operated in negative ionisation mode with a high cone voltage and a high collision energy setting in the CID cell. Precursor ion scans of m/z 395, 367 and 339 resulted in ions visualized in the m/z range 1000–1400. In this particular publication from Song *et al*., precursor ions were shown to be specific to individual mycobacterial species.

Szewczyk *et al*. and Song *et al*. both employed a shotgun lipidomics approach for mycobacterial species identification by infusing soluble lipid extracts originally obtained from mycobacterial clinical isolates. The use of LC prior to MS detection could provide improved accuracy with respect to mycobacterial species identification by analysing, integrating and comparing specific MA subclass molecules. The objectives of the study performed in this chapter thus aim to address the feasibility of using LC-MS/MS for mycobacterial species identification by way of accurate MA lipid class ratio determination.

2.3 Objectives

1. Develop a reproducible triple quadrupole based LC-MS/MS method for the detection and identification of major α-, keto- and methoxy- MA lipid class molecules.
2. Comparison of extracted and partially purified MAs from cultured *M. tb* to a commercially available MAs mixture (bovine strain) using the developed LC-MS/MS method.

<u>Note</u>: Non-derivatization sample preparation procedures were to be used to prevent the extracted MAs from being chemically altered, although chemical changes could have been introduced during the saponification process used for sample preparation.

2.4 Source of MA extracts

As part of a collaborative research study, purified MAs were obtained from the Department of Biochemistry (DOB) of the University of Pretoria. These molecules were from the department's collection of *M. tb* lipid extracts obtained by saponification, extraction and further purification of a laboratory grown strain of *M. tb*.

The DOB's preparation method is provided in more detail below:

M. tb laboratory strain H37Rv was cultured under different conditions for three weeks, harvested and homogenized in sterile phosphate-buffered saline (PBS) containing 0.01% Tween 80. Separate *M. tb* cultures were each grown under four different conditions:

1. mechanically stirred in Middlebrook 7H9 broth medium that was supplemented with albumin-dextrose-catalase,
2. stationary Middlebrook 7H9 broth medium that was supplemented with albumin-dextrose-catalase,
3. stationary Middlebrook 7H10 agar plates that were supplemented with oleic acid-albumin dextrose-catalase and
4. Lowenstein Jensen slants.

All *M. tb* cultures were incubated at 37 °C. After three weeks of culturing the *M. tb* were harvested and re-suspending in saline. Three centrifugation steps (3,500 x *g* for 20 minutes at 21°C) were used to remove dissolved proteins after which the mycobacteria were

inactivated by autoclaving the suspensions at 121°C for 60 min. Homogeneous bacterial cell pellets were re-suspended in a saponification solution (25% potassium hydroxide in methanol-water (1:1, v/v). Crude MA extracts were then purified using a counter current distribution method [125].

2.5 LC-MS/MS method development

2.5.1 Materials

2.5.1.1 Analytical Equipment

The following equipment was used for the initial experiments:

Harvard syringe pump with a glass one millilitre Hamilton® GASTIGHT® 4.61 mm ID syringe purchased from Separations, Randburg, South Africa; Shimadzu Prominence ultra-high pressure LC (UHPLC) system purchased from Shimadzu Corporation, Kyoto, Japan ; AB Sciex 3200 QTrap triple quadrupole tandem mass spectrometer (LC-MS/MS) purchased from Applied Biosystems, Concord, Canada.

2.5.1.2 Reagents and Consumables

Methanol (CH_3OH) 215 and Romil-SpS (super purity solvent) MS grade was purchased from Microsep, Johannesburg, South Africa; HPLC Plus grade Chloroform ($CHCl_3$) for HPLC analysis, ≥99.9% but containing amylene as stabilizer; Ammonium acetate ≥99.99%; formic acid (HCOOH) ACS reagent ≥96.0%; *Mycobacterium bovis* MA mixture were all purchased from Merck KGaA, Darmstadt, Germany; Clear glass HPLC 1.5 mL vials with wide screw neck, flat bottom 0.3 mL glass inserts and HPLC caps with split silicone septa were all purchased from Separations, Randburg, South Africa.

2.5.2 Methods

2.5.2.1 MS Method Development

This method was based on a combination of details from previous publications [65, 97, 98] where chloroform ($CHCl_3$) and methanol (CH_3OH) were used in various ratios to solubilize lipid extracts from *M. tb*. The commercially obtained MA extract (*M. tb* bovine strain),

purchased as a 5 mg freeze dried product in a 5 mL amber glass vial was reconstituted in 5 mL $CHCl_3$:CH_3OH (1:1, v/v) and dispensed into five 1 mL aliquots which were each dried to completion under a gentle stream of nitrogen. A 1 mg working stock was then reconstituted in 5 mL $CHCl_3$:CH_3OH (1:1, v/v) to obtain a 200 µg/mL working stock solution. A four times dilution of the working stock to 50 µg/mL using $CHCl_3$:CH_3OH (1:1, v/v) containing 10 mM ammonium acetate and 0.1% formic acid was then made for the LC-MS/MS method development. The addition of ammonium acetate and formic acid was to assist in the ionization of MA molecules as they entered the ion source.

The direct infusion analysis was performed using the Harvard syringe pump in combination with the AB Sciex 3200 QTrap MS/MS mass spectrometer to assess the complexity and mass range of all compounds present in the MA mixture (FIGURE 2.8). The syringe pump flow rate was set at 30 µL/min and the MS was set to scan all Q1 precursor ions in the m/z range 1000-1400 to obtain the low resolution negative ESI mass spectrum of the mixture. The ion source parameters including gas flows, declustering potential (DP), exit voltage (EV) and collision voltage (CE), were each manually optimized to provide the highest sensitivity for all resulting negative ions in the selected mass range. The manually optimised ion source parameters are shown in TABLE 2.2.

Table 2.2: Optimised ion source parameters used on the MS during the infusion experiments.

Manually optimized MS ion source	
Mode	ESI
Polarity	Negative
Scan type	MS1 (-Q1)
Curtain gas (nitrogen)	10
Temperature	500 °C
Gas 1 (dry air)	60
Gas 2 (nitrogen)	60
Ion spray voltage	-4500 V
DP	-145 V
EP	-10 V

Four batches of *M. tb* MA lipid extracts, each extracted from *M. tb* grown under the four different conditions as described in 2.4 were analysed using the optimised infusion method. The MS settings were optimized so as to obtain the highest sensitivity and specificity for detecting all MA precursor ions.

The next step in the method development process was to hyphenate the LC module with the MS. Initially, due to the availability of solvents, dichloromethane (CH_2Cl_2) in combination with CH_3OH was investigated as a mobile phase. Mobile phase A contained CH_3OH with 10 mM ammonium acetate and 0.1% formic acid, while mobile phase B contained CH_2Cl_2:CH_3OH (1:1) with 10 mM ammonium acetate and 0.1% formic acid. After assessing several different gradients, a long shallow binary gradient elution method was developed which provided the best chromatographic separation of the mixture of MA molecules for MS detection (TABLE 2.3 and FIGURE 2.7).

Table 2.3: Binary gradient elution method showing the total LC run time vs the % mobile phase A.

Total LC Run Time (mins)	Percentage (%) Mobile Phase B
0	40
5	40
6	80
25	95
42	95
43	40
47	40
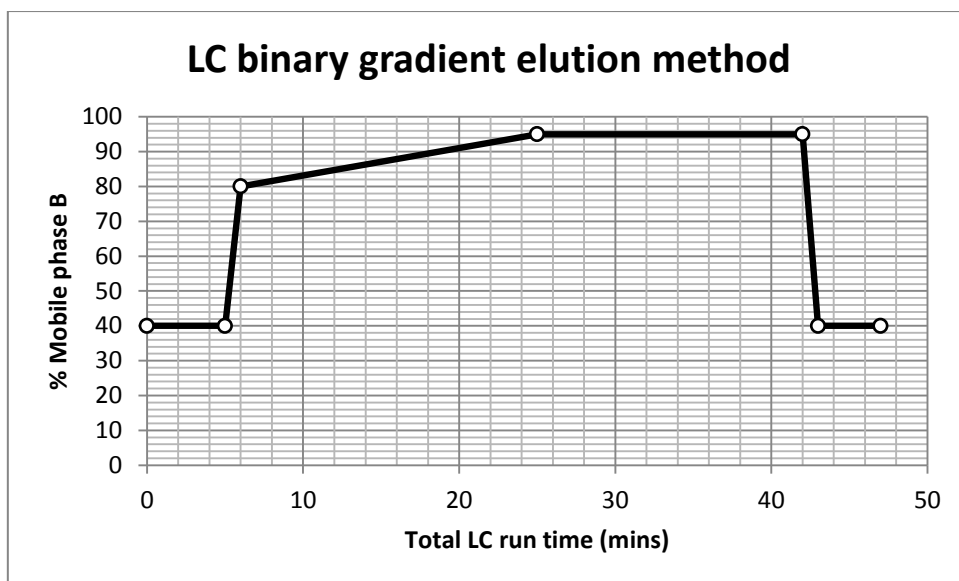
Figure 2.7: LC binary gradient elution method (total LC run time vs % mobile phase B)

During the optimisation phase of the chromatography, several different analytical column stationary phases were investigated. It was determined that an analytical column with a C18 stationary phase, packed with 3 µm particles with a 110 Å pore size and 150 mm in length provided the best peak resolution with acceptable efficiency for the separation of more than 20 different MA molecules present in the commercial as well as in the self-prepared MA extracts.

2.6   Results and Discussion

The results of the negative ionisation mode infusion experiments showed that the MAs were present in all samples and produced a complex combination of peaks that appeared to be separated by 12, 14 or 16 mass units apart. On closer inspection it became evident that each of the apparent broad peaks was a combination of several individual peaks with overlapping m/z isotopic distribution. The peaks of larger intensity were separated by approximately 28 Da, equivalent to the typical addition of $-(CH_2)_2-$ in a lipid chain. This addition of a two carbon unit is typical of biological processes in extending lipid chain length. The intervening low intensity peaks were offset by 14 Da, equivalent to a single carbon chain length extension or the difference in mass between the *cis-* and *trans-* isomers of the keto- and methoxy-MAs. A typical mass spectrum of the purified MA mixture is shown in FIGURE 2.8 below. It should be noted that each apparent monoisotopic m/z peak in FIGURE 2.8 is a complex combination of several isotopic m/z peaks with a narrow m/z separation. Upon closer inspection, and by referring to theoretical molecular masses of MAs, there is an overlapping isotopic distribution between mainly the keto- and methoxy-MA molecules in the m/z range of 1170 – 1340.
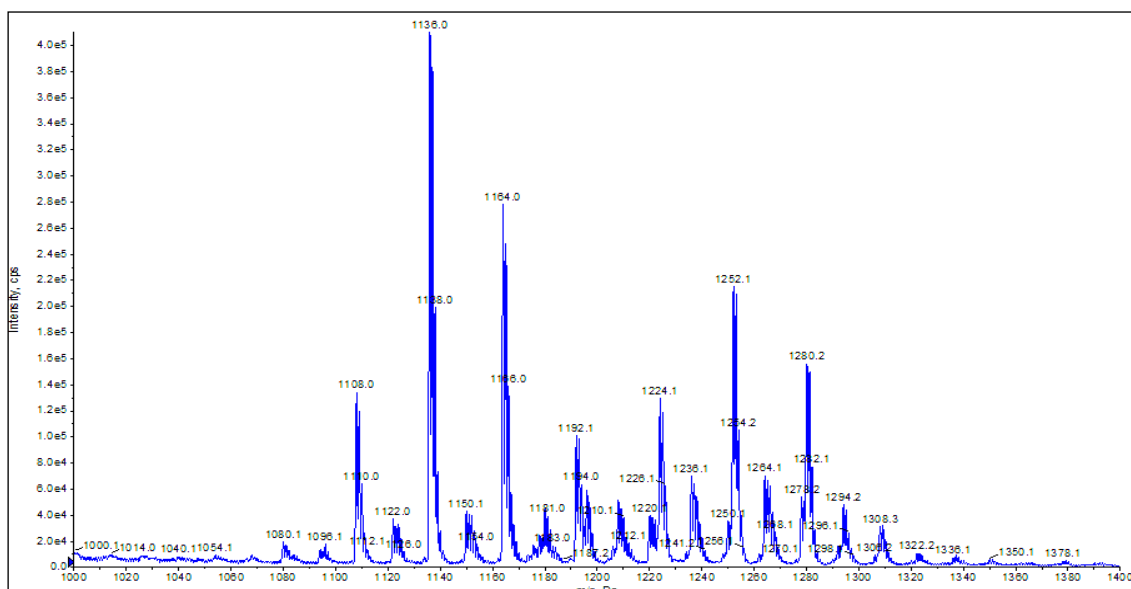
Figure 2.8: Negative ion mode mass spectrum of the initial direct infusion of a purified MA extract of MTB H37Rv, reconstituted in CHCl$_3$:CH$_3$OH (1:1) with 10 mM ammonium acetate and 0.1% formic acid, showing the 1000-1400 m/z range using the optimised conditions shown in TABLE 2.2. The spectrum was collected on an entry level LC-MS/MS at nominal mass accuracy.
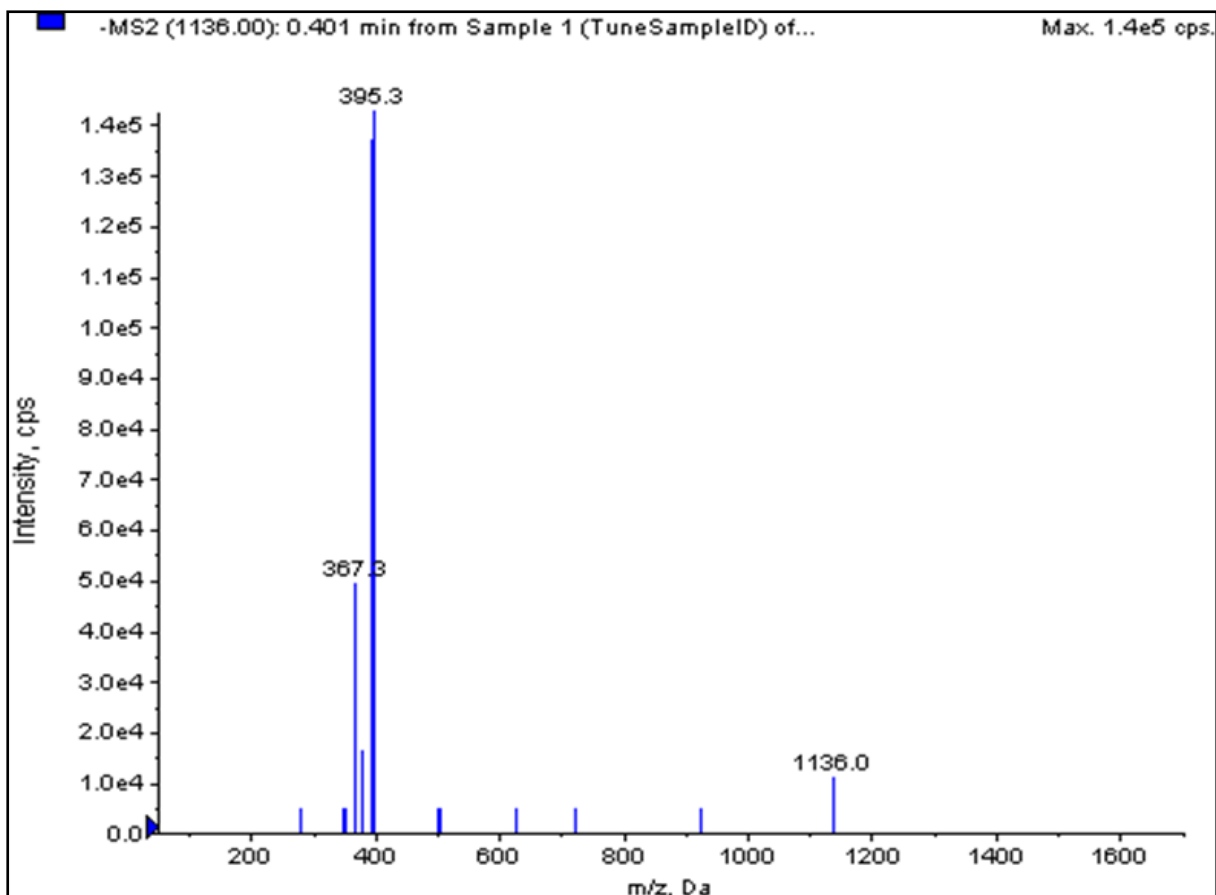
Figure 2.9: Product ion scan of precursor ion m/z 1136.0 producing fragment ions of m/z 367.3 and 395.3. The ion source parameters used were as shown in TABLE 2.2. The precursor ion of m/z 1136.0 was then pre-selected for fragmentation in a product ion scan by applying a collision energy of 25 V with collision cell entrance and exit potentials set at 10 V.

On performing product ion scans on selected precursor ions identified as major peaks it was found that the product ions of each selected precursor ions (m/z 1136, 1164, 1252 and 1236) resulted in exactly the same two product ions, m/z 367 and 395. As an example, the product ion scan of m/z 1136 is shown in FIGURE 2.9.

It was consequently found that a precursor ion scan of either m/z 367 or 395 (FIGURE 2.10) produced a mass spectrum that correlated closely to the initial precursor ion scan collected at Q1 (FIGURE 2.8). This result proved that both dominant product ions (m/z 367 or 395) were not unique to any particular precursor mass but were common product ions from all three different classes of MA molecules irrespective of the precursor ion that was selected for collision cell fragmentation. Either or both m/z 367 and 395 could therefore not be used as unique fragmentation ions for a MRM based LC-MS/MS method.
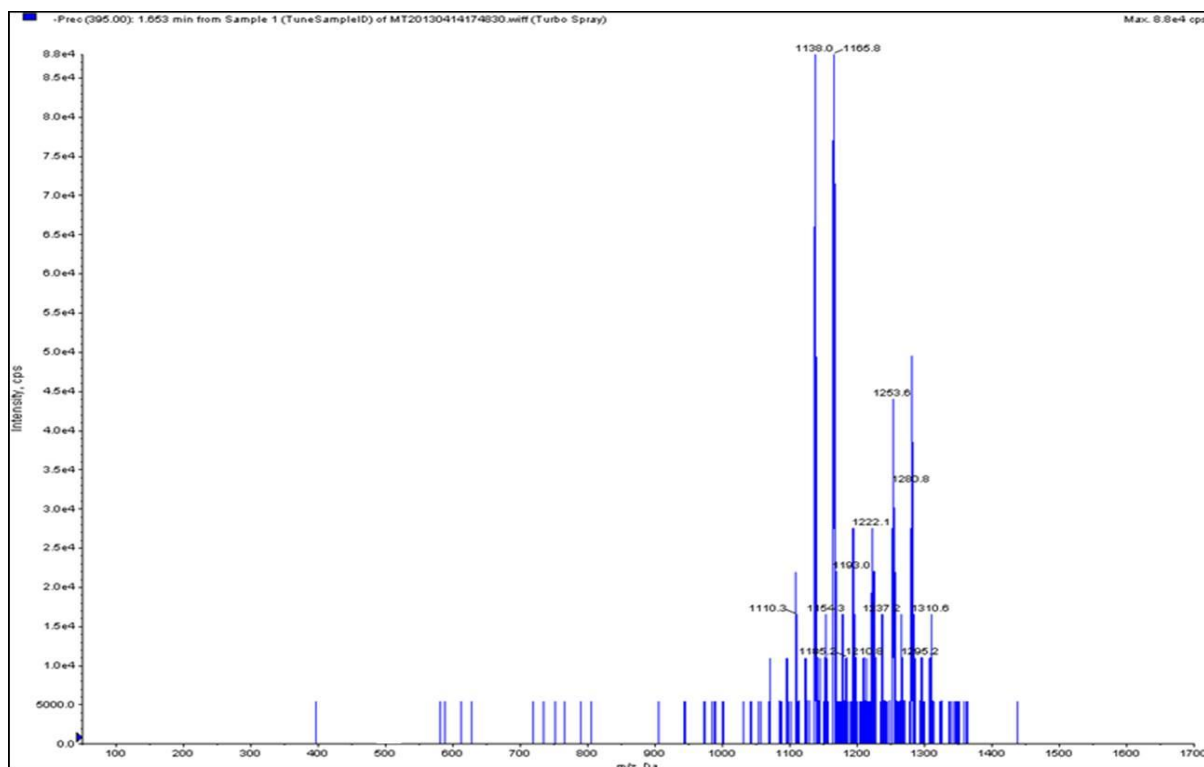
Figure 2.10: Precursor ion scan of the product ion with m/z 395 producing precursor ions correlating to the precursor ions for MAs from all three MA classes (α-, keto- and methoxy-MA).

A Q1 multiple ion scan method was instead created () which included 18 of the highest abundant "monoisotopic" m/z precursor ion signals that were obtained during the infusion experiments. Each of these $[M-H]^-$ precursor ions were assigned to a MA subclass (either α-, keto- or methoxy-MAs) according to previous reports on MA classifications that were based mainly on LC-MS/MS techniques [97, 98, 111].
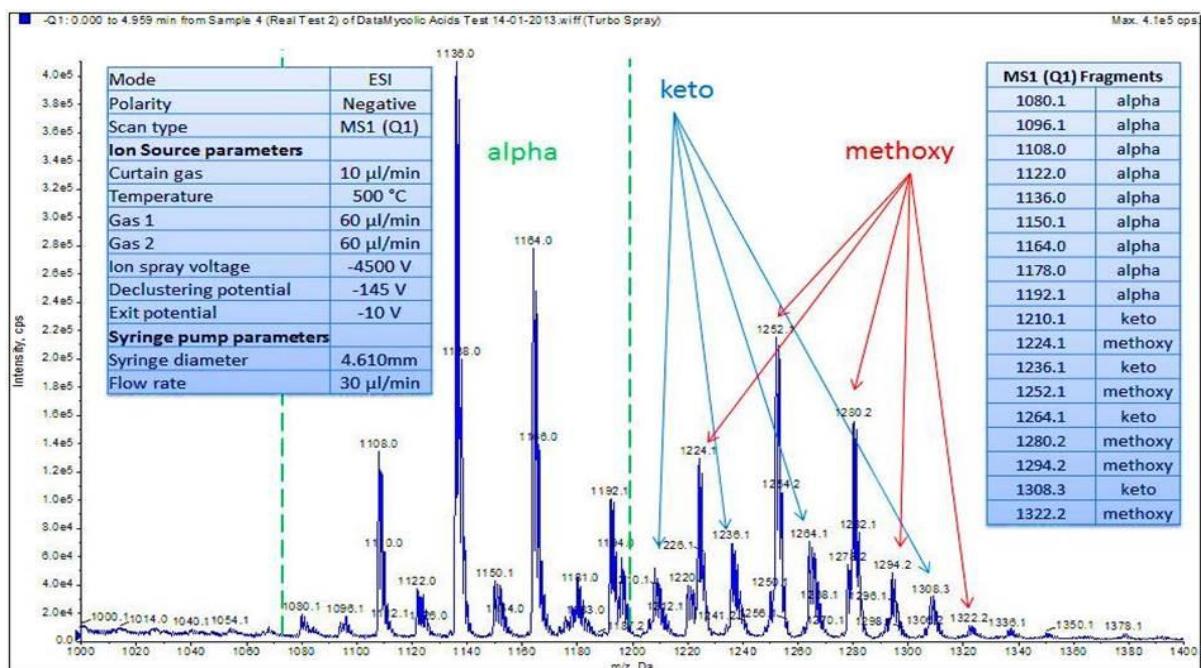
Figure 2.11: Mass spectrum between m/z 1000-1400 showing the three MA classes labelled with their respective subclasses. Optimized ion source parameters are shown in the top left inset and precursor ions used in the Q1 multiple ion scan method in the top right inset.

The ions that were selected for the Q1- multiple ion scan method were the most abundant ions obtained during the infusion analysis. Although the method included 18 different m/z ions that were monitored in negative mode, it is important to note that these were all precursor ions and not subjected to any CID. The method was therefore a targeted selective ion monitoring Q1- scan method that monitored for selected precursor ions only.

TABLE 2.4 shows the 18 precursor ions that were monitored in the Q1- multiple ion scan method. The isotopic distribution of each of the dominant α-, keto- and methoxy-MA precursor ions that were identified according to published data are shown in FIGURE 2.122, FIGURE 2.133 and FIGURE 2.144 respectively.

Table 2.4: List of 18 identifiable precursor ions that were monitored in a Q1- multiple ion scan method.

MA class ID	Q1- precursor ion (m/z)	Molecular empirical formula
α	1094.1	$C_{75}H_{146}O_3$
α	1108.2	$C_{76}H_{148}O_3$
α	1122.3	$C_{77}H_{150}O_3$
α	1136.4	$C_{78}H_{152}O_3$
α	1150.0	$C_{79}H_{154}O_3$
α	1164.2	$C_{80}H_{156}O_3$
α	1178.2	$C_{81}H_{158}O_3$
α	1192.2	$C_{82}H_{160}O_3$
keto	1209.2	$C_{82}H_{160}O_4$
methoxy	1220.4	$C_{83}H_{164}O_4$
keto	1236.3	$C_{84}H_{164}O_4$
methoxy	1252.3	$C_{85}H_{168}O_4$
keto	1264.3	$C_{86}H_{168}O_4$
methoxy	1280.3	$C_{87}H_{172}O_4$
methoxy	1294.4	$C_{88}H_{174}O_4$
keto	1308.4	$C_{89}H_{174}O_4$
methoxy	1322.4	$C_{90}H_{178}O_4$
methoxy	1336.4	$C_{91}H_{180}O_4$
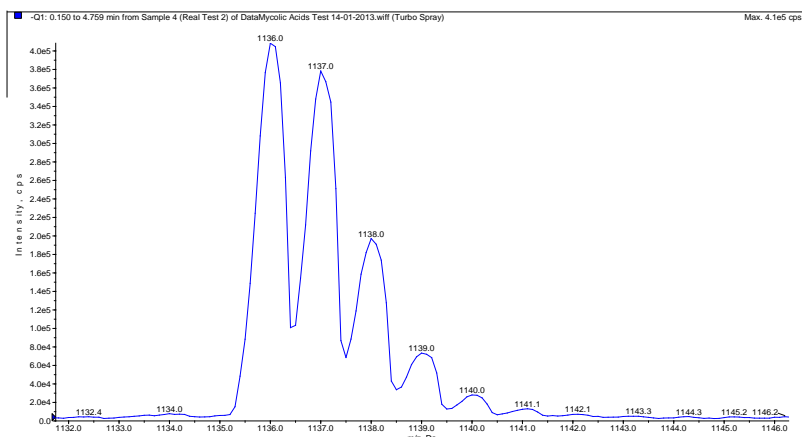
Figure 2.12: Isotopic distribution of the precursor ion at m/z 1136 representing the dominant α-MA molecule as collected on an entry level triple quadrupole mass spectrometer system during an infusion experiment using optimised source parameters as shown in Table 2.2.
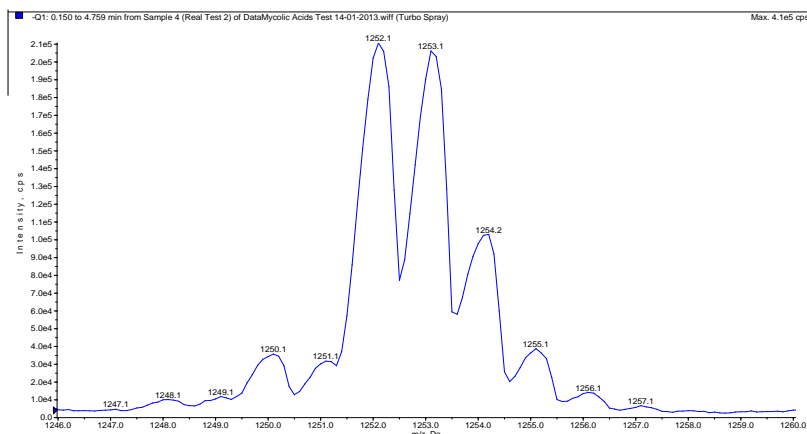
Figure 2.13: Isotopic distribution of the precursor ion at m/z 1252 representing the dominant methoxy-MA molecule.
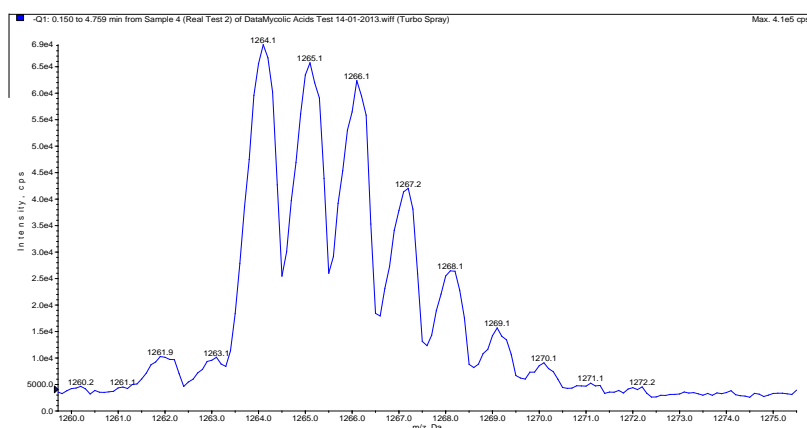
Figure 2.14: The unusual isotopic distribution of the precursor ion at m/z 1264 representing the dominant keto-MA molecule. This distribution indicates that there is overlap with an ion with m/z 1266.
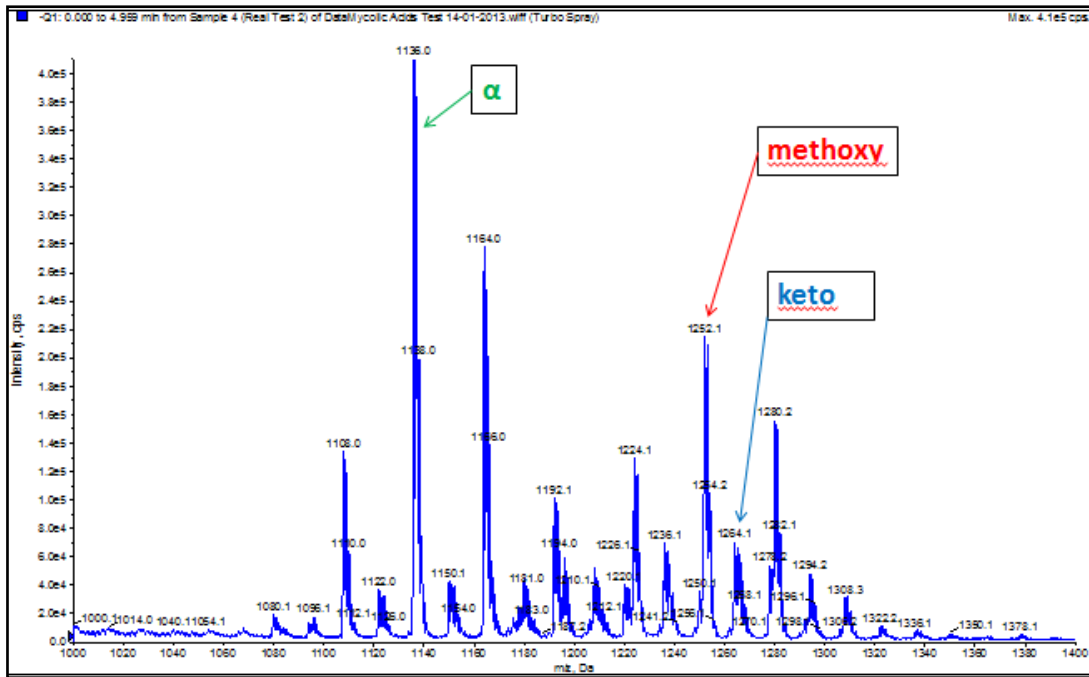
Figure 2.15: Continuous infusion-based negative ionisation mode mass spectrum of the m/z range 1000–1400 showing the 18 MA ions typically detected in the natural MA extracts on an entry level triple quadrupole mass spectrometer. Three most abundant ions from each of the α-, methoxy- and keto- MA subclasses (m/z 1136, 1252 and 1264 respectively) were chosen to be used in determining the relative MA class ratio.
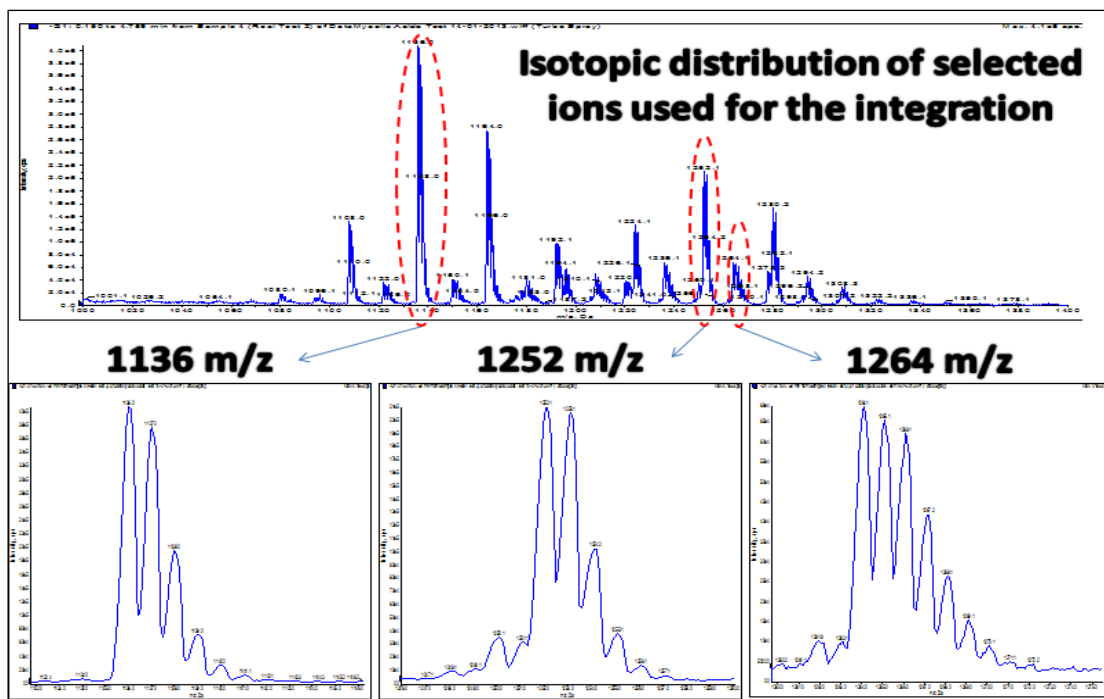
Figure 2.16: Infusion m/z spectrum of MA mixture showing ions between m/z 1000 and 1400. The expanded inserts show the isotopic distribution of the most abundant m/z ions that were used as representative of each MA subclass as an α- (m/z 1136), methoxy- (m/z 1252) or keto-MA (m/z). 1264).

48
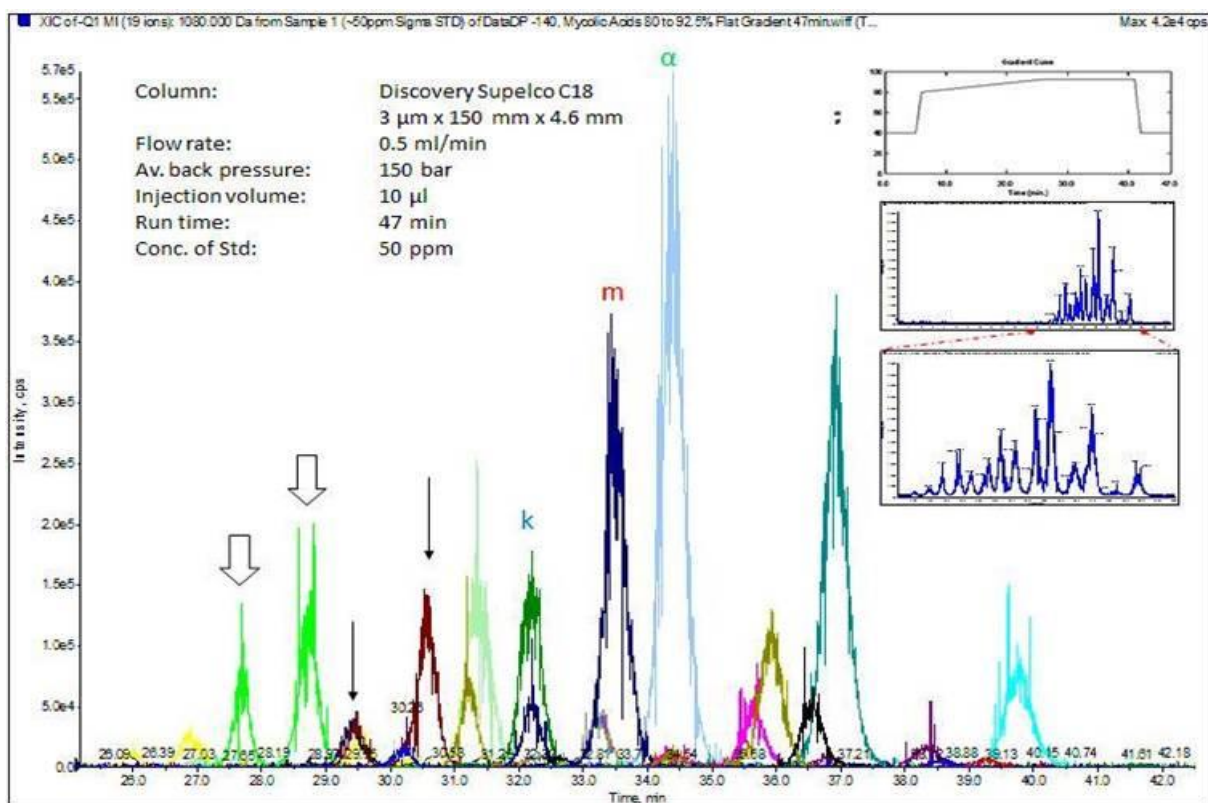
Figure 2.16: Extracted ion chromatogram showing select precursor ions; apparent isomers resolved (black arrows); major keto-, methoxy- and α- MA peaks indicated; Insets show the gradient curve used (top right inset) and total ion chromatogram (middle and zoomed in to the 19 – 42 min time range in the lower right inset).

Ions from each class extracted from TIC
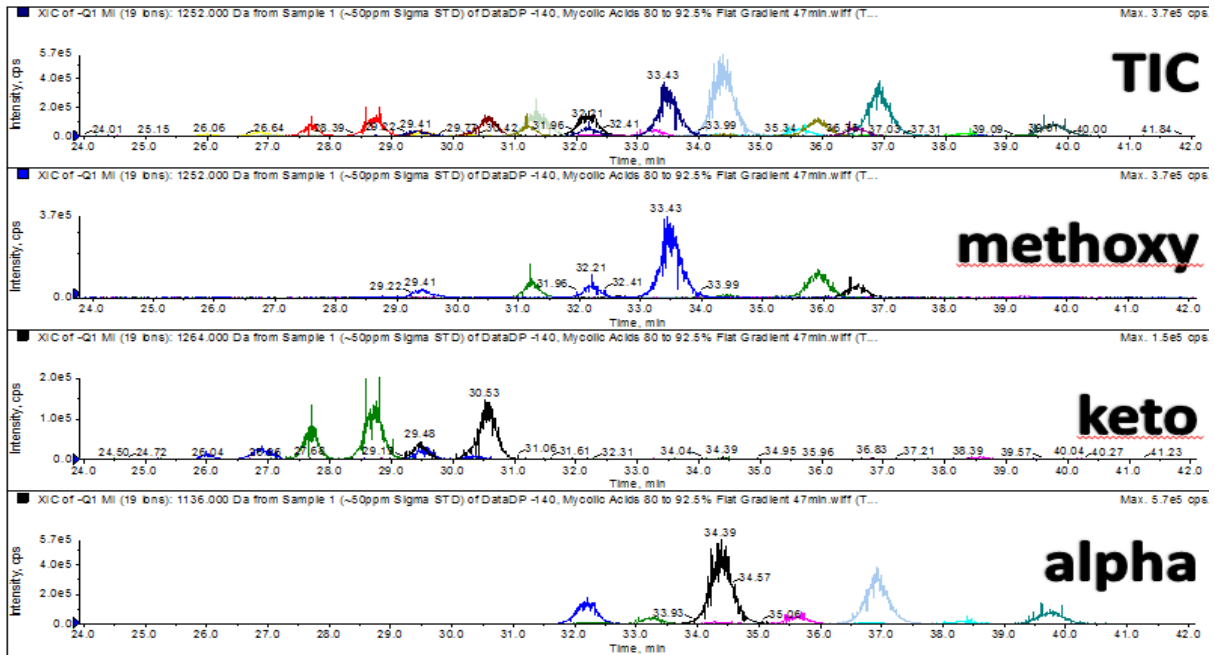
Figure 2.17: Extracted ion chromatograms of masses from each MA class from a TIC where 18 Q1-masses were selected from the original infusion m/z spectrum. The extracted ions were selected as masses identified as either methoxy-, keto- or α-MAs.
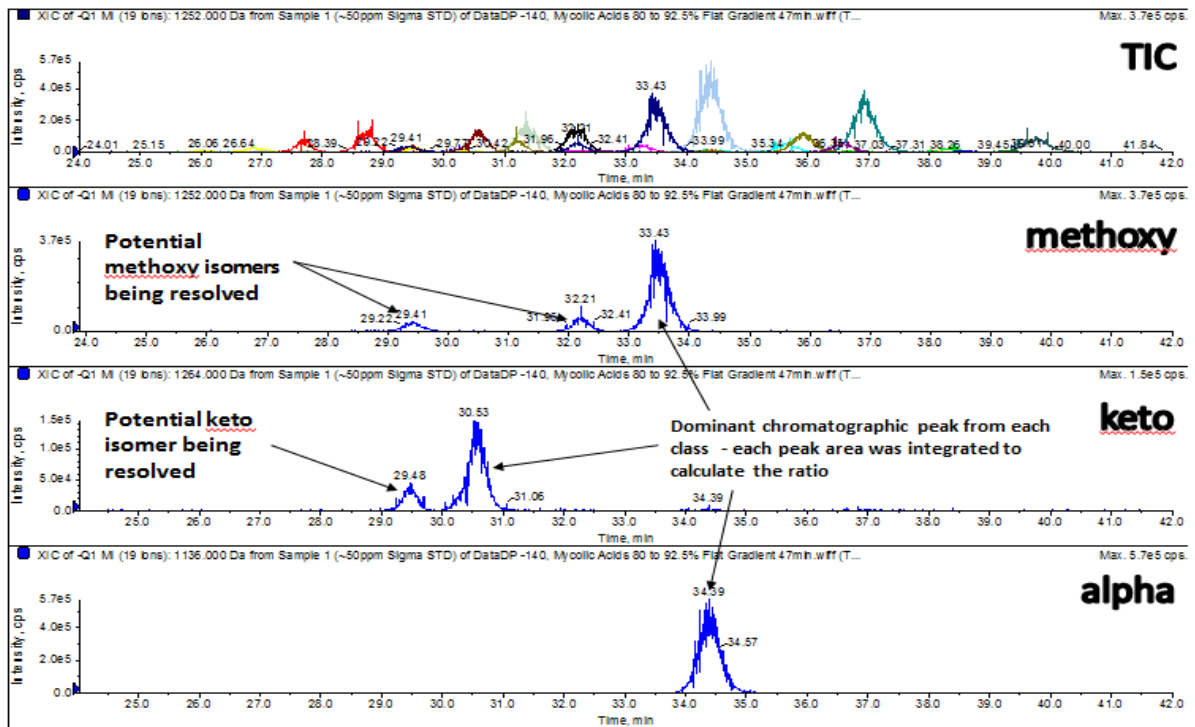
Figure 2.18: Extracted ion chromatograms of the single dominant m/z ions representing either α-methoxy- or keto- MAs

Using the LC-MS/MS method in negative ion precursor mode the ratios of MA subclasses were determined and used to differentiate between the two *M. tb* strains as proposed in SECTION 2.3. All MA subclasses from the *M. tb* H37Rv strain produced common product ions (m/z 367 & 395) with no unique ions associated with any MA subclass and as previously discussed, these non-unique product ions could therefore not be used to allocate the MA precursor ions to a specific MA subclass.

To determine a ratio of the three MA classes in a particular mixed MA extract, the single dominant m/z ion (highest signal) from each MA class was selected for integration using its correlating peak area in the chromatogram.

Results for the cultured *M. tb* and the commercially available *M. bovis* extracts revealed MAs ratios of α-, keto- and methoxy- MA subclasses of 65:7:28 for *M. tb* and 69:9:23 for *M. bovis*.

FIGURE 2.18 shows potential isomers being chromatographically resolved using the optimised LC-MS/MS method. These potential isomers were repeatedly identified in all analyses performed. Only the indicated α-, methoxy- and keto- peaks in the extracted ion chromatogram were used to determine the MA class ratio.

The most abundant m/z ion in each MA class was chosen for integration because of the proven overlap of eluting MA classes observed in the m/z infusion, especially with regard to keto- and methoxy-MA ions as can be seen in (FIGURE 2.11). The m/z ions chosen for the MA class ratio determination, namely m/z ions 1136, 1264 and 1252 (corresponding to α-, keto- and methoxy-MA respectively) were allocated according to previous reports from Sartain *et al*. [98], Layre *et al.* [97] and Shui *et al* [65] and by performing the calculations for the different classes of MAs.

Table 2.5: Acquired and integrated chromatogram peak data from the triplicate analysis of each of four batches of self-prepared MAs (Batch 1, 2, 3, 4) as well as triplicate analysis of the commercially available MA extract. The dominant precursor ion from each MA subclass is shown highlighted (yellow for α-, green for keto-, and blue for methoxy-MA) and selected for determining the percentage ratio between each of the MA subclasses.

	Sample Name	MA class ID	Analyte Mass Ranges	Analyte Peak Area (cps)	Sum of selected major peak areas	Percentage of selected peak area	MA class ID
Batch 1	**Batch 1A**	alpha	1097.100 Da	1.75E+06			
		alpha	1108.200 Da	1.12E+07			
		alpha	1122.300 Da	1.78E+06			
		alpha	1136.400 Da	2.90E+07		53.89	alpha
		alpha	1150.000 Da	9.20E+06			
		alpha	1164.200 Da	4.50E+07			
		alpha	1178.200 Da	2.79E+06			
		alpha	1192.200 Da	2.23E+07			
		keto	1209.200 Da	1.71E+06	5.38E+07		
		keto	1236.300 Da	2.98E+06		8.20	keto
		keto	1264.300 Da	4.41E+06			
		keto	1308.400 Da	4.30E+06			
		methoxy	1220.400 Da	5.91E+06			
		methoxy	1252.300 Da	2.04E+07			
		methoxy	1280.300 Da	2.04E+07			
		methoxy	1294.400 Da	3.97E+06		37.91	methoxy
		methoxy	1323.400 Da	7.39E+05			
		methoxy	1336.400 Da	7.61E+05			
	Batch 1B	alpha	1097.100 Da	2.07E+06			
		alpha	1108.200 Da	1.75E+07			
		alpha	1122.300 Da	2.28E+06			
		alpha	1136.400 Da	3.11E+07		49.47	alpha
		alpha	1150.000 Da	1.18E+07			
		alpha	1164.200 Da	6.49E+07			
		alpha	1178.200 Da	4.69E+06			
		alpha	1192.200 Da	3.34E+07			
		keto	1209.200 Da	2.73E+06	6.29E+07		
		keto	1236.300 Da	3.58E+06		9.18	keto
		keto	1264.300 Da	5.77E+06			
		keto	1308.400 Da	5.43E+06			
		methoxy	1220.400 Da	6.89E+06			
		methoxy	1252.300 Da	2.60E+07			
		methoxy	1280.300 Da	3.07E+07			
		methoxy	1294.400 Da	4.93E+06		41.36	methoxy
		methoxy	1323.400 Da	1.02E+06			
		methoxy	1336.400 Da	9.98E+05			
	Batch 1C	alpha	1097.100 Da	1.92E+06			
		alpha	1108.200 Da	1.13E+07			
		alpha	1122.300 Da	1.88E+06			
		alpha	1136.400 Da	3.10E+07		54.77	alpha
		alpha	1150.000 Da	1.07E+07			
		alpha	1164.200 Da	4.71E+07			
		alpha	1178.200 Da	2.88E+06			
		alpha	1192.200 Da	2.29E+07			
		keto	1209.200 Da	1.83E+06	5.66E+07		
		keto	1236.300 Da	3.21E+06		7.77	keto
		keto	1264.300 Da	4.40E+06			
		keto	1308.400 Da	4.60E+06			
		methoxy	1220.400 Da	6.46E+06			
		methoxy	1252.300 Da	2.12E+07			
		methoxy	1280.300 Da	2.10E+07			
		methoxy	1294.400 Da	3.92E+06		37.46	methoxy
		methoxy	1323.400 Da	7.33E+05			
		methoxy	1336.400 Da	8.08E+05			

Batch 2							
	Batch 2A	alpha	1097.100 Da	1.65E+06		56.76	alpha
		alpha	1108.200 Da	6.47E+06			
		alpha	1122.300 Da	1.85E+06			
		alpha	1136.400 Da	2.76E+07			
		alpha	1150.000 Da	1.05E+07			
		alpha	1164.200 Da	4.13E+07			
		alpha	1178.200 Da	3.20E+06			
		alpha	1192.200 Da	2.26E+07	4.86E+07		
		keto	1209.200 Da	1.08E+06		9.52	keto
		keto	1236.300 Da	2.64E+06			
		keto	1264.300 Da	4.63E+06			
		keto	1308.400 Da	5.43E+06			
		methoxy	1220.400 Da	9.29E+06		33.72	methoxy
		methoxy	1252.300 Da	1.64E+07			
		methoxy	1280.300 Da	1.88E+07			
		methoxy	1294.400 Da	4.57E+06			
		methoxy	1323.400 Da	1.05E+06			
		methoxy	1336.400 Da	1.23E+06			
	Batch 2B	alpha	1097.100 Da	1.94E+06		49.58	alpha
		alpha	1108.200 Da	1.16E+07			
		alpha	1122.300 Da	1.92E+06			
		alpha	1136.400 Da	2.66E+07			
		alpha	1150.000 Da	1.27E+07			
		alpha	1164.200 Da	6.70E+07			
		alpha	1178.200 Da	5.94E+06			
		alpha	1192.200 Da	3.86E+07	5.37E+07		
		keto	1209.200 Da	2.04E+06		11.84	keto
		keto	1236.300 Da	3.14E+06			
		keto	1264.300 Da	6.35E+06			
		keto	1308.400 Da	6.37E+06			
		methoxy	1220.400 Da	9.43E+06		38.58	methoxy
		methoxy	1252.300 Da	2.07E+07			
		methoxy	1280.300 Da	2.91E+07			
		methoxy	1294.400 Da	5.11E+06			
		methoxy	1323.400 Da	1.41E+06			
		methoxy	1336.400 Da	1.62E+06			
	Batch 2C	alpha	1097.100 Da	1.78E+06		56.22	alpha
		alpha	1108.200 Da	6.85E+06			
		alpha	1122.300 Da	1.72E+06			
		alpha	1136.400 Da	2.80E+07			
		alpha	1150.000 Da	1.10E+07			
		alpha	1164.200 Da	4.58E+07			
		alpha	1178.200 Da	3.29E+06			
		alpha	1192.200 Da	2.39E+07	4.98E+07		
		keto	1209.200 Da	1.13E+06		9.44	keto
		keto	1236.300 Da	2.66E+06			
		keto	1264.300 Da	4.70E+06			
		keto	1308.400 Da	5.28E+06			
		methoxy	1220.400 Da	8.77E+06		34.34	methoxy
		methoxy	1252.300 Da	1.71E+07			
		methoxy	1280.300 Da	1.92E+07			
		methoxy	1294.400 Da	4.21E+06			
		methoxy	1323.400 Da	9.92E+05			
		methoxy	1336.400 Da	1.17E+06			

Batch 3	**Batch 3A**	alpha	1097.100 Da	1.76E+06		55.14	alpha
		alpha	1108.200 Da	8.20E+06			
		alpha	1122.300 Da	2.62E+06			
		alpha	1136.400 Da	3.34E+07	6.06E+07		
		alpha	1150.000 Da	1.30E+07			
		alpha	1164.200 Da	4.04E+07			
		alpha	1178.200 Da	3.86E+06			
		alpha	1192.200 Da	2.19E+07			
		keto	1209.200 Da	1.68E+06		8.04	keto
		keto	1236.300 Da	3.58E+06			
		keto	1264.300 Da	4.87E+06			
		keto	1308.400 Da	6.00E+06			
		methoxy	1220.400 Da	9.81E+06		36.82	methoxy
		methoxy	1252.300 Da	2.23E+07			
		methoxy	1280.300 Da	2.10E+07			
		methoxy	1294.400 Da	4.91E+06			
		methoxy	1323.400 Da	1.01E+06			
		methoxy	1336.400 Da	1.12E+06			
	Batch 3B	alpha	1097.100 Da	2.00E+06		46.31	alpha
		alpha	1108.200 Da	1.63E+07			
		alpha	1122.300 Da	2.54E+06			
		alpha	1136.400 Da	2.94E+07	6.35E+07		
		alpha	1150.000 Da	1.60E+07			
		alpha	1164.200 Da	6.86E+07			
		alpha	1178.200 Da	7.69E+06			
		alpha	1192.200 Da	3.93E+07			
		keto	1209.200 Da	3.18E+06		10.38	keto
		keto	1236.300 Da	3.88E+06			
		keto	1264.300 Da	6.59E+06			
		keto	1308.400 Da	6.82E+06			
		methoxy	1220.400 Da	9.15E+06		43.31	methoxy
		methoxy	1252.300 Da	2.75E+07			
		methoxy	1280.300 Da	3.37E+07			
		methoxy	1294.400 Da	5.39E+06			
		methoxy	1323.400 Da	1.42E+06			
		methoxy	1336.400 Da	1.55E+06			
	Batch 3C	alpha	1097.100 Da	1.83E+06		52.68	alpha
		alpha	1108.200 Da	9.85E+06			
		alpha	1122.300 Da	2.41E+06			
		alpha	1136.400 Da	3.13E+07	5.94E+07		
		alpha	1150.000 Da	1.43E+07			
		alpha	1164.200 Da	4.76E+07			
		alpha	1178.200 Da	4.37E+06			
		alpha	1192.200 Da	2.52E+07			
		keto	1209.200 Da	1.75E+06		8.43	keto
		keto	1236.300 Da	3.60E+06			
		keto	1264.300 Da	5.01E+06			
		keto	1308.400 Da	5.53E+06			
		methoxy	1220.400 Da	9.00E+06		38.88	methoxy
		methoxy	1252.300 Da	2.31E+07			
		methoxy	1280.300 Da	2.25E+07			
		methoxy	1294.400 Da	4.55E+06			
		methoxy	1323.400 Da	9.86E+05			
		methoxy	1336.400 Da	1.12E+06			

Batch 4	**Batch 4A**	alpha	1097.100 Da	1.97E+06		56.87	alpha
		alpha	1108.200 Da	1.05E+07			
		alpha	1122.300 Da	2.29E+06			
		alpha	1136.400 Da	3.68E+07			
		alpha	1150.000 Da	1.06E+07			
		alpha	1164.200 Da	4.06E+07			
		alpha	1178.200 Da	2.53E+06			
		alpha	1192.200 Da	2.16E+07	6.47E+07		
		keto	1209.200 Da	1.47E+06		6.66	keto
		keto	1236.300 Da	3.34E+06			
		keto	1264.300 Da	4.31E+06			
		keto	1308.400 Da	5.20E+06			
		methoxy	1220.400 Da	7.84E+06		36.47	methoxy
		methoxy	1252.300 Da	2.36E+07			
		methoxy	1280.300 Da	2.10E+07			
		methoxy	1294.400 Da	4.11E+06			
		methoxy	1323.400 Da	6.31E+05			
		methoxy	1336.400 Da	8.89E+05			
	Batch 4B	alpha	1097.100 Da	2.44E+06		47.48	alpha
		alpha	1108.200 Da	2.06E+07			
		alpha	1122.300 Da	2.11E+06			
		alpha	1136.400 Da	3.01E+07			
		alpha	1150.000 Da	1.28E+07			
		alpha	1164.200 Da	7.10E+07			
		alpha	1178.200 Da	5.34E+06			
		alpha	1192.200 Da	3.97E+07	6.34E+07		
		keto	1209.200 Da	3.21E+06		8.98	keto
		keto	1236.300 Da	3.32E+06			
		keto	1264.300 Da	5.69E+06			
		keto	1308.400 Da	5.81E+06			
		methoxy	1220.400 Da	6.91E+06		43.54	methoxy
		methoxy	1252.300 Da	2.76E+07			
		methoxy	1280.300 Da	3.40E+07			
		methoxy	1294.400 Da	4.45E+06			
		methoxy	1323.400 Da	9.67E+05			
		methoxy	1336.400 Da	1.24E+06			
	Batch 4C	alpha	1097.100 Da	1.88E+06		56.04	alpha
		alpha	1108.200 Da	1.06E+07			
		alpha	1122.300 Da	1.83E+06			
		alpha	1136.400 Da	3.09E+07			
		alpha	1150.000 Da	1.01E+07			
		alpha	1164.200 Da	4.38E+07			
		alpha	1178.200 Da	2.73E+06			
		alpha	1192.200 Da	2.15E+07	5.51E+07		
		keto	1209.200 Da	1.48E+06		6.78	keto
		keto	1236.300 Da	2.77E+06			
		keto	1264.300 Da	3.74E+06			
		keto	1308.400 Da	4.23E+06			
		methoxy	1220.400 Da	6.33E+06		37.18	methoxy
		methoxy	1252.300 Da	2.05E+07			
		methoxy	1280.300 Da	2.01E+07			
		methoxy	1294.400 Da	3.48E+06			
		methoxy	1323.400 Da	5.56E+05			
		methoxy	1336.400 Da	7.10E+05			

Sigma-Aldrich	**Sigma-Aldrich MA a**	alpha	1097.100 Da	1.86E+05		56.45	alpha
		alpha	1108.200 Da	5.26E+06			
		alpha	1122.300 Da	2.12E+06			
		alpha	1136.400 Da	2.72E+07			
		alpha	1150.000 Da	1.18E+07			
		alpha	1164.200 Da	3.99E+07			
		alpha	1178.200 Da	3.46E+06			
		alpha	1192.200 Da	2.09E+07			
		keto	1209.200 Da	1.30E+06	4.82E+07	13.45	keto
		keto	1236.300 Da	4.14E+06			
		keto	1264.300 Da	6.48E+06			
		keto	1308.400 Da	3.05E+06			
		methoxy	1220.400 Da	8.57E+06		30.10	methoxy
		methoxy	1252.300 Da	1.45E+07			
		methoxy	1280.300 Da	1.24E+07			
		methoxy	1294.400 Da	2.71E+06			
		methoxy	1323.400 Da	5.95E+05			
		methoxy	1336.400 Da	6.38E+05			
	Sigma-Aldrich MA b	alpha	1097.100 Da	2.15E+05		46.36	alpha
		alpha	1108.200 Da	9.51E+06			
		alpha	1122.300 Da	1.90E+06			
		alpha	1136.400 Da	2.11E+07			
		alpha	1150.000 Da	1.39E+07			
		alpha	1164.200 Da	6.27E+07			
		alpha	1178.200 Da	6.32E+06			
		alpha	1192.200 Da	3.42E+07			
		keto	1209.200 Da	2.57E+06	4.55E+07	17.82	keto
		keto	1236.300 Da	4.08E+06			
		keto	1264.300 Da	8.11E+06			
		keto	1308.400 Da	3.03E+06			
		methoxy	1220.400 Da	7.54E+06		35.82	methoxy
		methoxy	1252.300 Da	1.63E+07			
		methoxy	1280.300 Da	1.77E+07			
		methoxy	1294.400 Da	2.67E+06			
		methoxy	1323.400 Da	8.00E+05			
		methoxy	1336.400 Da	7.30E+05			
	Sigma-Aldrich MA c	alpha	1097.100 Da	1.83E+05		56.27	alpha
		alpha	1108.200 Da	5.01E+06			
		alpha	1122.300 Da	1.72E+06			
		alpha	1136.400 Da	2.32E+07			
		alpha	1150.000 Da	1.09E+07			
		alpha	1164.200 Da	4.06E+07			
		alpha	1178.200 Da	3.31E+06			
		alpha	1192.200 Da	2.02E+07			
		keto	1209.200 Da	1.26E+06	4.12E+07	13.17	keto
		keto	1236.300 Da	3.32E+06			
		keto	1264.300 Da	5.43E+06			
		keto	1308.400 Da	2.45E+06			
		methoxy	1220.400 Da	6.70E+06		30.56	methoxy
		methoxy	1252.300 Da	1.26E+07			
		methoxy	1280.300 Da	1.12E+07			
		methoxy	1294.400 Da	2.21E+06			
		methoxy	1323.400 Da	5.33E+05			
		methoxy	1336.400 Da	4.97E+05			
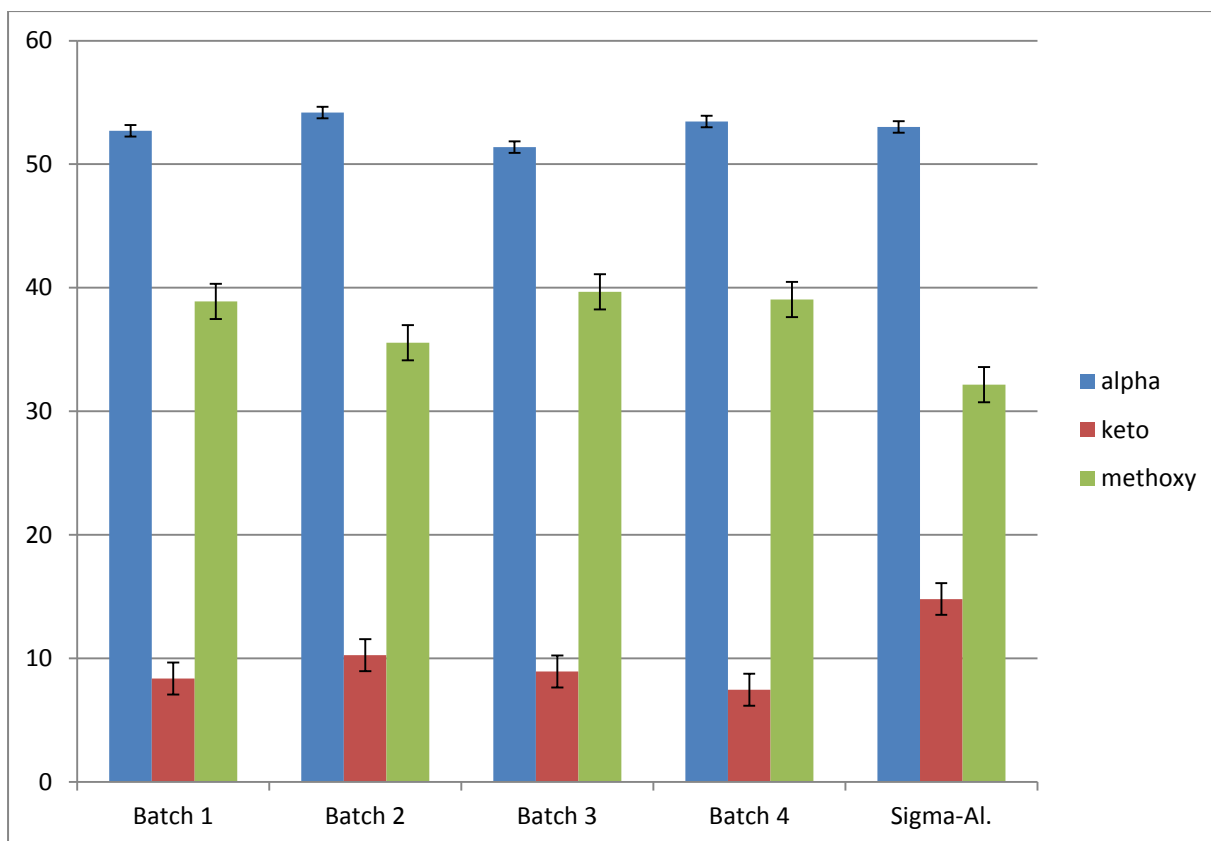
Figure 2.20: Ratios of α-, keto- and methoxy- MA subclasses of *M. tb* and commercially available *M. bovis* extracts revealed an average ratio of 53:8:38 for *M. tb* and 53:15:32 for *M. bovis* respectively.

Table 2.6: Summary of the percentage ratio determination between all four self-prepared batches of MAs and the commercially available MA extract.

Mean MA class percentage					
	Batch 1	Batch 2	Batch 3	Batch 4	Commercial MA
α-MA	53	54	51	53	53
keto-MA	8	10	9	7	15
methoxy-MA	39	36	40	39	32

2.7 Conclusion

Using negative ion mode with ESI ionisation it was possible to identify more than 20 different compounds with masses that match those of known MA that have previously been identified in MA extracts from *M. tb* during infusion experiments. This could quantify the different compounds based on peak height or peak area as seen from infusing different concentrations of the mixture of MA. This gave the basis of the precursor masses to select when scanning the LC eluent of an LC-MS/MS separation where the resolution of m/z for compounds with overlapping isotopic distribution could be identified and quantitated because of the retention time differences. These parameters could be used to characterise the individual compounds and to provide differentiating characteristics for compounds with less than two mass unit differences.

It was shown that chromatography based methods can be used effectively for targeted lipidomics where identification and quantitation of different MA classes was performed, allowing the determination of the ratios between the three MA classes in extracts from different mycobacterial growth conditions or species. The differences between MA class ratios are subtle in closely related mycobacterial species, but these can be accurately determined using effective LC coupled to a tandem mass spectrometer MS/MS. With a reproducible and robust sample preparation method coupled to a highly reproducibility analytical technique small class differences can be identified.

The traditional approach of performing a direct infusion of extractable lipids, followed by a visual comparison of the resulting mass spectral data to differentiate between mycobacterial species has been shown in this study to have potential spectral overlap of different compounds and would therefore be prone to miss-identification and poor quantitative outcomes. By making use of a hyphenated LC-MS method, whether an MRM or a Q1 precursor ion based method, the additional retention time information can resolve compounds of identical or similar mass thereby allowing more robust quantitative data for individual compounds within a complex mixture of compounds with similar lipophilicity.

The choice of mobile phase solvents, additives and the LC gradient profile all play a significant role in the efficiency of the final method used to resolve a mixture of MA molecules. A long, slow gradient is required to resolve these compounds which co-elute

when using shorter gradients and which provide an elution of overlapping peaks of compounds with similar lipophilicity as is the case of the long chain MA despite the increasing carbon number. There needs to be efficient and reproducible chromatographic resolution to be able to accurately integrate individual peaks and to compare single lipid molecules or groups of lipid molecules from extracts of mycobacteria grown under different conditions or extracted from different mycobacterial species.

The long, slow gradient LC method using lipophilic solvents, as developed and optimised in this study, was applied to the HR TOF MS method that was used to compare mass spectral data between drug-susceptible and drug-resistant *M. tb* clinical isolates.

3 Comparative lipidomics of drug-susceptible and drug-resistant *M. tb* clinical isolates.

3.1 Introduction

The emergence of drug-resistant TB was first reported in 1948 when increased resistance to streptomycin was observed in *M. tb* strains that were isolated from sputum samples collected from 12 positively diagnosed TB patients [126]. It was not until the early 1990s that drug-resistant TB began to receive global attention as a major public health threat. Outbreaks of drug-resistant TB were mostly associated with high mortality rates among patients co-infected with HIV [127-131]. Although combinational drug therapy showed promise in countering the emergence of drug resistance [132], patients infected with resistant *M. tb* strains remain less likely to be cured [133].

Drug-resistant TB thus continues to be a global health threat with at least 490 000 cases reported to have emerged in 2016 with an additional 110 000 cases that were reported as susceptible to INH but resistant to RIF treatment (RIF monoresistant *M. tb* (RR-TB)) [7]. The latter type of drug resistance is termed TB monoresistance [134-137]. Additionally and of growing concern is the recent increase in *M. tb* isolates that are susceptible to RIF but resistant to INH treatment (INH monoresistant *M. tb* (IR-TB)) [138-140]. MDR-TB on the other hand is currently defined as *M. tb* that is resistant to at least both RIF and INH [141-143]. As discussed at length in 1.5, MDR-TB requires treatment with a second-line drug treatment regimen.

By using the Xpert® MTB/RIF assay for the simultaneous detection of TB and determination of resistance to RIF [144-149], has shown a growing number of RR-TB cases [150-154]. RR-TB also requires treatment with second-line drugs [155]. The prompt and accurate diagnosis of any type of drug-resistant TB, followed by treatment in line with international standards can prevent deaths and further transmission of the infection [7]. The 2020 and 2025 milestones for reductions in TB incidence and TB deaths set out in the End TB Strategy requires the case fatality ratio to reduce to 10% by 2020 and to 6.5% by 2025 [7]. Early and accurate differentiation between drug-susceptible and drug-resistant TB therefore plays a crucial role in determining the correct treatment regimen for an infected TB patient.

3.2 Objectives

This chapter describes a comparative lipidomic study in which two different sample preparation methods were employed on identical cultures of isolated clinical resistant *M. tb* strains. The *M. tb* isolates under study were previously genotype-confirmed (with the Hain GenoType MTBDRplus® assay) to be either:

A. susceptible to both INH and RIF (IRS-TB),

B. resistant to INH but sensitive to RIF (IR-TB),

C. resistant to RIF but sensitive to INH (RR-TB) or

D. resistant to both INH and RIF (MDR-MTB).

The lipidomic analysis of ten isolates, grown in triplicate, from each group described above was performed on an LC-q-TOF-MS instrument.

The objectives of the study were to:

1) Identify lipid profiles or markers that can be associated with either mono- or multi-drug resistant *M.tb.*

2) Assess the feasibility of using Kendrick mass defect analyses and/or Van Krevelen analyses to differentiate between main lipid classes.

3.3 Materials, Methods and Procedure

Ten triplicate cultures each of (A) IRS-TB, (B) IR-TB, (C) RR-TB and (D) MDR-MTB *M. tb* strains were each initially isolated from BACTEC® MGIT® liquid culture vessels (Becton, Dickinson and Company, New Jersey, USA). Each primary liquid culture was sub-cultured in triplicate on agar-based Middlebrook 7H11 media (MEDIA-MAGE, Johannesburg, South Africa) for a period of 8 weeks. Apart from the *M. tb* H37Rv strain used for group A, which was sub-cultured from an American Type Culture Collection (ATCC) strain, each sub-cultured resistant strain was initially isolated from a clinical sputum sample.

After 8 weeks of incubation at 40°C in an Economy Oven 40 L (Scientific Engineering (Pty) Ltd, Stormill Ext 10, South Africa) each of the grown cultures, from the groups A, B, C and D

were harvested by collecting two loops of bacterial colonies from each culture plate using 10 µL sterile disposable inoculating loops. Each 2 x ~10 µL collection was made in 10 mL clear glass vials with screwcap neck (O.D. × H × I.D. 22 mm × 45 mm × 12.5 mm, purchased from Merck KGaA, Darmstadt, Germany). Capping after collecting the colonies was made with magnetic screw caps (18 mm thread and silicone septum with septum thickness 1.3 mm, also purchased from Merck KGaA).

Each colony collection was made in two different solvent systems (solution in the 10 mL clear glass vials). The two solvent systems used were:

(I)   2 mL of a 65% potassium hydroxide (KOH), 35% methanol (MeOH) solution - called a saponification reagent [156-158]

(II)   2 mL of double distilled deionized water (ddH$_2$O)

The use of a saponification reagent (I) for colony collection was containing KOH aimed at completely hydrolysing the bacterial cellular membrane before further sample preparation for instrumental analysis. The use of (II) was to extract and analyse lipid content in the absence of a hydrolysis reagent which would potentially allow for possible conjugated MA compounds to be analysed and identified.

After harvesting into (I) and (II) above the collected bacterial cells were denatured by autoclaving at 121°C for 1 hour and allowed to cool for 12 hours to reach room temperature (25°C). The cooled 10 mL sample vials were then stored at 4°C until further sample preparation was required for LC-q-TOF-MS analysis.

In preparing each sample for LC-q-TOF-MS analysis, a solution of hydrochloric acid (HCl) pH 4.4 was prepared and 3 mL dispensed into each 10 mL vial from (I) to acidify the contents. For both sample collection methods ((I) and (II)), 3 mL of a chloroform:methanol (CHCl$_3$:MeOH) (1:1, v/v) solution was dispensed into each 10 mL vial. All samples were then vortex mixed for 1 min and allowed to phase separate for 30 minutes at 22°C (preparation here was done in a Bioflow cabinet where the inside temperature was recorded at 22°C).

One millilitre of the heavier CHCl$_3$ phase, which remained at the bottom of the 10 mL vials, was transferred to a 5 mL glass tube using a GILSON® 1 mL micropipette. Each CHCl$_3$ extract was then dried down completely under a gentle stream of nitrogen in a Thermo Scientific™

Reacti-Vap™ Evaporator system for 1 hour at 25°C to ensure complete dehydration. Each dried extract was then reconstituted in 200 μL of CHCl$_3$:MeOH (1:1, v/v), vortex mixed for 30 seconds to ensure complete dissolution, clarified by centrifugation at 16 000 x g for 10 minutes at 21°C and finally 150 μL transferred to 350 μL flat-based glass inserts in 2 mL HPLC autosampler vials (Waters, Millford, USA) for LC-q-TOF-MS analysis (FIGURE 3.1).
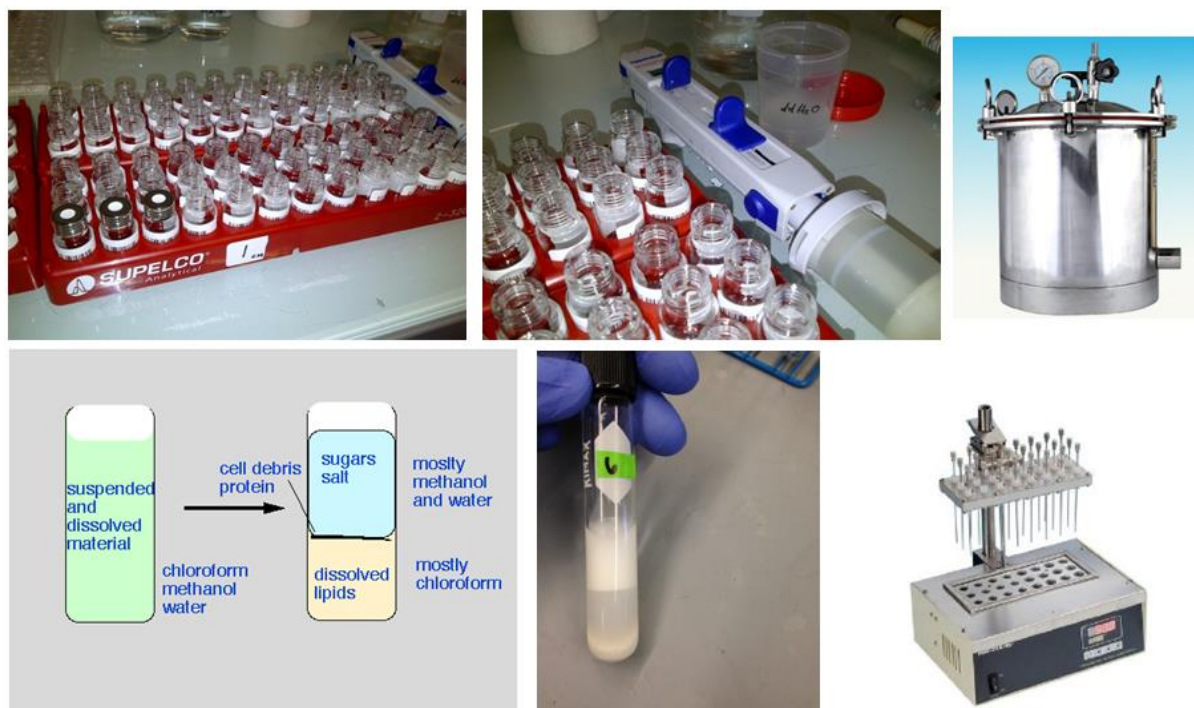
Figure 3.1: Pictorial montage of the sample preparation procedure showing the 10 mL collection vials in top left and middle insets, typical autoclave equipment used at the far right inset, diagram of solvent extraction procedure in the bottom left inset, the heavier CHCl$_3$ phase at the bottom of the 10 mL glass tube that resulted after vortex mixing - shown in the bottom middle inset, and the typical nitrogen drying equipment that was used is shown in the bottom right inset.

The LC-q-TOF-MS analysis was performed on a Waters Synapt G2 UHPLC-TOF-MS/MS. An initial infusion of purified MAs was carried out using the on-board infusion pump system. The infusion was performed at a flow rate of 25 μL/min and ion source and detector parameters were manually optimized (TABLE 2.1). The MS method was setup to only analyse for all precursor ions in each sample and not perform the CID due the major m/z product ions of 367 and 395 being the same for all MA molecules, as found in chapter 2. Upon optimization of the MS parameters it was determined that the positive polarity mode resulted in the highest sensitivity.

Table 3.1: Manually optimized MS conditions on Waters Synapt G2 UHPLC-q-TOF-MS/MS

MS Parameter	Value or Option selected
Acquisition mode	Resolution mode (centroid)
Capillary	1.5 kV
Sampling cone	30 V
Extraction cone	5 V
Source temperature	300 °C
Desolvation gas temperature	500 °C
Desolvation gas flow	800 L/h
Cone gas flow	50 L/h
Lock spray	m/z 922.009798 (+ ion) [ESI-L Low Concentration Tuning Mix 100mL, Agilent and Supelco Analytical]
Scan range	m/z 50 to 3000
Scan time	0.3 s
Calibration	Sodium Iodide

For the LC method it was decided to employ a similar gradient to that used previously (TABLE 2.3) in order obtain adequate separation of lipid molecules from different classes. Mobile phase A contained MeOH with 10 mM ammonium acetate and 0.1% formic acid; mobile phase B contained $CHCl_3$:MeOH (1:1) with 10 mM ammonium acetate and 0.1% formic acid. A Supelco Discovery C_{18} (150 x 4.6 mm with 3 μ m particles) analytical column was again used with a 45 min binary gradient elution method at a total flow rate of 500 µL/min. The LC gradient conditions were set as shown in

TABLE 3.2 and graphically illustrated in FIGURE 3.2.

Total LC Run Time (mins)	Percentage (%) Mobile Phase B
0	50
5	50
25	100
38	100
40	50
45	50
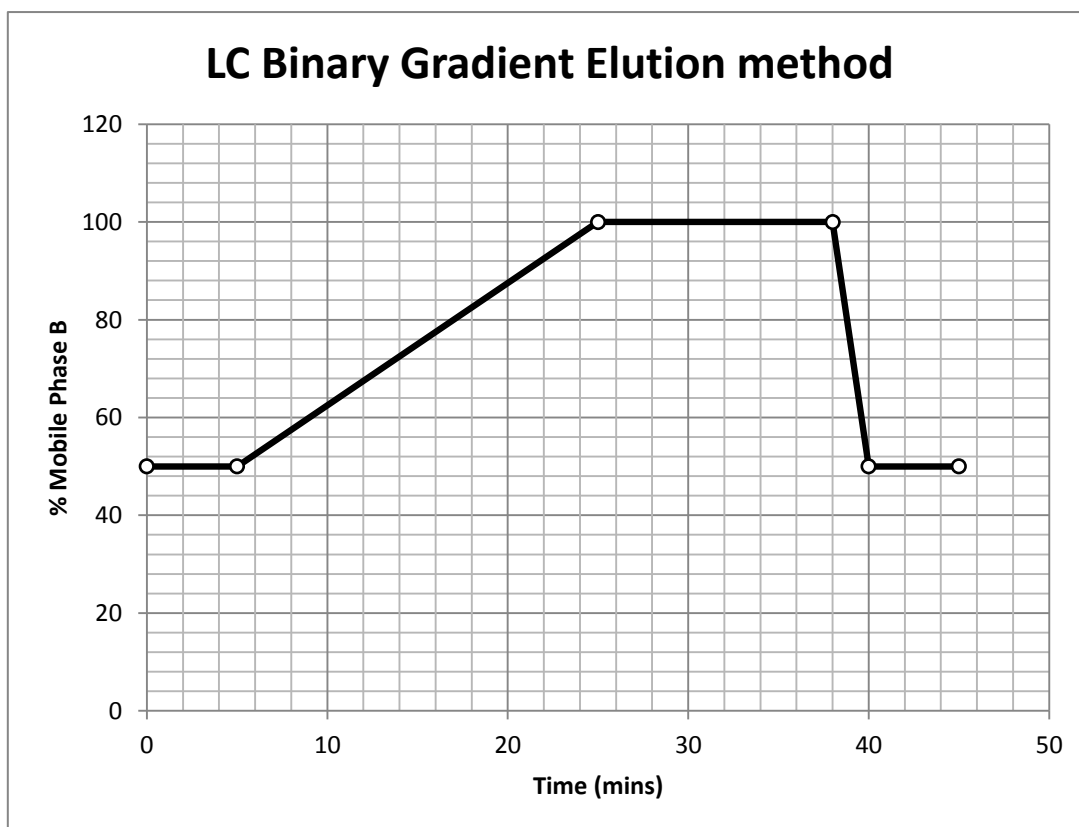
Figure 3.2: LC binary gradient elution method used on the LC-q-TOF-MS/MS (total LC run time vs % mobile phase B).

3.4 Results and Discussion

All samples were analysed as per the triplicate sample collections made and the two types of extraction procedures followed ((I) and (II)). An illustration of the LC-q-TOF-MS method's reproducibility in analysing biological repeats is shown in Figure 3.3 and Figure 3.4.
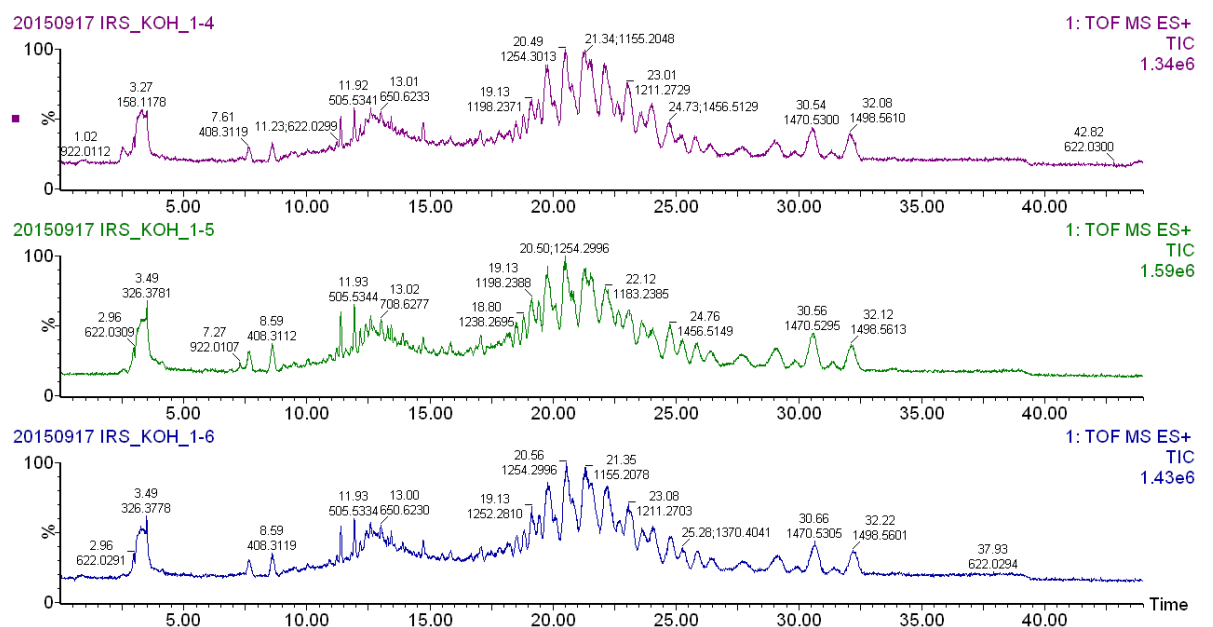
Figure 3.3: Stacked chromatogram of a saponification prepared drug susceptible strain which was grown in triplicate and each triplicate analysed individually, showing a slight shift in retention time, however the chromatographic peak selectivity remained unchanged.
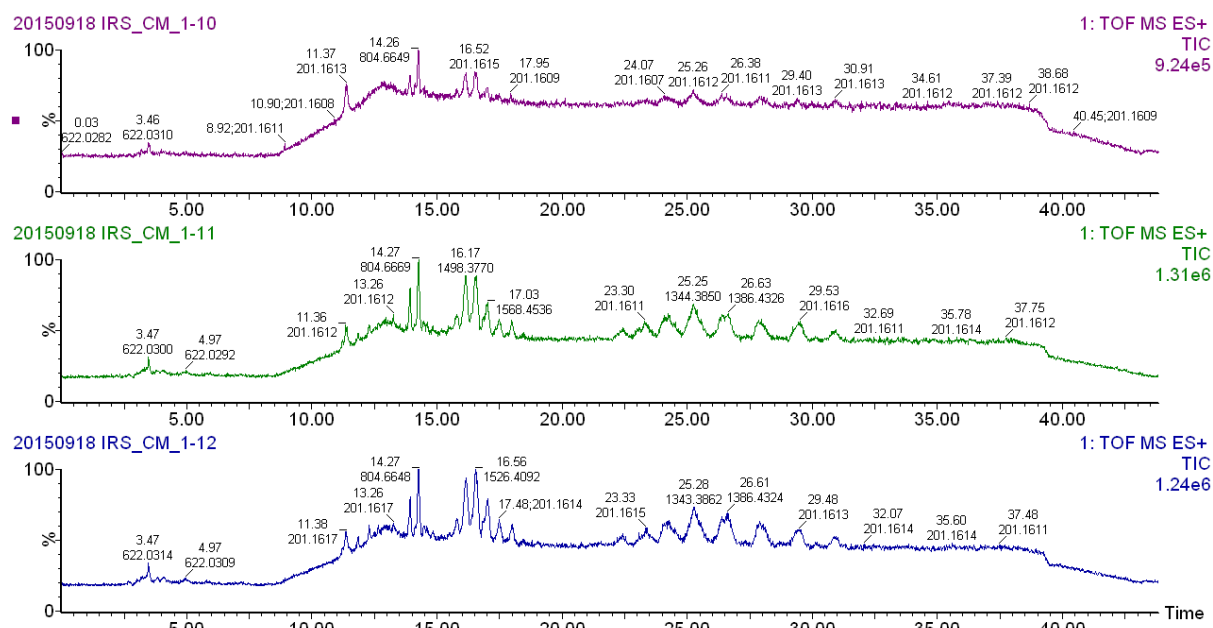
Figure 3.4: Stacked chromatogram of a non-hydrolysis prepared drug susceptible strain which was grown in triplicate and each triplicate analysed individually.

A closer comparison of chromatograms from the same sample that underwent sample preparation methods (I) and (II) showed that several peaks between retention times 15 and 25 minutes, which were observed from using sample preparation method (I), were not present in the chromatograms of samples that underwent sample preparation method (II) (FIGURE 3.5).
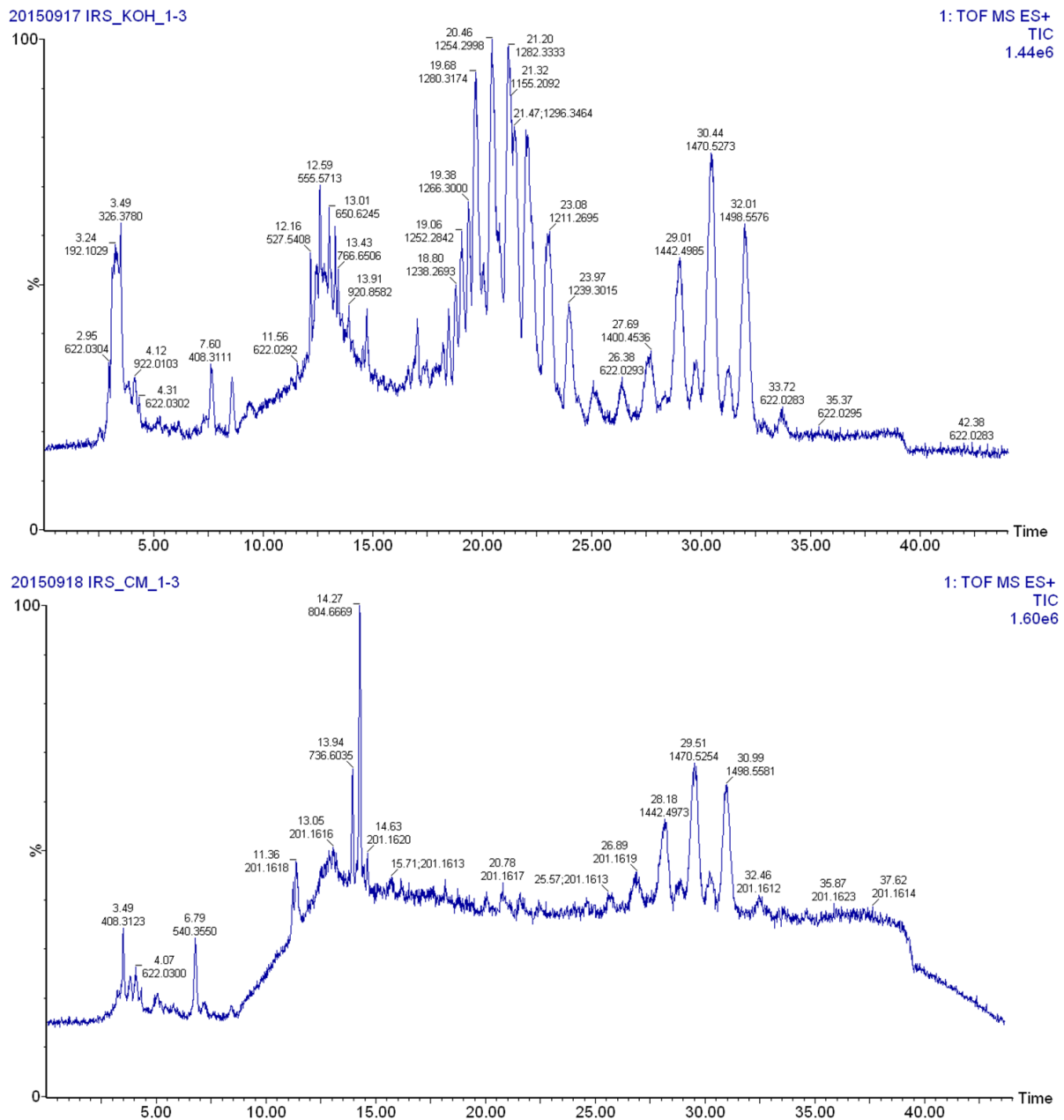
Figure 3.5: Comparison of chromatograms of the same sample which underwent sample preparation method (I) above and sample preparation method (II) below.

A stacked view of chromatograms from a category B sample which underwent sample preparation methods (I) and (II) (**Error! Not a valid bookmark self-reference.**), showed the general absence of eluting lipids after 25 minutes post injection from sample preparation method (I). Similar results were also obtained for samples in category C and D (Figure 3.7 and Figure 3.8 respectively). This possibly indicates that making use of a hydrolysis or saponification reagent can result in altering the chemical structure of the intact lipid molecule and hence alter its interaction with the stationary phase material.
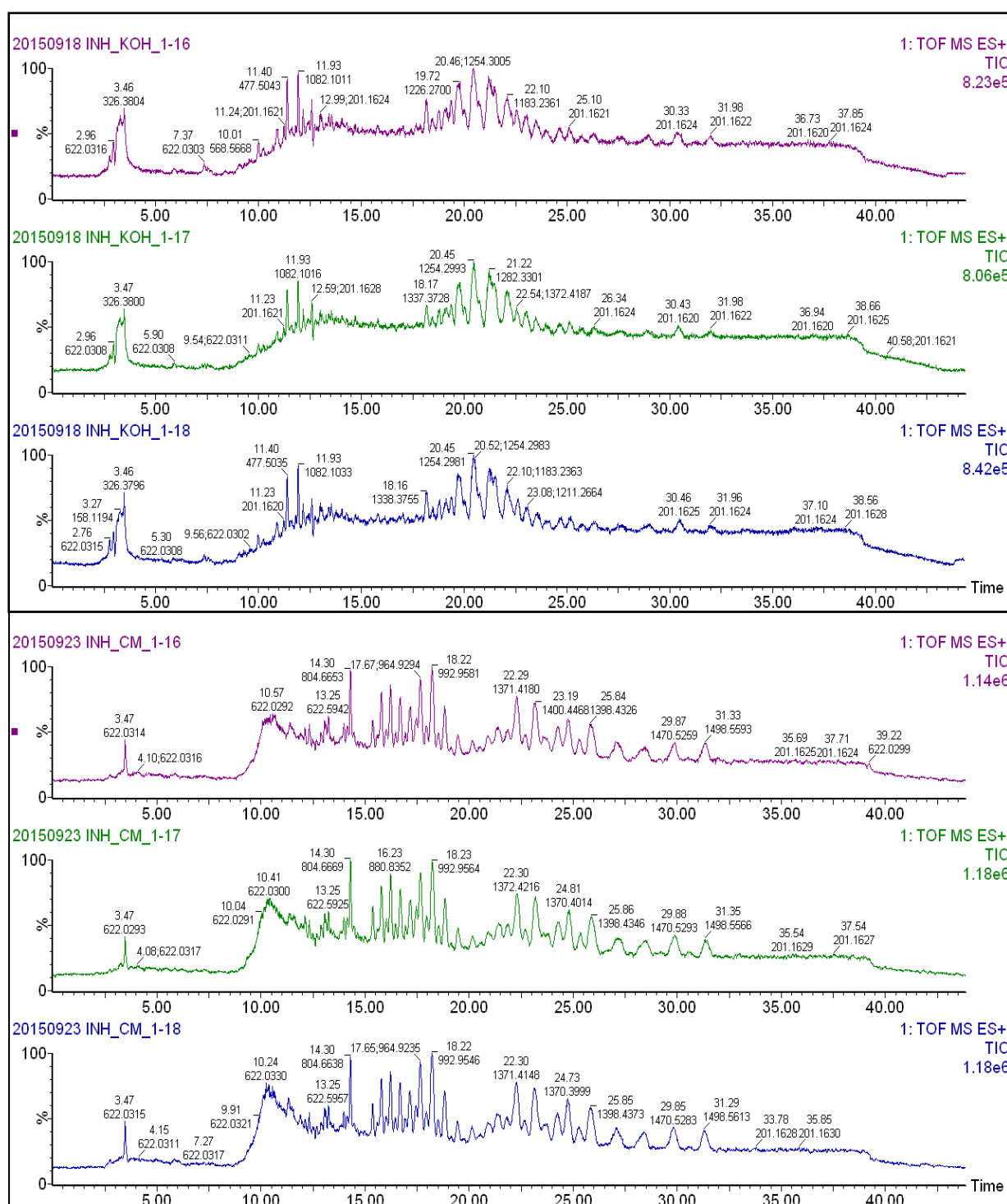
Figure 3.6: A stacked view of all chromatograms of a category B sample which underwent sample preparation methods (I) (top three chromatograms) and (II) (bottom three chromatograms).
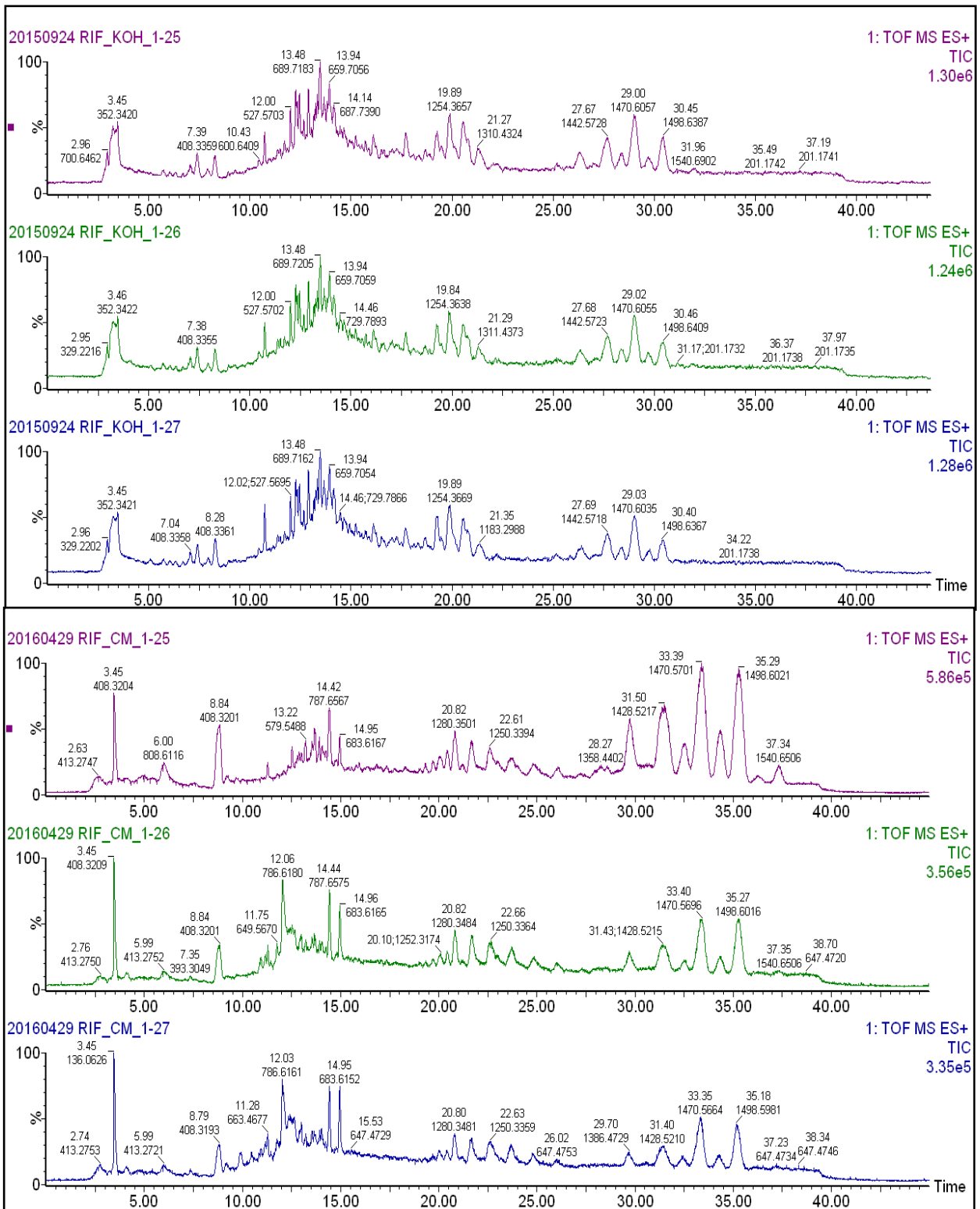
Figure 3.7: A stacked view of all chromatograms of a category C sample which underwent sample preparation methods (I) (top three chromatograms) and (II) (bottom three chromatograms).
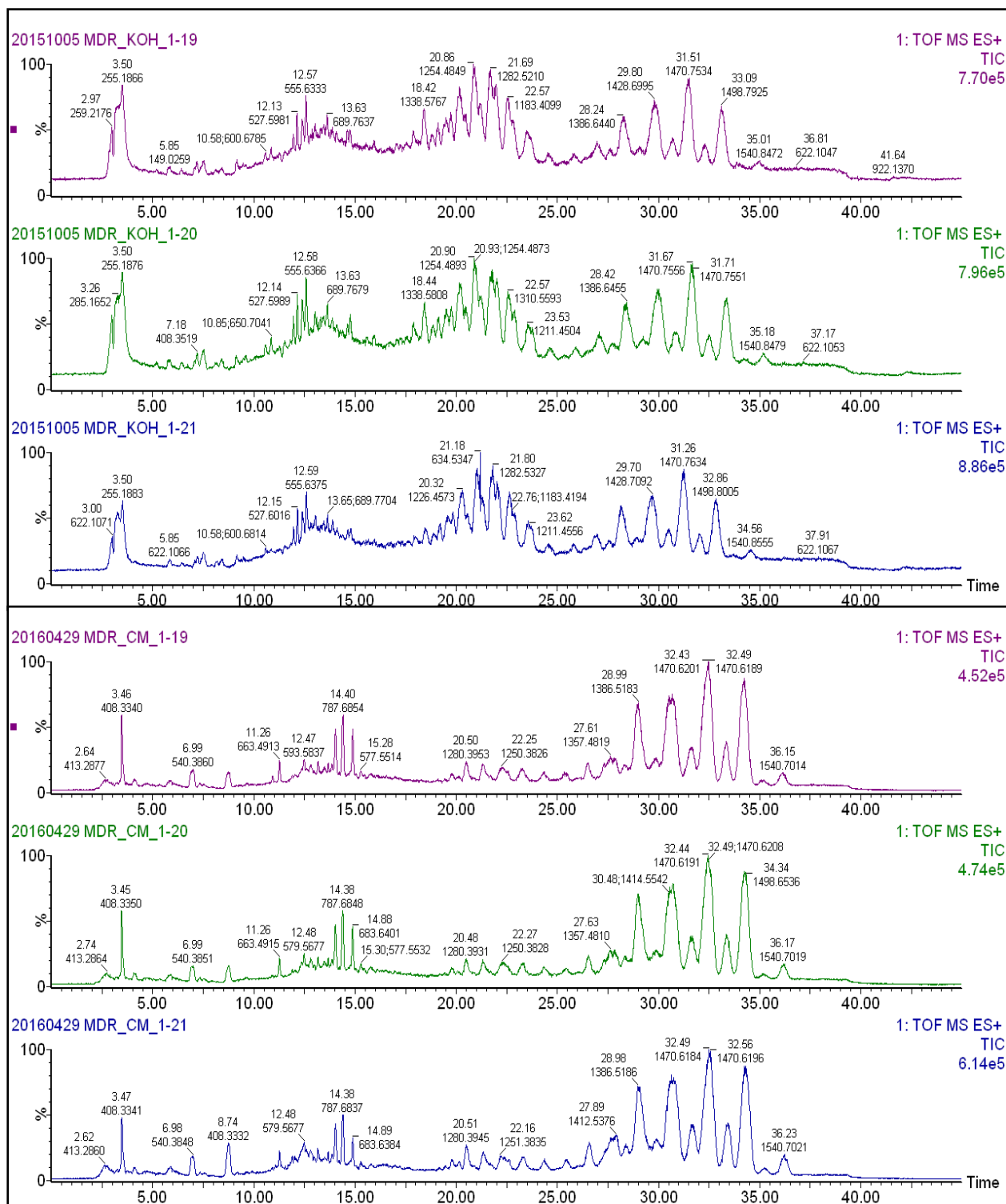
Figure 3.8: A stacked view of all chromatograms of a category D sample which underwent sample preparation methods (I) (top three chromatograms) and (II) (bottom three chromatograms).

Using freely available MS processing software (MZmine version 2.32) each data file could be processed to view either a 2-dimensional (Figure 3.9) or 3-dimensional (Figure 3.10) chromatogram. Both these type of graphical displays can differentiate between different lipid class molecules that elute at similar retention times.
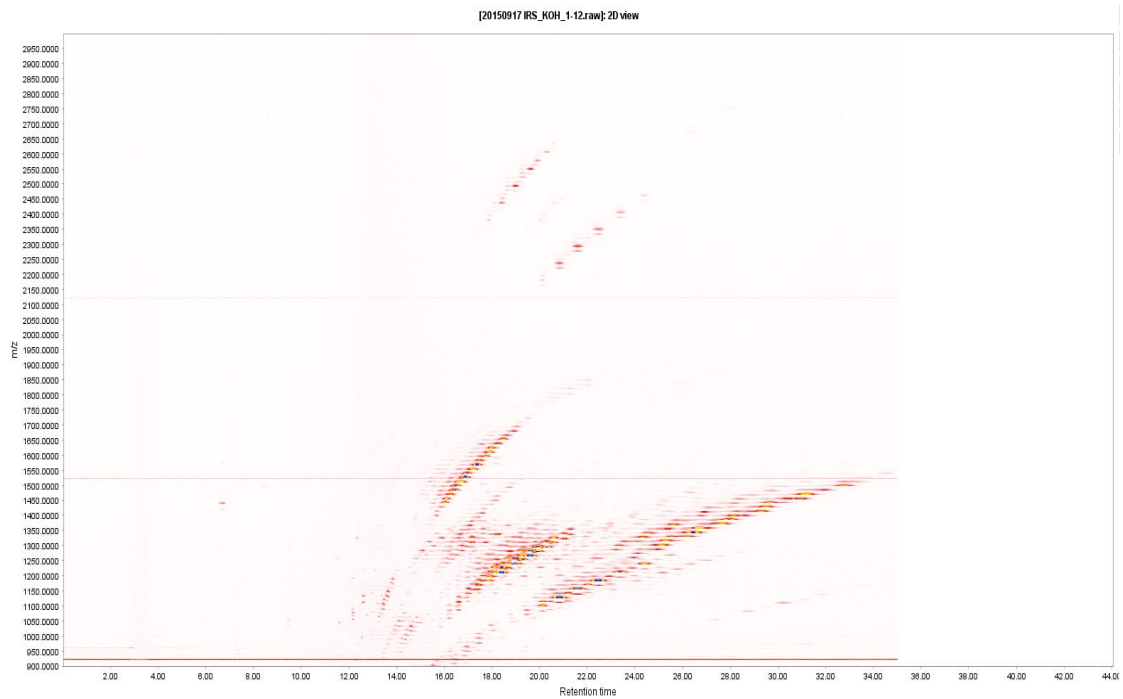
Figure 3.9: 2-dimensional chromatographic visualization of lipids extracted from a drug susceptible strain of *M. tb.*
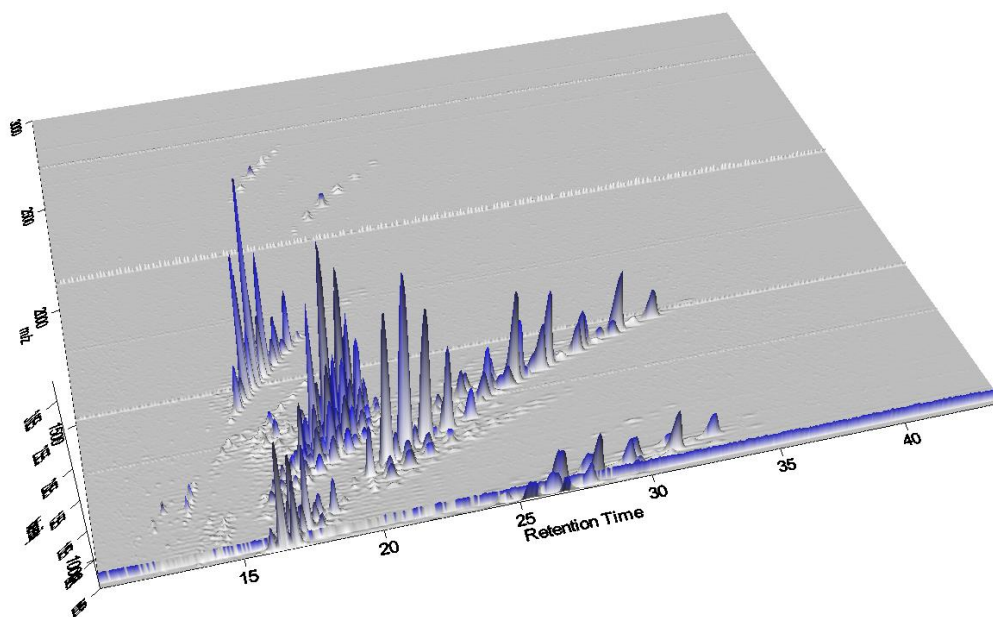
Figure 3.10: 3-dimensional chromatographic visualization of lipids extracted from a drug susceptible strain of *M. tb*.

In processing the resulting chromatograms of each sample from each category a combined mass spectrum in the m/z range 1,000-1,650 was obtained. A comparison of m/z data between each category was inconclusive since there was no unique set of biomarkers that could be found (FIGURE 3.11, FIGURE 3.12, FIGURE 3.13 and FIGURE 3.14). The m/z data can however be carefully de-isotoped using available MS analytical tools, preliminarily identified upon performing a LipidMaps™ or MSLamp™ library search and then compared to each other in a Van Krevelen type diagram () which plots the hydrogen-to-carbon (H/C) ratio against the oxygen-to-carbon (O/C) ratio.
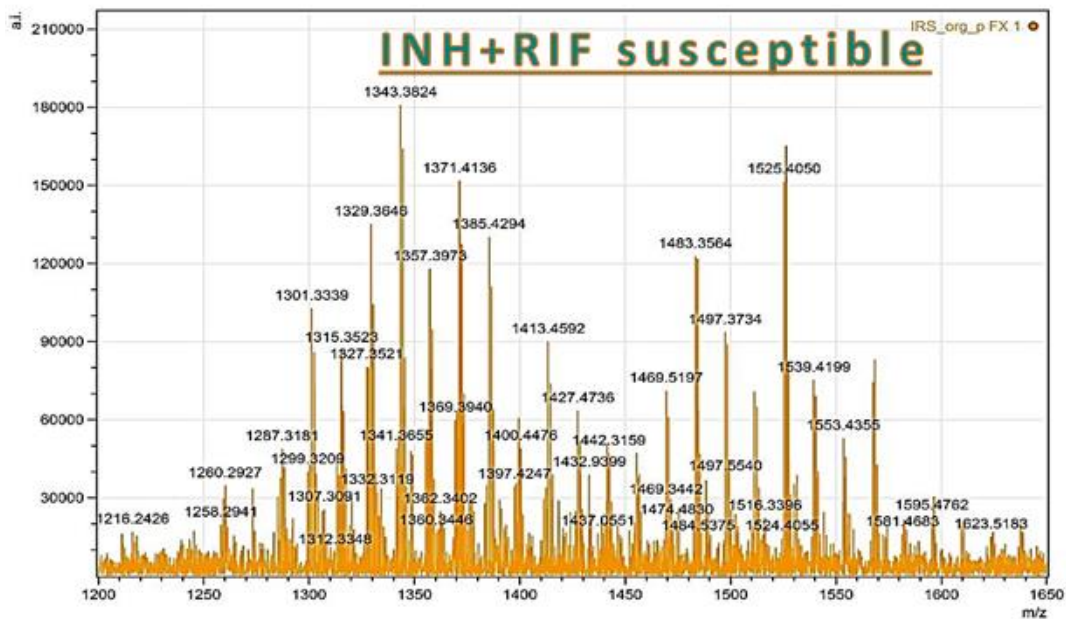
Figure 3.11: Typical combined mass spectrum in the m/z range 1,200-1,650 for a sample from category A (INH and RIF susceptible strain).
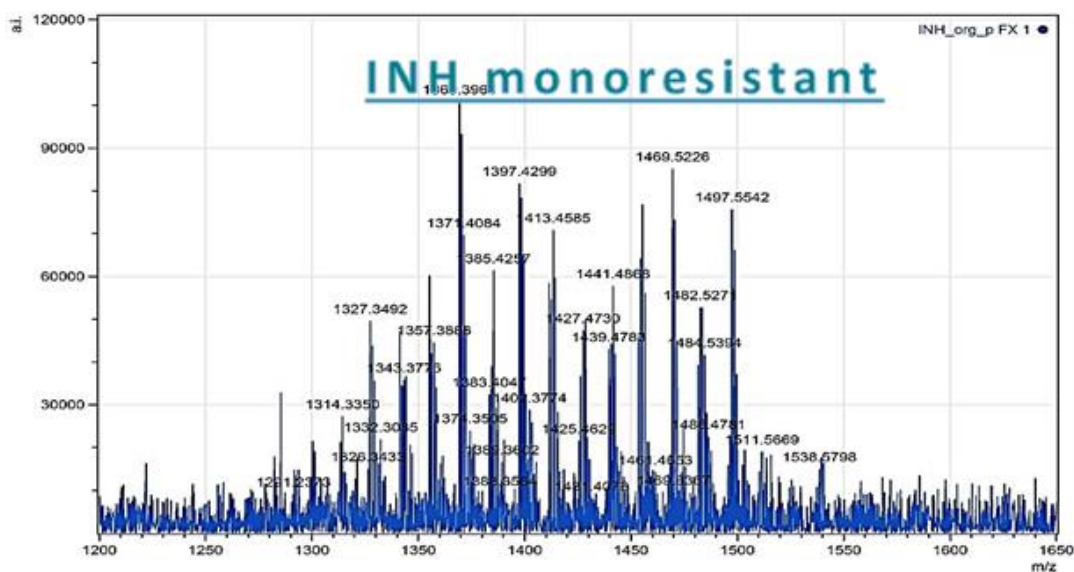
Figure 3.12: Typical combined mass spectrum in the m/z range 1,200-1,650 for a sample from category B (INH mono-resistant strain).
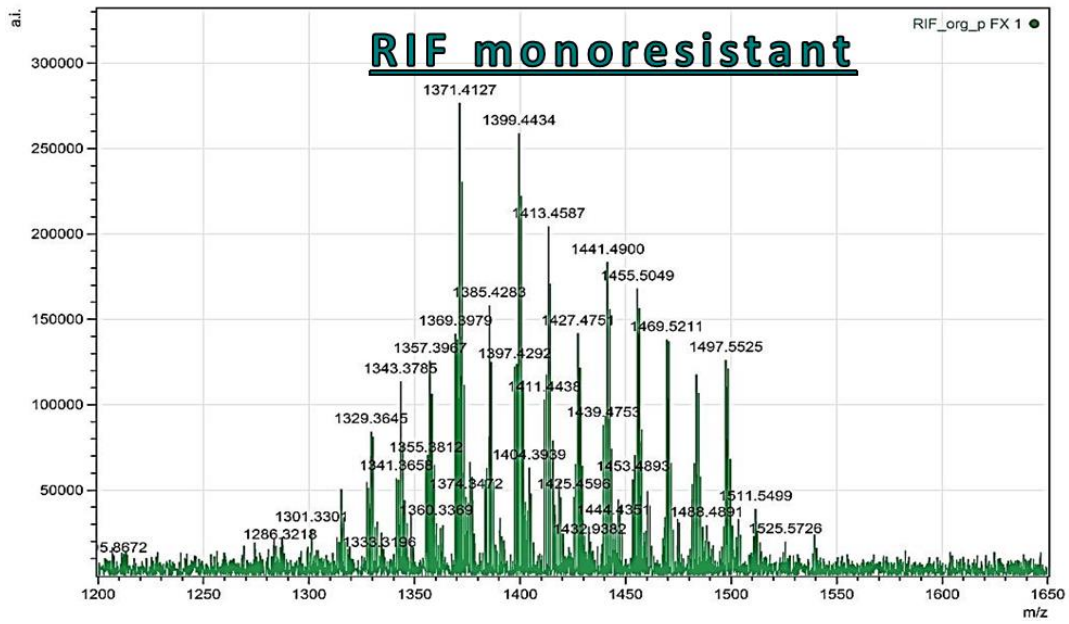
Figure 3.13: Typical combined mass spectrum in the m/z range 1,200-1,650 for a sample from category C (RIF mono-resistant strain).
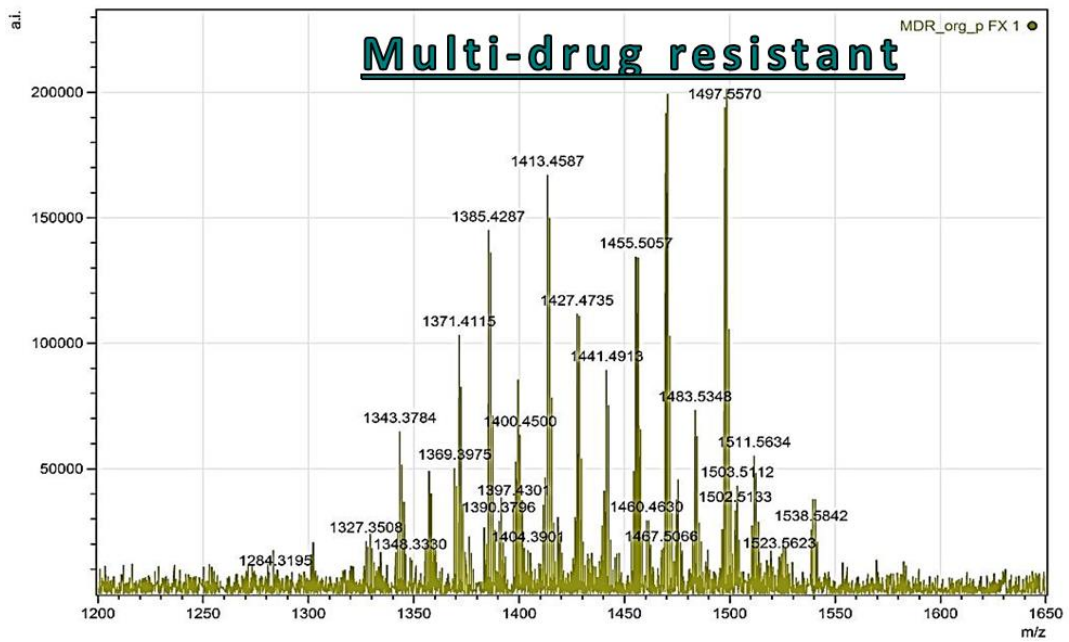
Figure 3.14: Typical combined mass spectrum in the m/z range 1,200-1,650 for a sample from category D (Multi-drug resistant strain).

The m/z data of each analysed sample was processed using the de-isotoping function in MZmine version 2.32 to obtain a Van Krevelen diagram of the H/C ratio against the O/C ratio. Typical Van Krevelen diagrams are shown in FIGURE 3.15 and FIGURE 3.16. The main benefit of using a Van Krevelen diagram to plot the identifiable lipid molecules present in a sample is the ability to further categorize lipids according to their class. Lipid molecules that follow a diagonal linear trend all belong to the same lipid class. For example, upon magnification of the m/z data of MA molecules, a clear distinction between the α-, methoxy- and keto-MAs can be seen FIGURE 3.17.
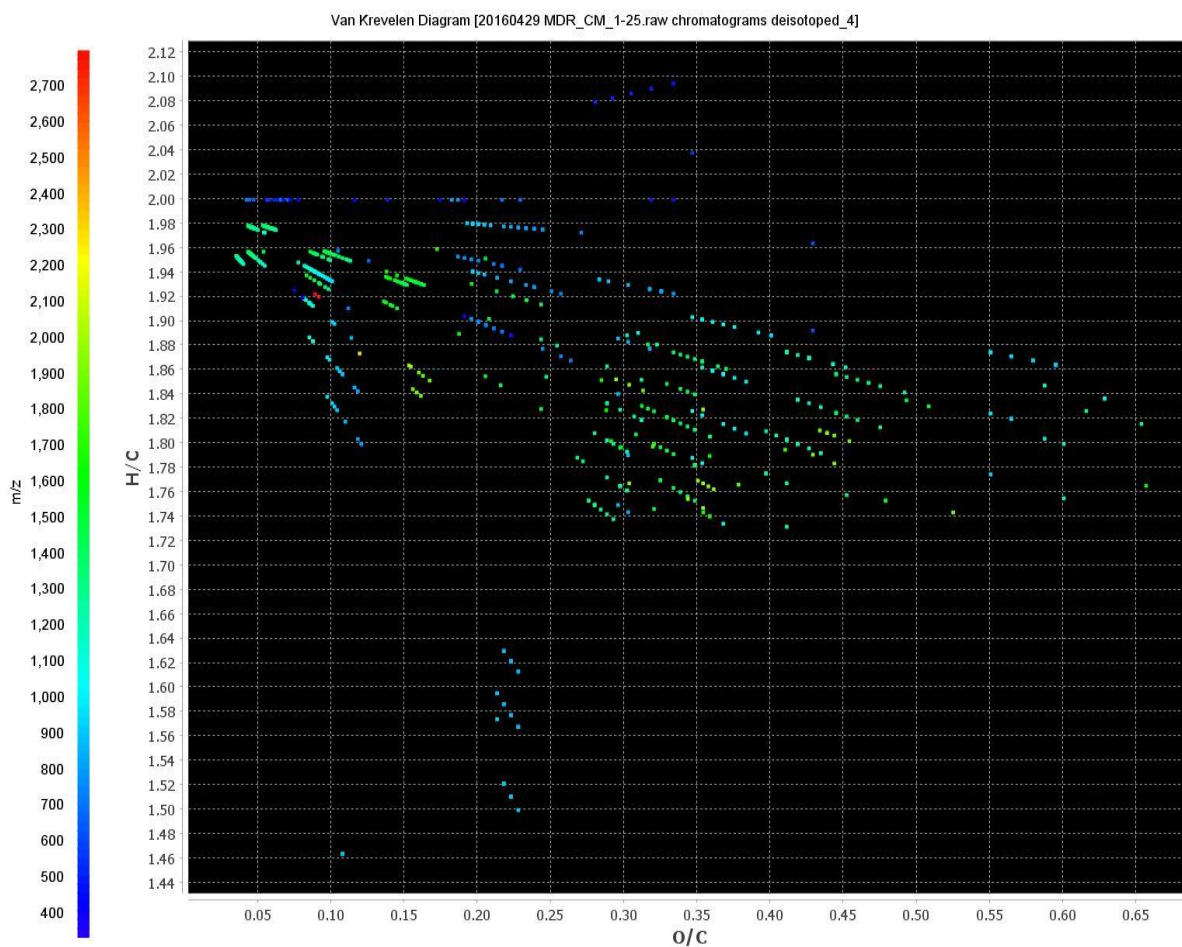
Figure 3.15: Van Krevelen diagram showing the H/C ratio vs O/C ratio in a MDR strain.
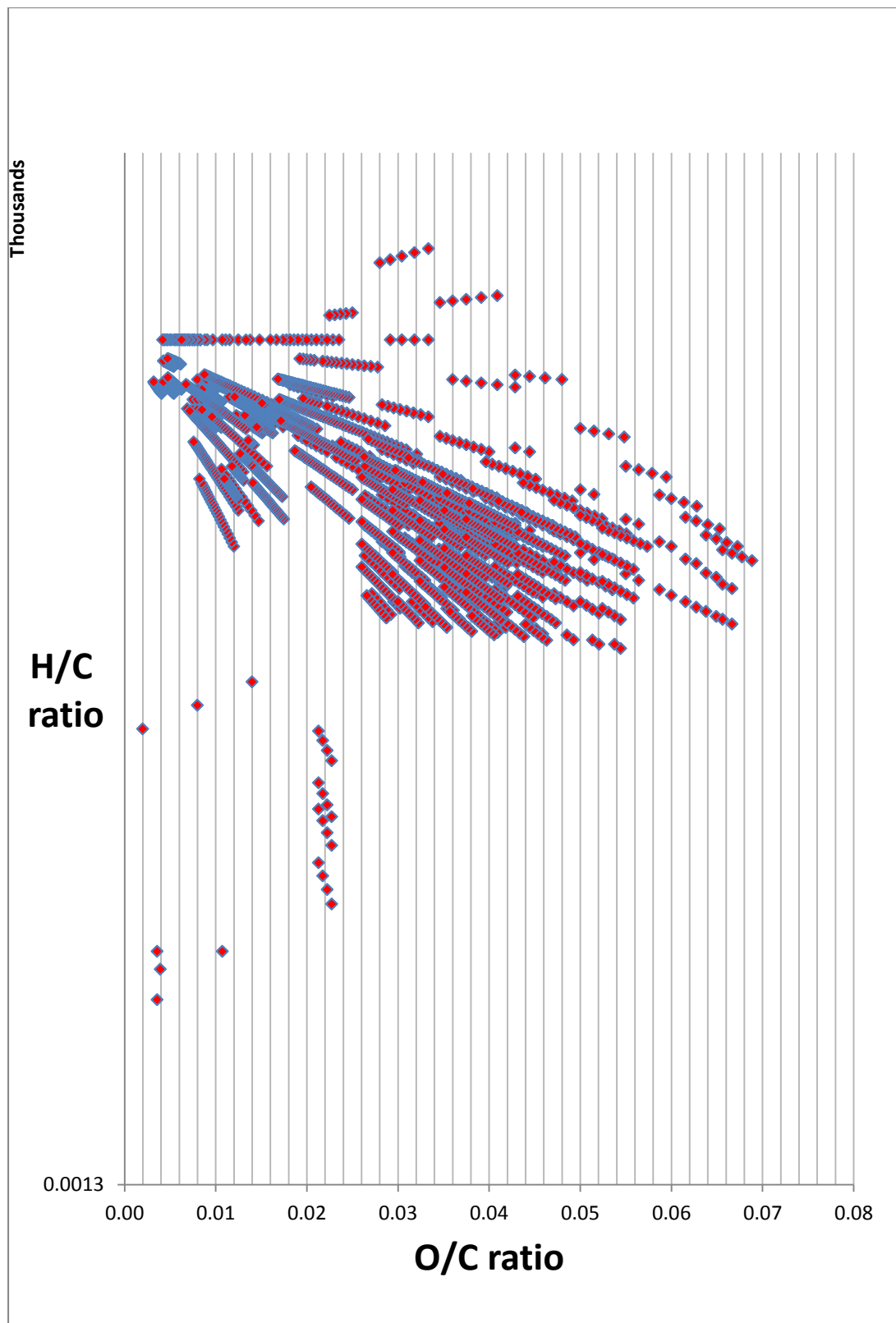
Figure 3.16: : Van Krevelen diagram showing the H/C ratio vs O/C ratio from theoretical m/z data
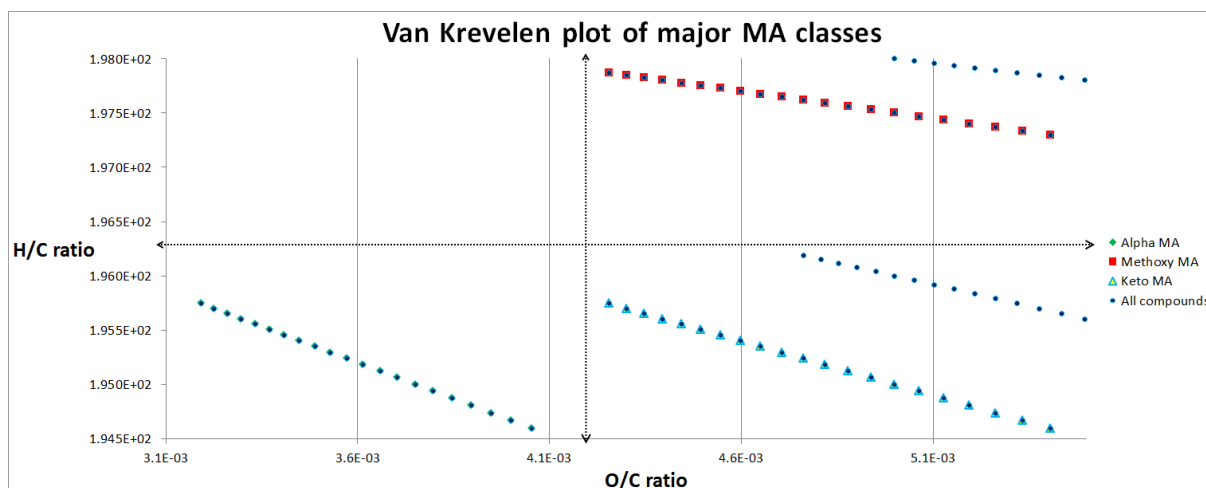
Figure 3.17: Van Krevelen digram of the MA class of molecules showing the H/C ratio vs the O/C ratio.

An alternative analytical tool to visually separate the m/z data obtained for MA subclass molecules or other lipid classes is by making use of calculated Kendrick mass defect analyses. The Kendrick mass is conventionally defined by setting the mass of a chosen molecular fragment, for example CH_2, to an integer value in atomic mass units [159]. It is different from the IUPAC definition, which is based on setting the mass of a ^{12}C isotope to exactly 12 u. The Kendrick mass is often used to identify homologous compounds that differ only by a number of base units in high resolution mass spectra [160]. FIGURE 3.18 shows the calculated Kendrick mass defect vs Kendrick mass for theoretical molecular ion [M-H] m/z values of all naturally occurring α-, methoxy- and keto-MAs. FIGURE 3.19 shows the calculated Kendrick mass defect vs Kendrick mass values in the m/z range 50-2000 for experimentally observed molecular ion [M+NH$_4$] m/z data of all extractable lipid molecules in a sub-cultured MDR patient sample.
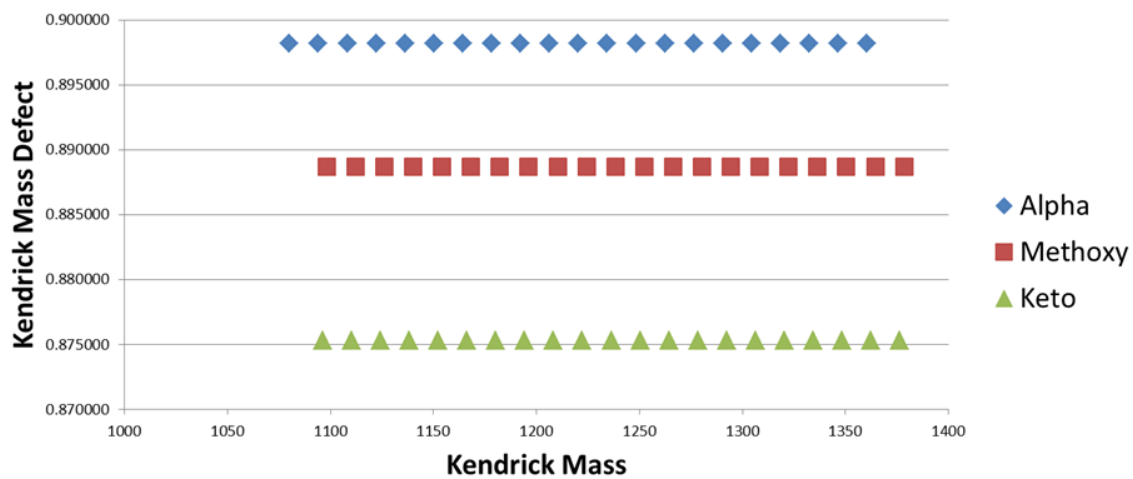
Figure 3.18: Calculated Kendrick mass defect vs Kendrick mass for theoretical [M-H] m/z values of all naturally occurring alpha-, methoxy- and keto-MAs.
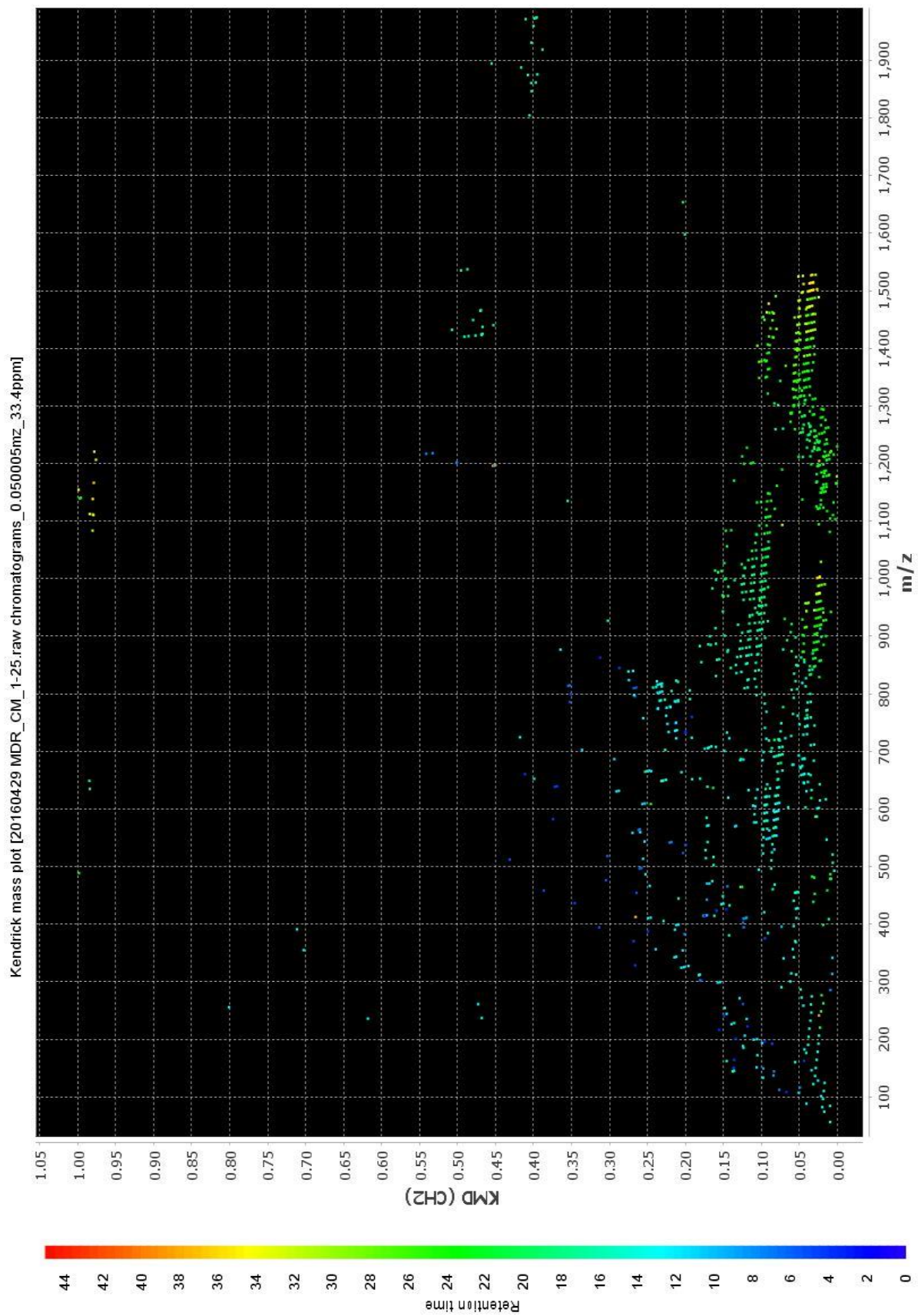
Figure 3.19: Calculated Kendrick mass defect vs Kendrick mass values in the m/z range 50-2000 for theoretical [M+NH4] m/z data of all extractable lipid molecules in a sub-cultured MDR patient sample.

A key finding from the study performed was the difference in m/z data values from the same samples which had undergone both a KOH/MeOH saponification and a detergent-free ddH$_2$O sample preparation method.

3.20 shows a typical comparison of [M+NH$_4$] m/z values in the m/z range 1,000 - 1,700 of a MDR sample from category 4 which had undergone both types of sample preparation methods. This finding was consistent in all the samples analysed from each category.

The main reason for the difference in m/z values can possibly be attributed to a hydrolysis reaction that occurs with larger lipids such as the PDIMs in the KOH/MeOH solvent system. With the KOH/MeOH solvent system essentially performing a detergent function, the exclusion of these chemical additives in a ddH$_2$O type of collection and extraction revealed that there is indeed a hydrolysis reaction taking place when using a KOH/MeOH mixture as a solvent extraction system. Take note that both solvent extraction systems underwent autoclaving at 121°C for 1 hour followed by cooling to room temperature (24°C), acidification with HCl to neutralize the pH and a further chloroform extraction which was then carefully transferred and concentrated by drying with a gentle stream of nitrogen before the LC-q-TOF-MS anlaysis and data collection occurred.

In comparing the m/z data between each sample analysed in triplicate it was found that the most appropriate means of visualizing the data was a two-dimensional gel type of plot using mMass version 5.0 (an open source MS tool) as can be seen in , , and for all samples in category A, B, C and D respectively.

Although similar dominant m/z values can be found across all samples within a category there was no conclusive evidence of there being a distinct biomarker or set of biomarkers which could differentiate one category from another. The m/z values 1371 (+/- 0.05) and 1470 (+/- 0.05) are certainly pronounced in all four categories and could possibly be used in a future diagnostic trial for screening purposes, but their use in distinguishing between drug susceptible and drug resistant TB may require further in depth investigation and a larger sample pool.

It should be significantly noted that this study was performed on patient sample material that had been cultured and further sub-cultured before analytical sample preparation occurred. The study was therefore not performed directly on clinical samples.

Figure 3.20: Comparison of KOH/MeOH to ddH2O solvent extraction systems.
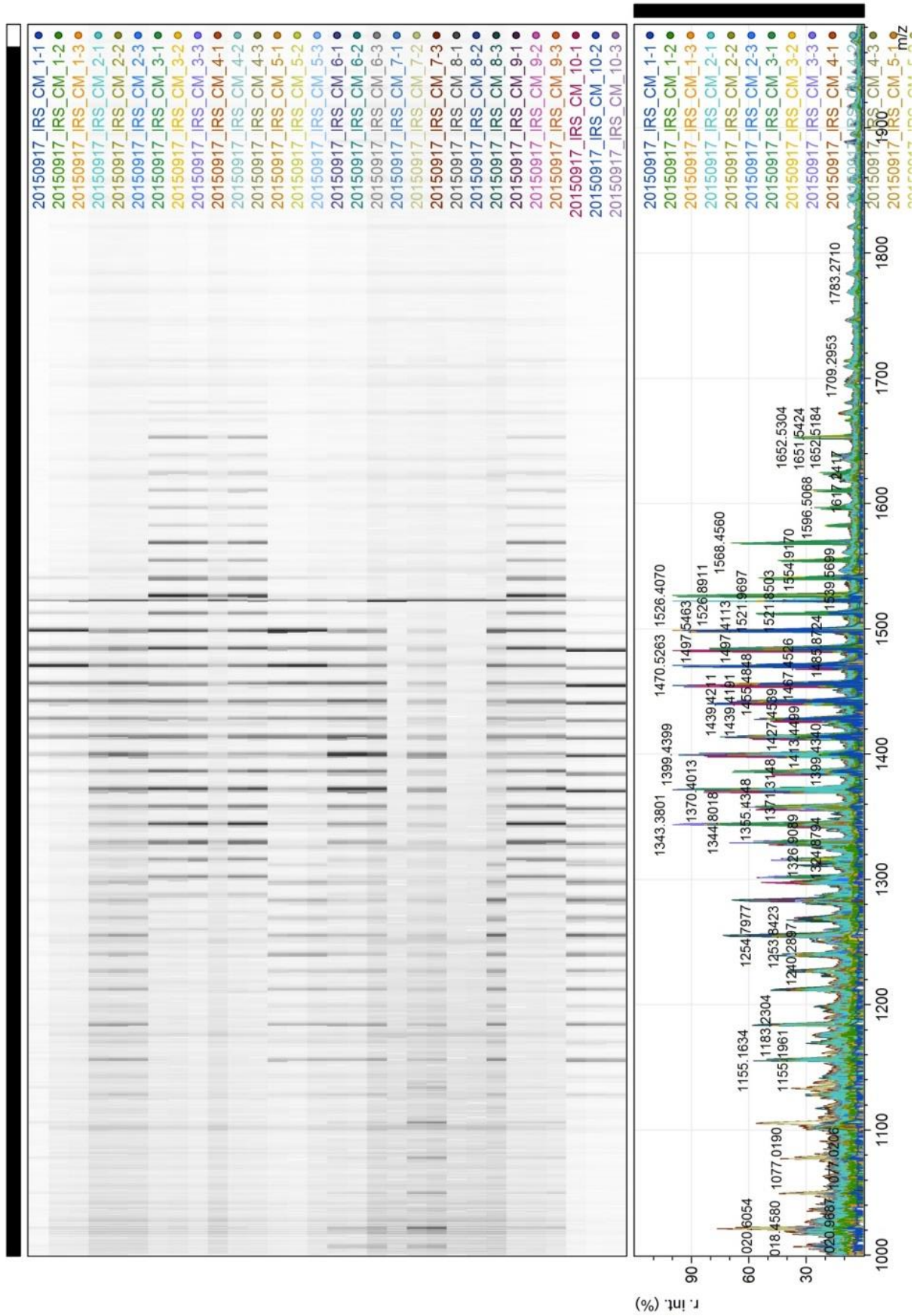
Figure 3.21: 2-dimensional gel type of comparison between all samples analysed in triplicate from category A in the m/z range 1,000-2,000.
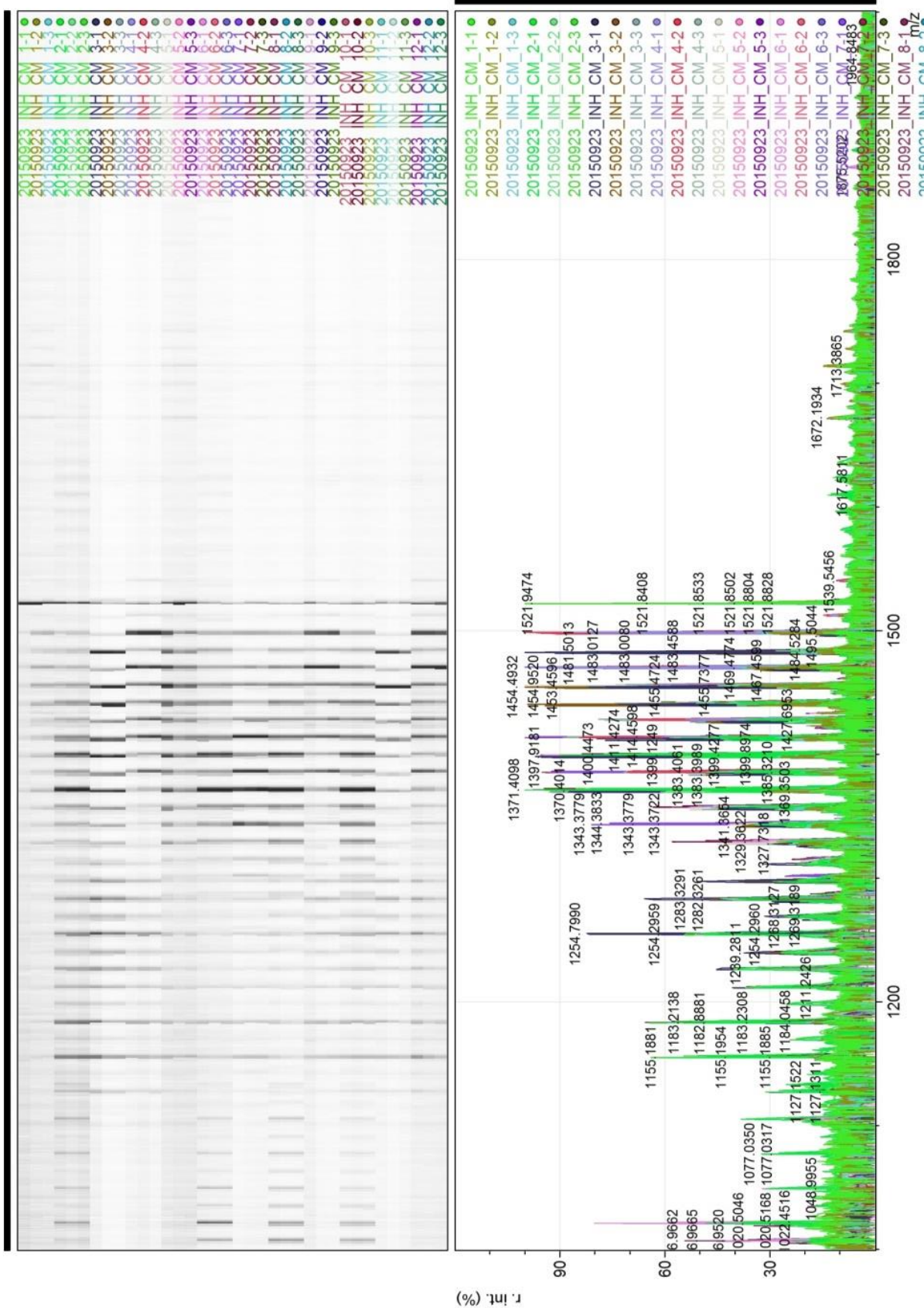
Figure 3.22: : 2-dimensional gel type of comparison between all samples analysed in triplicate from category B in the m/z range 1,000-2,000.
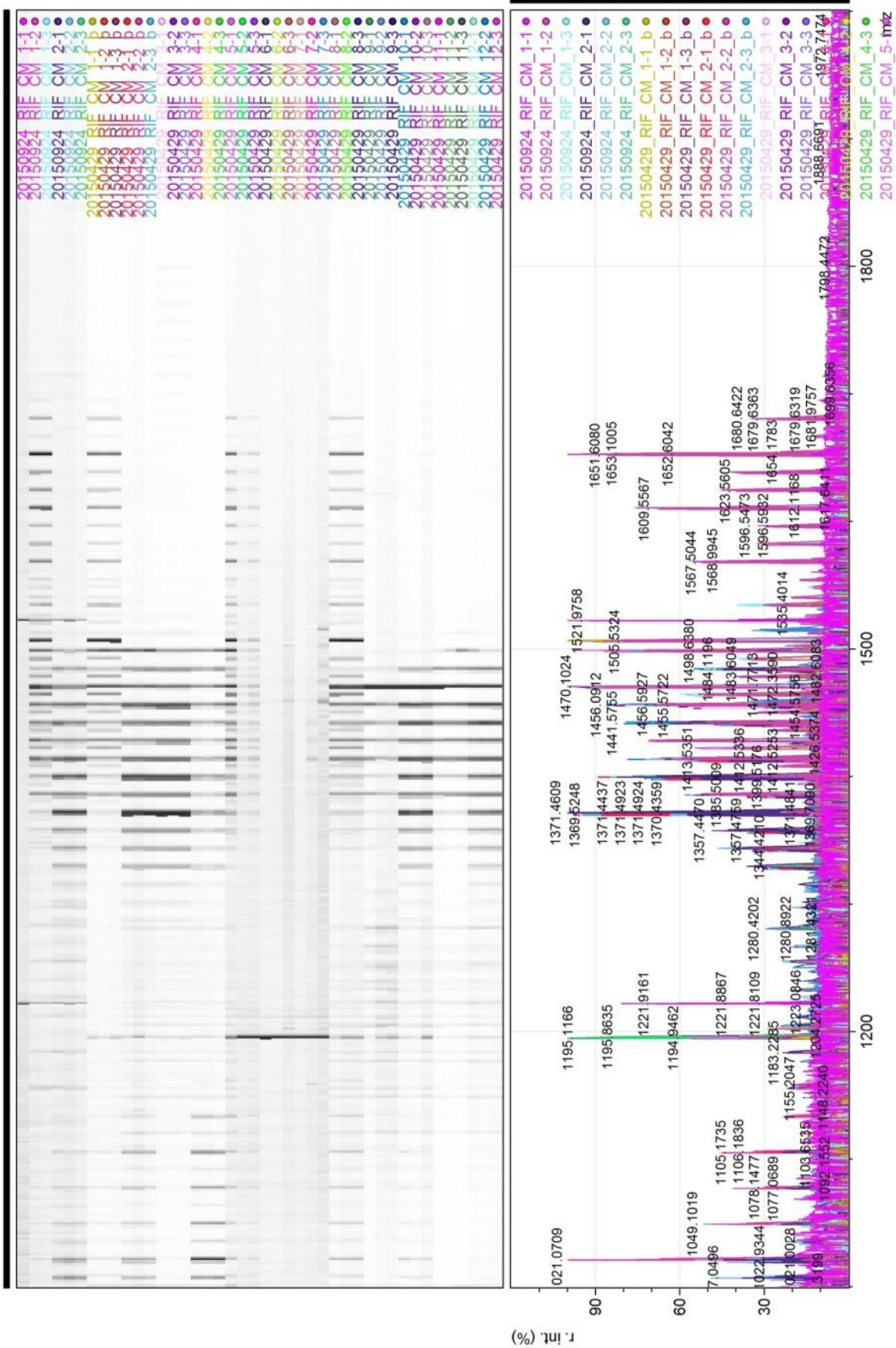
Figure 3.23: 2-dimensional gel type of comparison between all samples analysed in triplicate from category C in the m/z range 1,000-2,000.
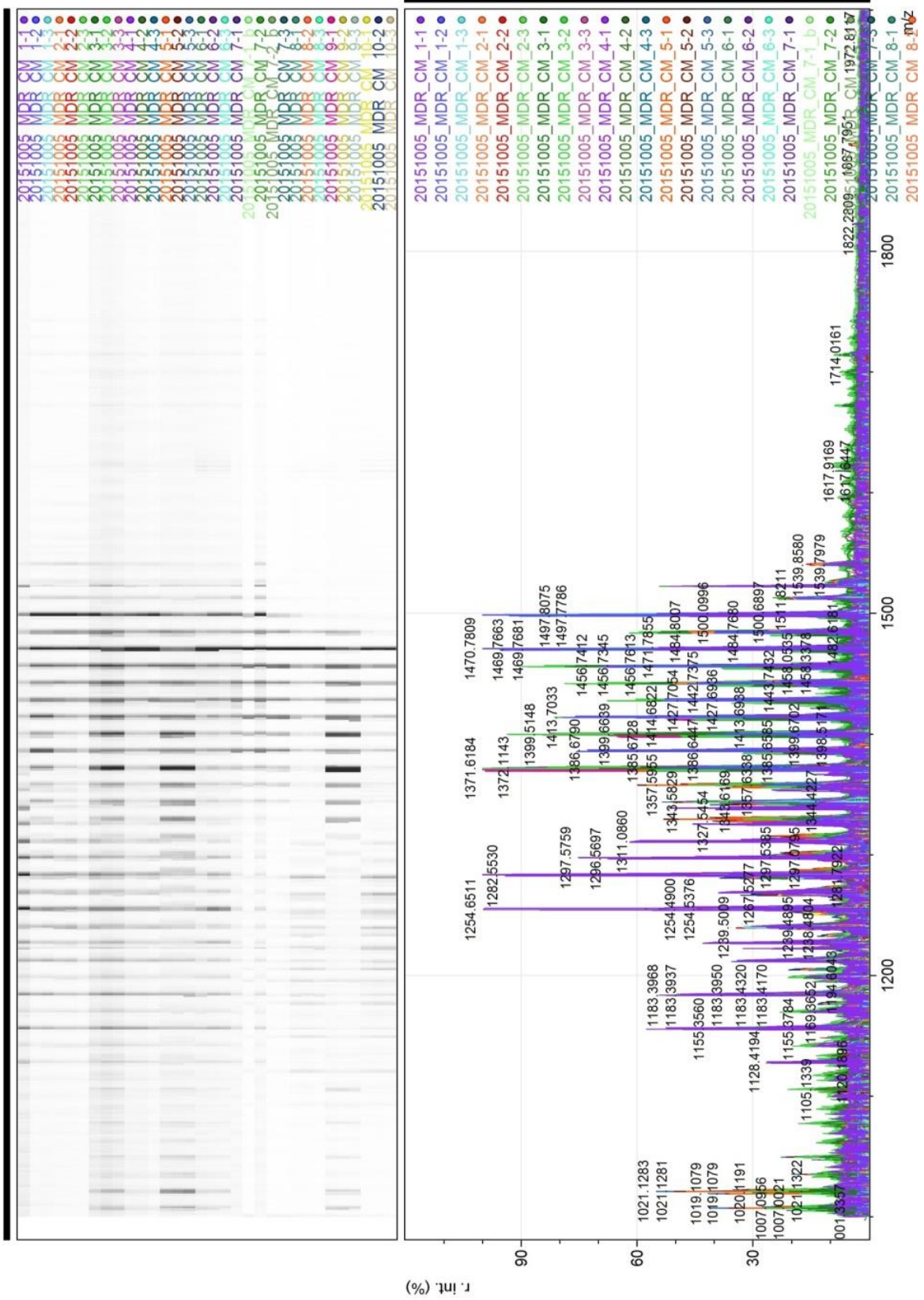
Figure 3.24: 2-dimensional gel type of comparison between all samples analysed in triplicate from category D in the m/z range 1,000-2,000.

3.5 Conclusion

There have been several techniques employed to study the lipid content of *M. tb*'s cellular envelope and these vary from thin layer chromatography [106, 161, 162] to nuclear magnetic resonance [162, 163] to HRMS [53]. HRMS in particular has been largely employed in TB lipidomics [164]. The use of HRMS is ultimately intended to measure the accurate (or exact) mass of a molecule to the fifth or sixth decimal place and thus differentiate it from a molecule with the same nominal (or integer) mass. A nominal mass analyser has a mass resolution of approximately 1 Da or 1 m/z value and can distinguish between m/z values that are around 1 unit apart. Commercially available MS instruments are classified as either nominal or accurate mass resolution type mass analysers.

Structurally related molecules where the nominal mass and subsequent m/z values are similar can overlap in an acquired nominal mass spectrum. These molecules can however be resolved using efficient chromatographic separation before being introduced to the ion source. They can also be further resolved using HRMS in order to obtain an accurate mass for identification purposes. Non-polar lipid molecules tend to ionize inefficiently under atmospheric chemical ionization (APCI) source conditions. The use of electrospray ionization (ESI) sources with appropriate chemical additives to assist in the ionization has been successfully employed in recent lipidomics studies [97, 98, 165].

To conclusively identify and classify lipid molecules when using MS, an accurate or exact mass value is unavoidably required. The use of HRMS techniques in lipidomics studies is therefore crucial for the identification and classification of lipids. HRMS, combined with high efficiency LC techniques, is currently presented with the complex analytical challenge of accurately resolving thousands of mycobacterial lipids in the search for unique biomarkers or even ratios of different lipids that could indicate resistance toward current therapeutics.

The study performed in this chapter revealed significant findings that may require further investigation using a larger sample cohort. The use of Van Krevelen diagrams and Kendrick mass defect analyses showed promise in visually separating closely related lipid subclasses and can be used in future for the exact identification of *M. tb* lipid molecules. These analytical tools unavoidably require HRMS data that is both technically and biologically reproducible.

The difference in m/z data that was obtained from using a detergent-free sample preparation method compared to a detergent-containing (KOH/MeOH) sample preparation method is a key finding that will play a significant role in future *M. tb* lipidomics experimental designs. The possibility that MAs could be formed as a result of adding a detergent to the extraction solvent which causes hydrolysis of larger lipid molecules needs to be carefully considered when interpreting the m/z data obtained from large *M. tb* lipidomic studies.

4   Conclusion

M. tb lipidomics studies that require the use of MS techniques have been at the forefront of TB research in recent times. Through their use of HRMS analysers and interrogative data interpretation Sartain *et al*. [111] and Layre *et al*. [97] have each developed a detailed *M. tb* lipid database for lipid identification purposes. These databases are closely correlated with respect to the mass accuracy and have the potential to be used as reference libraries for the confirmatory presence of TB biomarkers - at thresholds that are yet to be determined from the direct analysis of clinical samples though.

From the study performed in chapter 3 it was shown that by employing two different sample preparation procedures MA molecules may not exist in the cell wall membrane of *M. tb* as an isolated lipid class, but may instead be the result of an alteration of the PDIM lipid class molecules upon performing a saponification (hydrolysis) type of lipid extraction. The latter view has recently been proven to a certain extent in the *M. tb* outer membrane investigations performed by Daffe *et al* [166]. Hence, it is becoming evident that chemically non-reactive extraction procedures are crucially required in analysing and accurately depicting the lipid layer content of the outer membrane of *M. tb*.

The final LC-q-TOF-MS method that was employed for this study analysed for all precursor ions in the m/z range 50-3000. The product ions of MA molecules in particular are not unique to any of their precursor ions. With the higher m/z resolution achievable the LC-q-TOF-MS instrument and the ability to obtain accurate m/z data, all MS analytical tools that

were used to process the m/z data were in an effort to individually identify each eluting lipid molecules monoisotope that could be further processed and shown in 2D or 3D graphic visualizations that take into account m/z value, retention time and m.z intensity.

The study of the outer membrane of *M. tb* plays a significant role in furthering our understanding of the organism's phenotypic expression at a certain point in time and correlating this phenotype to the genotypic profile at that particular time. By connecting the dots between the inherent genotype and the expressed phenotype, we will be able to investigate the detailed biochemical pathway with which *M. tb* expressed its hydrophobic exterior, especially in MDR-TB and XDR-TB cases. The information present in a proposed biochemical pathway, such as the specific enzymes which are required for the upregulation of PDIMa or PDIMb, will be pivotal in developing new anti-TB therapies.

There are also proteins, metallo-proteins and other metabolites that could play a significant role in *M. tb* immune-recognition and immune activity. Hence, there is a dire need for designing "multi-omic" studies of *M. tb* in future. HRMS is already being used extensively in *M. tb* proteomic investigations. Inorganic MS techniques by way of high resolution ICP-MS for example needs to be carefully considered and included in multi-omic approaches in order to obtain useful information on the metal content and its role in efflux mechanisms when *M. tb* starts developing resistance to current and future drug therapies.

Without doubt there still lies an unresolved analytical challenge of chromatographically separating non-derivatized *M. tb* lipids. Although a thorough investigation was carried out into the use of different chemical solvent mixtures with various chemical additives, reverse phase LC performed on conventional C_{18} stationary phase material or even hydrophilic type stationary phase material (not shown here) remains challenging and unfortunately requires long periods and slow flow rates in order to achieve separation of the subtly different *M. tb* lipid molecules.

Nano-flow LC seems a plausible alternative to resolve this but is yet to be reported for *M. tb* lipidomic investigations. Using supercritical CO_2 as a primary mobile phase in combination with HRMS is also yet to be investigated for its usefulness in *M. tb* lipidomic studies. The use of C_{30} type stationary phase material and possibly with two or three analytical columns in series for LC analysis of *M. tb* lipids also needs further investigation.

Developing a lengthy and laborious approach to achieve efficient chromatographic separation of *M. tb* lipids may not be immediately favourable as a diagnostic tool in clinical settings but can certainly add value in multi-omic biochemical studies of the pathogen as we enter the age of antimicrobial resistance and the search for novel alternative medicines to tackle TB.

A preliminary investigation was made post study into the use of long LC runtimes (up to 5 hours per injection) and low flow rates (down to 0.05 mL/min) for analysing a purified MA mixture. The results of using the latter LC parameters showed promise in achieving a clear visual separation between the three main subclasses of MAs upon performing a partitioned ion extraction (XIC) of the TIC chromatogram. Further investigation into the feasibility of this processing technique will need to be carried out using similar LC parameters on a HRMS instrument.

The main aim of this project in developing a selective and sensitive LC-MS/MS method to identify and determine the relative ratios of the α-, keto- and methoxy-MA classes to differentiate between different *Mycobacterium* phenotypes was successfully achieved in differentiating between extracted and purified MAs from *M. tb* and *M. bovis*.

In so doing, we chromatographically separated a mixture of MA molecules and were able to identify the class of each MA molecule by using LC-MS/MS. The ratio between the three main classes of MAs in isolated MA's (*M. tb*) and commercially available MA preparations (*M. bovis*) was shown to be different in both mycobacterial species analysed.

The use of accurate mass data from a q-TOF-MS to classify MA using measured mass defects was shown to be feasible. The assessment of whether *M. tb* lipid fraction profiles determined by LC-MS/MS can be used to identify drug resistant phenotypes as confirmed by genotypic data is inconclusive and may require a mass analyser with resolving power in excess of 100,000 such as a fourier transform-orbitrap MS or a fourier transform ion cyclon resonance MS. Additionally, chromatographic technologies that are capable of resolving non-derivatized complex mixtures of large (C_{60}-C_{100}) nonpolar lipid molecules may require further develepment.

References

1. Zumla A, Petersen E: **The Historic and Unprecedented United Nations General Assembly High Level Meeting on Tuberculosis (UNGA-HLM-TB)-'United to End TB-An Urgent Global Response to a Global Epidemic'.** *International Journal of Infectious Diseases: IJID: Official Publication of the International Society for Infectious Diseases* 2018.

2. Nakajima H: **Tuberculosis: a global emergency.** *World Health* 1993, **46:**3.

3. Herbert N, Sharma V, Masham BS, Sheehan BS, Hauser J, Zumla A: **Concrete action now: UN High-Level Meeting on Tuberculosis.** *The Lancet Infectious Diseases* 2018.

4. Murray JF, Schraufnagel DE, Hopewell PC: **Treatment of tuberculosis. A historical perspective.** *Annals of the American Thoracic Society* 2015, **12:**1749-1759.

5. Wells CD, Cegielski JP, Nelson LJ, Laserson KF, Holtz TH, Finlay A, Castro KG, Weyer K: **HIV infection and multidrug-resistant tuberculosis: the perfect storm.** *The Journal of Infectious Diseases* 2007, **196 Suppl 1:**S86-107.

6. Pawlowski A, Jansson M, Sköld M, Rottenberg ME, Källenius G: **Tuberculosis and HIV co-infection.** *PLoS Pathogens* 2012, **8:**e1002464.

7. Global W: **tuberculosis report 2017.** *World Health Organization Geneva* 2018.

8. Organization WH: **Global TB Report 2017.** *Accessed on 19th March* 2018.

9. Gernaey AM, Minnikin DE, Copley M, Dixon RA, Middleton J, Roberts C: **Mycolic acids and ancient DNA confirm an osteological diagnosis of tuberculosis.** *Tuberculosis* 2001, **81:**259-265.

10. Lee JY: **Diagnosis and treatment of extrapulmonary tuberculosis.** *Tuberculosis and respiratory diseases* 2015, **78:**47-55.

11. Sharma S, Mohan A: **Extrapulmonary tuberculosis.** *Indian Journal of Medical Research* 2004, **120:**316-353.

12. Heemskerk D, Caws M, Marais B, Farrar J: *Tuberculosis in Adults and Children.* Springer; 2016.

13. De Jong BC, Antonio M, Gagneux S: **Mycobacterium africanum—review of an important cause of human tuberculosis in West Africa.** *PLoS Neglected Tropical Diseases* 2010, **4:**e744.

14. Nicas M, Nazaroff WW, Hubbard A: **Toward understanding the risk of secondary airborne infection: emission of respirable pathogens.** *Journal of Occupational and Environmental Hygiene* 2005, **2:**143-154.

15.   Barry CE, Boshoff HI, Dartois V, Dick T, Ehrt S, Flynn J, Schnappinger D, Wilkinson RJ, Young D: **The spectrum of latent tuberculosis: rethinking the biology and intervention strategies.** *Nature Reviews Microbiology* 2009, **7:**845-855.

16.   Gagneux S: **Ecology and evolution of Mycobacterium tuberculosis.** *Nature Reviews Microbiology* 2018, **16:**202.

17.   Murray JF: **History of Tuberculosis and of Warfare.** In *Tuberculosis and War. Volume* 43: Karger Publishers; 2018: 2-19

18.   Todar K: *Todar's online textbook of bacteriology.* University of Wisconsin-Madison Department of Bacteriology; 2006.

19.   Barksdale L, Kim KS: **Mycobacterium.** *Bacteriological Reviews* 1977, **41:**217-372.

20.   **Diagnostic Standards and Classification of Tuberculosis in Adults and Children. This official statement of the American Thoracic Society and the Centers for Disease Control and Prevention was adopted by the ATS Board of Directors, July 1999. This statement was endorsed by the Council of the Infectious Disease Society of America, September 1999.** *Am J Respir Crit Care Med* 2000, **161:**1376-1395.

21.   Neyrolles O, Hernández-Pando R, Pietri-Rouxel F, Fornès P, Tailleux L, Payán JAB, Pivert E, Bordat Y, Aguilar D, Prévost M-C: **Is adipose tissue a place for Mycobacterium tuberculosis persistence?** *PLoS One* 2006, **1:**e43.

22.   Brzostek A, Pawelczyk J, Rumijowska-Galewicz A, Dziadek B, Dziadek J: **Mycobacterium tuberculosis is able to accumulate and utilize cholesterol.** *Journal of Bacteriology* 2009, **191:**6584-6591.

23.   Balabanova Y, Drobniewski F, Nikolayevskyy V, Kruuner A, Malomanova N, Simak T, Ilyina N, Zakharova S, Lebedeva N, Alexander HL: **An integrated approach to rapid diagnosis of tuberculosis and multidrug resistance using liquid culture and molecular methods in Russia.** *PLoS One* 2009, **4:**e7129.

24.   Moure R, Muñoz L, Torres M, Santin M, Martín R, Alcaide F: **Rapid detection of Mycobacterium tuberculosis complex and rifampin resistance in smear-negative clinical samples by use of an integrated real-time PCR method.** *Journal of Clinical Microbiology* 2011, **49:**1137-1139.

25.   Anochie PI, Onyeneke EC, Ogu AC, Onyeozirila AC, Aluru S, Onyejepu N, Zhang J, Efere L, Adetunji MA, Sanchez JG: **Recent advances in the diagnosis of Mycobacterium tuberculosis.** *Germs* 2012, **2:**110-120.

26. Beige J, Lokies J, Schaberg T, Finckh U, Fischer M, Mauch H, Lode H, Köhler B, Rolfs A: **Clinical evaluation of a Mycobacterium tuberculosis PCR assay.** *Journal of Clinical Microbiology* 1995, **33:**90-95.

27. D'Amato RF, Hochstein LH, Colaninno PM, Scardamaglia M, Kim K, Mastellone AJ, Patel RC, Alkhuja S, Tevere VJ, Miller A: **Application of the Roche Amplicor, Mycobacterium tuberculosis (PCR) test to specimens other than respiratory secretions.** *Diagnostic microbiology and infectious disease* 1996, **24:**15-17.

28. Ioannidis P, Papaventsis D, Karabela S, Nikolaou S, Panagi M, Raftopoulou E, Konstantinidou E, Marinou I, Kanavaki S: **Cepheid GeneXpert MTB/RIF assay for Mycobacterium tuberculosis detection and rifampin resistance identification in patients with substantial clinical indications of tuberculosis and smear-negative microscopy results.** *Journal of Clinical Microbiology* 2011, **49:**3068-3070.

29. Holland CA, Kiechle FL: **Point-of-care molecular diagnostic systems—past, present and future.** *Current Opinion in Microbiology* 2005, **8:**504-509.

30. Ling DI, Zwerling AA, Pai M: **GenoType MTBDR assays for the diagnosis of multidrug-resistant tuberculosis: a meta-analysis.** *European Respiratory Journal* 2008, **32:**1165-1174.

31. Barnard M, Albert H, Coetzee G, O'Brien R, Bosman ME: **Rapid molecular screening for multidrug-resistant tuberculosis in a high-volume public health laboratory in South Africa.** *American Journal of Respiratory and Critical Care Medicine* 2008, **177:**787-792.

32. Hillemann D, Weizenegger M, Kubica T, Richter E, Niemann S: **Use of the genotype MTBDR assay for rapid detection of rifampin and isoniazid resistance in Mycobacterium tuberculosis complex isolates.** *Journal of Clinical Microbiology* 2005, **43:**3699-3703.

33. Omer ZB, Mekonnen Y, Worku A, Zewde A, Medhin G, Mohammed T, Pieper R, Ameni G: **Evaluation of the GenoType MTBDRplus assay for detection of rifampicin-and isoniazid-resistant Mycobacterium tuberculosis isolates in central Ethiopia.** *International Journal of Mycobacteriology* 2016, **5:**475-481.

34. Luetkemeyer AF, Kendall MA, Wu X, Lourenço MC, Jentsch U, Swindells S, Qasba SS, Sanchez J, Havlir DV, Grinsztejn B: **Evaluation of two line probe assays for rapid detection of Mycobacterium tuberculosis, tuberculosis (TB) drug resistance, and non-TB Mycobacteria in HIV-infected individuals with suspected TB.** *Journal of Clinical Microbiology* 2014, **52:**1052-1059.

35. Du Toit LC, Pillay V, Danckwerts MP: **Tuberculosis chemotherapy: current drug delivery approaches.** *Respir Res* 2006, **7:**118.

36.   Iseman M: **Tuberculosis therapy: past, present and future.** *European Respiratory Journal* 2002, **20:**87S-94s.

37.   Yee D, Valiquette C, Pelletier M, Parisien I, Rocher I, Menzies D: **Incidence of serious side effects from first-line antituberculosis drugs among patients treated for active tuberculosis.** *American Journal of Respiratory and Critical Care Medicine* 2003, **167:**1472-1477.

38.   Schaberg T, Rebhan K, Lode H: **Risk factors for side-effects of isoniazid, rifampin and pyrazinamide in patients hospitalized for pulmonary tuberculosis.** *European Respiratory Journal* 1996, **9:**2026-2030.

39.   Awofeso N: **Anti-tuberculosis medication side-effects constitute major factor for poor adherence to tuberculosis treatment.** *Bulletin of the World Health Organization* 2008, **86:**B-D.

40.   Gülbay BE, Gürkan ÖU, Yıldız ÖA, Önen ZP, Erkekol FÖ, Baççıoğlu A, Acıcan T: **Side effects due to primary antituberculosis drugs during the initial phase of therapy in 1149 hospitalized patients for tuberculosis.** *Respiratory medicine* 2006, **100:**1834-1842.

41.   Zumla A, Nahid P, Cole ST: **Advances in the development of new tuberculosis drugs and treatment regimens.** *Nature Reviews Drug Discovery* 2013, **12:**388-404.

42.   Fitzwater SP, Sechler GA, Jave O, Coronel J, Mendoza A, Gilman RH, Friedland JS, Moore DAJ: **Second-line anti-tuberculosis drug concentrations for susceptibility testing in the MODS assay.** *European Respiratory Journal* 2013, **41:**1163-1171.

43.   Pontali E, Sotgiu G, D'Ambrosio L, Centis R, Migliori GB: **Bedaquiline and multidrug-resistant tuberculosis: a systematic and critical analysis of the evidence.** *European Respiratory Journal* 2016, **47:**394-402.

44.   Cox E, Laessig K: **FDA Approval of Bedaquiline — The Benefit–Risk Balance for Drug-Resistant Tuberculosis.** *New England Journal of Medicine* 2014, **371:**689-691.

45.   Ryan NJ, Lo JH: **Delamanid: first global approval.** *Drugs* 2014, **74:**1041-1045.

46.   Skripconoka V, Danilovits M, Pehme L, Tomson T, Skenders G, Kummik T, Cirule A, Leimane V, Kurve A, Levina K: **Delamanid improves outcomes and reduces mortality in multidrug-resistant tuberculosis.** *European Respiratory Journal* 2013, **41:**1393-1400.

47.   Jarlier V, Nikaido H: **Mycobacterial cell wall: structure and role in natural resistance to antibiotics.** *FEMS Microbiology Letters* 1994, **123:**11-18.

48.   Danilchanka O, Pires D, Anes E, Niederweis M: **The Mycobacterium tuberculosis outer membrane channel protein CpnT confers susceptibility to toxic molecules.** *Antimicrobial Agents and Chemotherapy* 2015**:**AAC. 04222-04214.

49. Park S-H, Bendelac A: **CD1-restricted T-cell responses and microbial infection.** *Nature* 2000, **406:**788-792.

50. Torrelles JB: *Broadening our view about the role of Mycobacterium tuberculosis cell envelope components during infection: a battle for survival.* INTECH Open Access Publisher; 2012.

51. Barry CE, Mdluli K: **Drug sensitivity and environmental adaptation of myocobacterial cell wall components.** *Trends in Microbiology* 1996, **4:**275-281.

52. Lederer E, Adam A, Ciorbaru R, Petit J-F, Wietzerbin J: **Cell walls of mycobacteria and related organisms; chemistry and immunostimulant properties.** *Molecular and Cellular Biochemistry* 1975, **7:**87-104.

53. Crick PJ, Guan XL: **Lipid metabolism in mycobacteria—Insights using mass spectrometry-based lipidomics.** *Biochimica et Biophysica Acta (BBA)-Molecular and Cell Biology of Lipids* 2016, **1861:**60-67.

54. Marrakchi H, Lanéelle M-A, Daffé M: **Mycolic acids: structures, biosynthesis, and beyond.** *Chemistry & Biology* 2014, **21:**67-85.

55. Nataraj V, Varela C, Javid A, Singh A, Besra GS, Bhatt A: **Mycolic acids: deciphering and targeting the Achilles' heel of the tubercle bacillus.** *Mol Microbiol* 2015, **98:**7-16.

56. Hammerschlag A: **Bacteriologisch-Chemische Untersuchungen der Tuberkelbacillen.** *Monatshefte für Chemie/Chemical Monthly* 1889, **10:**9-18.

57. Verschoor JA, Baird MS, Grooten J: **Towards understanding the functional diversity of cell wall mycolic acids of Mycobacterium tuberculosis.** *Prog Lipid Res* 2012, **51:**325-339.

58. Gebhardt H, Meniche X, Tropis M, Krämer R, Daffe M, Morbach S: **The key role of the mycolic acid content in the functionality of the cell wall permeability barrier in Corynebacterineae.** *Microbiology* 2007, **153:**1424-1434.

59. Sutcliffe IC: **Cell envelope composition and organisation in the genus Rhodococcus.** *Antonie van Leeuwenhoek* 1998, **74:**49-58.

60. Nishiuchi Y, Baba T, Hotta HH, Yano I: **Mycolic acid analysis in Nocardia species: the mycolic acid compositions of Nocardia asteroides, N. farcinica, and N. nova.** *Journal of Microbiological Methods* 1999, **37:**111-122.

61. Hsu F-F, Soehl K, Turk J, Haas A: **Characterization of mycolic acids from the pathogen Rhodococcus equi by tandem mass spectrometry with electrospray ionization.** *Analytical Biochemistry* 2011, **409:**112-122.

62. Portevin D, de Sousa-D'Auria C, Houssin C, Grimaldi C, Chami M, Daffé M, Guilhot C: **A polyketide synthase catalyzes the last condensation step of mycolic acid biosynthesis in**

mycobacteria and related organisms. *Proceedings of the National Academy of Sciences* 2004, **101:**314-319.

63.   Vilchèze C, Morbidoni HR, Weisbrod TR, Iwamoto H, Kuo M, Sacchettini JC, Jacobs WR: **Inactivation of the inhA-encoded fatty acid synthase II (FASII) enoyl-acyl carrier protein reductase induces accumulation of the FASI end products and cell lysis of Mycobacterium smegmatis.** *Journal of Bacteriology* 2000, **182:**4059-4067.

64.   Groenewald W, Baird MS, Verschoor JA, Minnikin DE, Croft AK: **Differential spontaneous folding of mycolic acids from Mycobacterium tuberculosis.** *Chem Phys Lipids* 2014, **180:**15-22.

65.   Shui GH, Bendt AK, Jappar IA, Lim HM, Laneelle M, Herve M, Via LE, Chua GH, Bratschi MW, Rahim SZZ, et al: **Mycolic acids as diagnostic markers for tuberculosis case detection in humans and drug efficacy in mice.** *EMBO Molecular Medicine* 2012, **4:**27-37.

66.   Astarie-Dequeker C, Le Guyader L, Malaga W, Seaphanh F-K, Chalut C, Lopez A, Guilhot C: **Phthiocerol dimycocerosates of M. tuberculosis participate in macrophage invasion by inducing changes in the organization of plasma membrane lipids.** *PLoS Pathog* 2009, **5:**e1000289.

67.   Rousseau C, Winter N, Pivert E, Bordat Y, Neyrolles O, Avé P, Huerre M, Gicquel B, Jackson M: **Production of phthiocerol dimycocerosates protects Mycobacterium tuberculosis from the cidal activity of reactive nitrogen intermediates produced by macrophages and modulates the early immune response to infection.** *Cellular Microbiology* 2004, **6:**277-287.

68.   Bisson GP, Mehaffy C, Broeckling C, Prenni J, Rifat D, Lun DS, Burgos M, Weissman D, Karakousis PC, Dobos K: **Upregulation of the phthiocerol dimycocerosate biosynthetic pathway by rifampin-resistant, rpoB mutant Mycobacterium tuberculosis.** *Journal of Bacteriology* 2012, **194:**6441-6452.

69.   Kolattukudy P, Fernandes ND, Azad A, Fitzmaurice AM, Sirakova TD: **Biochemistry and molecular genetics of cell-wall lipid biosynthesis in mycobacteria.** *Molecular Microbiology* 1997, **24:**263-270.

70.   Yu J, Tran V, Li M, Huang X, Niu C, Wang D, Zhu J, Wang J, Gao Q, Liu J: **Both phthiocerol dimycocerosates and phenolic glycolipids are required for virulence of Mycobacterium marinum.** *Infection and Immunity* 2012, **80:**1381-1389.

71.   Reed MB, Domenech P, Manca C, Su H, Barczak AK, Kreiswirth BN, Kaplan G, Barry CE: **A glycolipid of hypervirulent tuberculosis strains that inhibits the innate immune response.** *Nature* 2004, **431:**84-87.

72.   Cox JS, Chen B, McNeil M, Jacobs WR: **Complex lipid determines tissue-specific replication of Mycobacterium tuberculosis in mice.** *Nature* 1999, **402:**79-83.

73.   Camacho LR, Constant P, Raynaud C, Lanéelle M-A, Triccas JA, Gicquel B, Daffé M, Guilhot C: **Analysis of the Phthiocerol Dimycocerosate Locus ofMycobacterium tuberculosis EVIDENCE THAT THIS LIPID IS INVOLVED IN THE CELL WALL PERMEABILITY BARRIER.** *Journal of Biological Chemistry* 2001, **276:**19845-19854.

74.   Cambier C, Takaki KK, Larson RP, Hernandez RE, Tobin DM, Urdahl KB, Cosma CL, Ramakrishnan L: **Mycobacteria manipulate macrophage recruitment through coordinated use of membrane lipids.** *Nature* 2014, **505:**218.

75.   Flentie KN, Stallings CL, Turk J, Minnaard AJ, Hsu F-F: **Characterization of phthiocerol and phthiodiolone dimycocerosate esters of M. tuberculosis by multiple-stage linear ion-trap MS.** *Journal of Lipid Research* 2016, **57:**142-155.

76.   Minnikin DE, Kremer L, Dover LG, Besra GS: **The methyl-branched fortifications of Mycobacterium tuberculosis.** *Chemistry & Biology* 2002, **9:**545-553.

77.   O'Sullivan DM, Nicoara SC, Mutetwa R, Mungofa S, Lee OY, Minnikin DE, Bardwell MW, Corbett EL, McNerney R, Morgan GH: **Detection of Mycobacterium tuberculosis in sputum by gas chromatography-mass spectrometry of methyl mycocerosates released by thermochemolysis.** *PLoS One* 2012, **7:**e32836.

78.   Daffe M, Draper P: **The envelope layers of mycobacteria with reference to their pathogenicity.** *Advances in Microbial Physiology* 1997, **39:**131-203.

79.   Rolim AEH, Henrique-Araújo R, Ferraz EG, Dultra FKdAA, Fernandez LG: **Lipidomics in the study of lipid metabolism: Current perspectives in the omic sciences.** *Gene* 2015, **554:**131-139.

80.   Sethi S, Brietzke E: **Recent Advances in Lipidomics: Analytical and Clinical Perspectives.** *Prostaglandins & Other Lipid Mediators* 2016.

81.   Mirsaeidi M, Banoei MM, Winston BW, Schraufnagel DE: **Metabolomics: applications and promise in Mycobacterial disease.** *Annals of the American Thoracic Society* 2015, **12:**1278-1287.

82.   Li L, Han J, Wang Z, Liu Ja, Wei J, Xiong S, Zhao Z: **Mass spectrometry methodology in lipid analysis.** *International Journal of Molecular Sciences* 2014, **15:**10492-10507.

83.   de Hoffmann E: **Tandem mass spectrometry: a primer.** *Journal of Mass Spectrometry* 1996, **31:**129-137.

84.   Chernushevich IV, Loboda AV, Thomson BA: **An introduction to quadrupole–time-of-flight mass spectrometry.** *Journal of Mass Spectrometry* 2001, **36:**849-865.

85. Stodola F, Lesuk A, Anderson R: **The chemistry of the lipids of tubercle bacilli liv. The isolation and properties of mycolic acid.** *Journal of Biological Chemistry* 1938, **126:**505-513.

86. Anderson R, Creighton M: **THE CHEMISTRY OF THE LIPIDS OF TUBERCLE BACILLI LVII. THE MYCOLIC ACIDS OF THE AVIAN TUBERCLE BACILLUS WAX.** *Journal of Biological Chemistry* 1939, **129:**57-63.

87. Lesuk A, Anderson R: **The Chemistry of the Lipids of Tubercle Bacilli. LXII. Studies on Mycolic Acid.** *Journal of Biological Chemistry* 1940, **136:**603-613.

88. Korf J, Stoltz A, Verschoor J, De Baetselier P, Grooten J: **The Mycobacterium tuberculosis cell wall component mycolic acid elicits pathogen-associated host innate immune responses.** *Eur J Immunol* 2005, **35:**890-900.

89. Murphy RC, Fiedler J, Hevko J: **Analysis of nonvolatile lipids by mass spectrometry.** *Chem Rev* 2001, **101:**479-526.

90. Toriyama S, Ikuya Y, Masui M, Masamichi K, Kusunose E: **Separation of C50–60 and C70–80 mycolic acid molecular species and their changes by growth temperatures in Mycobacterium phlei.** *FEBS Letters* 1978, **95:**111-115.

91. Butler WR, Ahearn DG, Kilburn JO: **High-Performance Liquid-Chromatography of Mycolic Acids as a Tool in the Identification of Corynebacterium, Nocardia, Rhodococcus, and Mycobacterium Species.** *Journal of Clinical Microbiology* 1986, **23:**182-185.

92. Han X, Gross RW: **Global analyses of cellular lipidomes directly from crude extracts of biological samples by ESI mass spectrometry: a bridge to lipidomics.** *J Lipid Res* 2003, **44:**1071-1079.

93. Hou W, Zhou H, Elisma F, Bennett SA, Figeys D: **Technological developments in lipidomics.** *Brief Funct Genomic Proteomic* 2008, **7:**395-409.

94. Butler WR, Jost KC, Jr., Kilburn JO: **Identification of mycobacteria by high-performance liquid chromatography.** *J Clin Microbiol* 1991, **29:**2468-2472.

95. Butler WR, Guthertz LS: **Mycolic acid analysis by high-performance liquid chromatography for identification of Mycobacterium species.** *Clin Microbiol Rev* 2001, **14:**704-726, table of contents.

96. Shinnick TM, Iademarco MF, Ridderhof JC: **National plan for reliable tuberculosis laboratory services using a systems approach.** *MMWR Recommend Rep* 2005, **54:**1-12.

97. Layre E, Sweet L, Hong S, Madigan CA, Desjardins D, Young DC, Cheng TY, Annand JW, Kim K, Shamputa IC, et al: **A comparative lipidomics platform for chemotaxonomic analysis of Mycobacterium tuberculosis.** *Chem Biol* 2011, **18:**1537-1549.

98. Sartain MJ, Dick DL, Rithner CD, Crick DC, Belisle JT: **Lipidomic analyses of Mycobacterium tuberculosis based on accurate mass measurements and the novel "Mtb LipidDB".** *J Lipid Res* 2011, **52:**861-872.

99. Pal R, Hameed S, Kumar P, Singh S, Fatima Z: **Comparative lipidomics of drug sensitive and resistant Mycobacterium tuberculosis reveals altered lipid imprints.** *3 Biotech* 2017, **7:**325.

100. Stackebrandt E, Rainey FA, Ward-Rainey NL: **Proposal for a new hierarchic classification system, Actinobacteria classis nov.** *International Journal of Systematic and Evolutionary Microbiology* 1997, **47:**479-491.

101. Eggeling L, Bott M: *Handbook of Corynebacterium glutamicum.* CRC press; 2005.

102. Barry CE, Lee RE, Mdluli K, Sampson AE, Schroeder BG, Slayden RA, Yuan Y: **Mycolic acids: structure, biosynthesis and physiological functions.** *Progress in lipid research* 1998, **37:**143-179.

103. Collins M, Goodfellow M, Minnikin D: **A survey of the structures of mycolic acids in Corynebacterium and related taxa.** *Microbiology* 1982, **128:**129-149.

104. Asselineau J, Lanéelle G: **Mycobacterial lipids: a historical perspective.** *Front Biosci* 1998, **3:**e164-e174.

105. Asselineau J, Lederer E: **Structure of the mycolic acids of mycobacteria.** *Nature* 1950, **166:**782.

106. Minnikin D, Hutchinson IG, Caldicott A, Goodfellow M: **Thin-layer chromatography of methanolysates of mycolic acid-containing bacteria.** *Journal of Chromatography A* 1980, **188:**221-233.

107. Butler W, Ahearn D, Kilburn J: **High-performance liquid chromatography of mycolic acids as a tool in the identification of Corynebacterium, Nocardia, Rhodococcus, and Mycobacterium species.** *Journal of Clinical Microbiology* 1986, **23:**182-185.

108. Butler W, Jost K, Kilburn J: **Identification of mycobacteria by high-performance liquid chromatography.** *Journal of Clinical Microbiology* 1991, **29:**2468-2472.

109. Butler W, Kilburn JO: **High-performance liquid chromatography patterns of mycolic acids as criteria for identification of Mycobacterium chelonae, Mycobacterium fortuitum, and Mycobacterium smegmatis.** *Journal of Clinical Microbiology* 1990, **28:**2094-2098.

110. Steck PA, Schwartz BA, Rosendahl MS, Gray GR: **Mycolic acids. A reinvestigation.** *Journal of Biological Chemistry* 1978, **253:**5625-5629.

111. Szewczyk R, Kowalski K, Janiszewska-Drobinska B, Druszczyńska M: **Rapid method for Mycobacterium tuberculosis identification using electrospray ionization tandem mass**

spectrometry analysis of mycolic acids. *Diagnostic Microbiology and Infectious Disease* 2013, **76:**298-305.

112. Welker M, Moore ER: **Applications of whole-cell matrix-assisted laser-desorption/ionization time-of-flight mass spectrometry in systematic microbiology.** *Systematic and applied microbiology* 2011, **34:**2-11.

113. Lopez B, Aguilar D, Orozco H, Burger M, Espitia C, Ritacco V, Barrera L, Kremer K, HERNANDEZ-PANDO R, Huygen K: **A marked difference in pathogenesis and immune response induced by different Mycobacterium tuberculosis genotypes.** *Clinical & Experimental Immunology* 2003, **133:**30-37.

114. Caws M, Thwaites G, Dunstan S, Hawn TR, Lan NTN, Thuong NTT, Stepniewska K, Huyen MNT, Bang ND, Loc TH: **The influence of host and bacterial genotype on the development of disseminated disease with Mycobacterium tuberculosis.** *PLoS pathogens* 2008, **4:**e1000034.

115. Zhang Y, Post-Martens K, Denkin S: **New drug candidates and therapeutic targets for tuberculosis therapy.** *Drug Discovery Today* 2006, **11:**21-27.

116. Farhat MR, Shapiro BJ, Kieser KJ, Sultana R, Jacobson KR, Victor TC, Warren RM, Streicher EM, Calver A, Sloutsky A: **Genomic analysis identifies targets of convergent positive selection in drug-resistant Mycobacterium tuberculosis.** *Nature Genetics* 2013, **45:**1183.

117. Devallois A, Goh KS, Rastogi N: **Rapid identification of mycobacteria to species level by PCR-restriction fragment length polymorphism analysis of the hsp65 gene and proposition of an algorithm to differentiate 34 mycobacterial species.** *Journal of Clinical Microbiology* 1997, **35:**2969-2973.

118. Leão SC, Bernardelli A, Cataldi A, Zumarraga M, Robledo J, Realpe T, Mejía GI, da Silva Telles MA, Chimara E, Velazco M: **Multicenter evaluation of mycobacteria identification by PCR restriction enzyme analysis in laboratories from Latin America and the Caribbean.** *Journal of Microbiological Methods* 2005, **61:**193-199.

119. Telenti A, Marchesi F, Balz M, Bally F, Böttger E, Bodmer T: **Rapid identification of mycobacteria to the species level by polymerase chain reaction and restriction enzyme analysis.** *Journal of Clinical Microbiology* 1993, **31:**175-178.

120. Brunello F, Ligozzi M, Cristelli E, Bonora S, Tortoli E, Fontana R: **Identification of 54 Mycobacterial Species by PCR-restriction fragment length polymorphism analysis of the hsp65Gene.** *Journal of Clinical Microbiology* 2001, **39:**2799-2806.

121. Wang H-y, Kim H, Kim S, Kim D-k, Cho S-N, Lee H: **Performance of a real-time PCR assay for the rapid identification of Mycobacterium species.** *Journal of Microbiology* 2015, **53:**38-46.

122. Wilson JF: **Long-suffering lipids gain respect: technical advances and enhanced understanding of lipid biology fuel a trend toward lipidomics.(Lab consumer).** *The Scientist* 2003, **17:**34-37.

123. Ranković M: **Photon and electron action spectroscopy of trapped biomolecular ions-from isolated to nanosolvated species.** Univerzitet u Beogradu-Fizički fakultet, 2016.

124. Song SH, Park KU, Lee JH, Kim EC, Kim JQ, Song J: **Electrospray ionization-tandem mass spectrometry analysis of the mycolic acid profiles for the identification of common clinical isolates of mycobacterial species.** *J Microbiol Methods* 2009, **77:**165-177.

125. Goodrum M, Siko D, Niehues T, Eichelbauer D, Verschoor J: **Mycolic acids from Mycobacterium tuberculosis: purification by countercurrent distribution and T-cell stimulation.** *Microbios* 2000, **106:**55-67.

126. Crofton J, Mitchison D: **Streptomycin resistance in pulmonary tuberculosis.** *British Medical Journal* 1948, **2:**1009.

127. Control CfD: **Nosocomial transmission of multidrug-resistant tuberculosis among HIV-infected persons--Florida and New York, 1988-1991.** *MMWR Morbidity and Mortality Weekly Report* 1991, **40:**585.

128. Frieden TR, Sterling T, Pablos-Mendez A, Kilburn JO, Cauthen GM, Dooley SW: **The emergence of drug-resistant tuberculosis in New York City.** *New England Journal of Medicine* 1993, **328:**521-526.

129. Monno L, Carbonara S, Costa D, Angarano G, Coppola S, Quarto M, Pastore G: **Emergence of drug-resistant Mycobacterium tuberculosis in HIV-infected patients.** *The Lancet* 1991, **337:**852.

130. Moro ML, Gori A, Errante I, Infuso A, Franzetti F, Sodano L, Iemoli E, Group IM-RTOS: **An outbreak of multidrug-resistant tuberculosis involving HIV-infected patients of two hospitals in Milan, Italy.** *Aids* 1998, **12:**1095-1102.

131. Campos PE, Suarez PG, Sanchez J, Zavala D, Arevalo J, Ticona E, Nolan CM, Hooton TM, Holmes KK: **Multidrug-resistant Mycobacterium tuberculosis in HIV-infected persons, Peru.** *Emerging Infectious Diseases* 2003, **9:**1571.

132. Cohn ML, Middlebrook G, Russell WF: **Combined drug treatment of tuberculosis. I. Prevention of emergence of mutant populations of tubercle bacilli resistant to both streptomycin and isoniazid in vitro.** *The Journal of Clinical Investigation* 1959, **38:**1349-1355.

133. Mitchison D, Nunn A: **Influence of initial drug resistance on the response to short-course chemotherapy of pulmonary tuberculosis.** *American Review of Respiratory Disease* 1986, **133:**423-430.

134. Pang Y, Lu J, Wang Y, Song Y, Wang S, Zhao Y: **Study of the rifampin mono-resistance mechanism in Mycobacterium tuberculosis.** *Antimicrobial agents and chemotherapy* 2012**:**AAC. 01024-01012.

135. Vernon A, Burman W, Benator D, Khan A, Bozeman L, Consortium TT: **Acquired rifamycin monoresistance in patients with HIV-related tuberculosis treated with once-weekly rifapentine and isoniazid.** *The Lancet* 1999, **353:**1843-1847.

136. Ridzon R, Whitney CG, McKENNA MT, Taylor JP, Ashkar SH, Nitta AT, Harvey SM, Valway S, Woodley C, Cooksey R: **Risk factors for rifampin mono-resistant tuberculosis.** *American journal of respiratory and critical care medicine* 1998, **157:**1881-1884.

137. Traore H, Fissette K, Bastian I, Devleeschouwer M, Portaels F: **Detection of rifampicin resistance in Mycobacterium tuberculosis isolates from diverse countries by a commercial line probe assay as an initial indicator of multidrug resistance.** *The International Journal of Tuberculosis and Lung Disease* 2000, **4:**481-484.

138. Menzies D, Benedetti A, Paydar A, Royce S, Pai M, Burman W, Vernon A, Lienhardt C: **Standardized treatment of active tuberculosis in patients with previous treatment and/or with mono-resistance to isoniazid: a systematic review and meta-analysis.** *PLoS Medicine* 2009, **6:**e1000150.

139. Hazbón MH, Brimacombe M, del Valle MB, Cavatore M, Guerrero MI, Varma-Basil M, Billman-Jacobe H, Lavender C, Fyfe J, García-García L: **Population genetics study of isoniazid resistance mutations and evolution of multidrug-resistant Mycobacterium tuberculosis.** *Antimicrobial agents and chemotherapy* 2006, **50:**2640-2649.

140. Cattamanchi A, Dantes RB, Metcalfe JZ, Jarlsberg LG, Grinsdale J, Kawamura LM, Osmond D, Hopewell PC, Nahid P: **Clinical characteristics and treatment outcomes of patients with isoniazid-monoresistant tuberculosis.** *Clinical Infectious Diseases* 2009, **48:**179-185.

141. Control CfD, Prevention: **Emergence of Mycobacterium tuberculosis with extensive resistance to second-line drugs--worldwide, 2000-2004.** *MMWR Morbidity and Mortality Weekly Report* 2006, **55:**301.

142. Millard J, Ugarte-Gil C, Moore DA: **Multidrug resistant tuberculosis.** *Bmj* 2015, **350:**h882.

143. Falzon D, Mirzayev F, Wares F, Baena IG, Zignol M, Linh N, Weyer K, Jaramillo E, Floyd K, Raviglione M: **Multidrug-resistant tuberculosis around the world: what progress has been made?** *European Respiratory Journal* 2015, **45:**150-160.

144. Steingart KR, Schiller I, Horne DJ, Pai M, Boehme CC, Dendukuri N: **Xpert® MTB/RIF assay for pulmonary tuberculosis and rifampicin resistance in adults.** *The Cochrane Database of Systematic Reviews* 2014**:1**.

145. Boehme CC, Nicol MP, Nabeta P, Michael JS, Gotuzzo E, Tahirli R, Gler MT, Blakemore R, Worodria W, Gray C: **Feasibility, diagnostic accuracy, and effectiveness of decentralised use of the Xpert MTB/RIF test for diagnosis of tuberculosis and multidrug resistance: a multicentre implementation study.** *The Lancet* 2011, **377:**1495-1505.

146. Lawn SD, Mwaba P, Bates M, Piatek A, Alexander H, Marais BJ, Cuevas LE, McHugh TD, Zijenah L, Kapata N: **Advances in tuberculosis diagnostics: the Xpert MTB/RIF assay and future prospects for a point-of-care test.** *The Lancet Infectious Diseases* 2013, **13:**349-361.

147. Marlowe EM, Novak-Weekley SM, Cumpio J, Sharp SE, Momeny MA, Babst A, Carlson JS, Kawamura M, Pandori M: **Evaluation of the Cepheid Xpert MTB/RIF assay for direct detection of Mycobacterium tuberculosis complex in respiratory specimens.** *Journal of Clinical Microbiology* 2011, **49:**1621-1623.

148. Theron G, Zijenah L, Chanda D, Clowes P, Rachow A, Lesosky M, Bara W, Mungofa S, Pai M, Hoelscher M: **Feasibility, accuracy, and clinical effect of point-of-care Xpert MTB/RIF testing for tuberculosis in primary-care settings in Africa: a multicentre, randomised, controlled trial.** *The Lancet* 2014, **383:**424-435.

149. Nicol MP, Workman L, Isaacs W, Munro J, Black F, Eley B, Boehme CC, Zemanay W, Zar HJ: **Accuracy of the Xpert MTB/RIF test for the diagnosis of pulmonary tuberculosis in children admitted to hospital in Cape Town, South Africa: a descriptive study.** *The Lancet Infectious Diseases* 2011, **11:**819-824.

150. Dlamini-Mvelase NR, Werner L, Phili R, Cele LP, Mlisana KP: **Effects of introducing Xpert MTB/RIF test on multi-drug resistant tuberculosis diagnosis in KwaZulu-Natal South Africa.** *BMC Infectious Diseases* 2014, **14:**442.

151. Horng Y-T, Soo P-C: **The Molecular Mechanism and WHO-endorsed Diagnosis of Rifampicin Resistance in Mycobacterium tuberculosis.** *Journal of Biomedical & Laboratory Sciences* 2015, **27:**115-124.

152. Kohli M, Schiller I, Dendukuri N, Dheda K, Denkinger CM, Schumacher SG, Steingart KR: **Xpert® MTB/RIF assay for extrapulmonary tuberculosis and rifampicin resistance.** *The Cochrane Database of Systematic Reviews* 2018.

153. Dorman SE, Schumacher SG, Alland D, Nabeta P, Armstrong DT, King B, Hall SL, Chakravorty S, Cirillo DM, Tukvadze N: **Xpert MTB/RIF Ultra for detection of Mycobacterium**

tuberculosis and rifampicin resistance: a prospective multicentre diagnostic accuracy
study.** *The Lancet Infectious Diseases* 2018, **18:**76-84.

154. Santos A, Leung J, Malaquias T, Vieira M, Kritski A, Mello F: **The Reliability of Rifampicin
Resistance Identified on Xpert® MTB/RIF as a Proxy for Multidrug-Resistant Tuberculosis
(MDR-TB) in a Reference Center for MDR-TB in Rio de Janeiro, Brazil.** In *C62 Tuberculosis:
Bench to Bedside.* American Thoracic Society; 2018: A5544-A5544

155. Falzon D, Schünemann HJ, Harausz E, González-Angulo L, Lienhardt C, Jaramillo E, Weyer K:
**World Health Organization treatment guidelines for drug-resistant tuberculosis, 2016
update.** *European Respiratory Journal* 2017, **49:**1602308.

156. Singh P, Sinha R, Tandon R, Tyagi G, Khatri P, Reddy LCS, Saini NK, Pathak R, Varma-Basil M,
Prasad AK: **Revisiting a protocol for extraction of mycobacterial lipids.** *International journal
of mycobacteriology* 2014, **3:**168-172.

157. Junior CAC, de la Torre CAL, de Souza Figueiredo EE, Lilenbaum W, Paschoalin VMF:
**Application of High Performance Liquid Chromatography for Identification of
Mycobacterium spp.** In *Tuberculosis-Expanding Knowledge.* InTech; 2015

158. Furlanetto LV, Conte-Júnior CA, de Souza Figue EE, Duarte RS, Lilenbaum W, Silva JT,
Paschoalin VMF: **HPLC protocol for identification of Mycobacterium spp. from clinical
samples of human and veterinary.** *Journal of Microbiology Research* 2014, **4:**193-200.

159. Kendrick E: **A Mass Scale Based on CH2= 14.0000 for High Resolution Mass Spectrometry of
Organic Compounds.** *Analytical Chemistry* 1963, **35:**2146-2154.

160. Marshall AG, Rodgers RP: **Petroleomics: the next grand challenge for chemical analysis.**
Accounts of Chemical Research 2004, **37:**53-59.

161. Takayama K, Wang L, David HL: **Effect of isoniazid on the in vivo mycolic acid synthesis, cell
growth, and viability of Mycobacterium tuberculosis.** *Antimicrobial agents and
chemotherapy* 1972, **2:**29-35.

162. Ojha AK, Baughn AD, Sambandan D, Hsu T, Trivelli X, Guerardel Y, Alahari A, Kremer L, Jacobs
Jr WR, Hatfull GF: **Growth of Mycobacterium tuberculosis biofilms containing free mycolic
acids and harbouring drug-tolerant bacteria.** *Molecular microbiology* 2008, **69:**164-174.

163. Qureshi N, Takayama K, Jordi HC, Schnoes HK: **Characterization of the purified components
of a new homologous series of alpha-mycolic acids from Mycobacterium tuberculosis
H37Ra.** *Journal of Biological Chemistry* 1978, **253:**5411-5417.

164. Layre E, Moody DB: **Lipidomic profiling of model organisms and the world's major
pathogens.** *Biochimie* 2013, **95:**109-115.

165.   Howard NC, Marin ND, Ahmed M, Rosa BA, Martin J, Bambouskova M, Sergushichev A,
         Loginicheva E, Kurepina N, Rangel-Moreno J: **Mycobacterium tuberculosis carrying a
         rifampicin drug resistance mutation reprograms macrophage metabolism through cell wall
         lipid changes.** *Nature microbiology* 2018, **3:**1099.

166.   Chiaradia L, Lefebvre C, Parra J, Marcoux J, Burlet-Schiltz O, Etienne G, Tropis M, Daffé M:
         **Dissecting the mycobacterial cell envelope and defining the composition of the native
         mycomembrane.** *Scientific reports* 2017, **7:**12807.

Appendix

Mycobacterium komaniense sp. nov., a rapidly growing non-tuberculous Mycobacterium species detected in South Africa

Nomakorinte Gcebe,[1,2,*] Victor P. M. G. Rutten,[2,3] Nicolaas Gey van Pittius,[4] Brendon Naicker[5] and Anita L. Michel[2]

Abstract

Some species of non-tuberculous mycobacteria (NTM) have been reported to be opportunistic pathogens of animals and humans. Recently there has been an upsurge in the number of cases of NTM infections, such that some NTM species are now recognized as pathogens of humans and animals. From a veterinary point of view, the major significance of NTM is the cross–reactive immune response they elicit against *Mycobacterium bovis* antigens, leading to misdiagnosis of bovine tuberculosis. Four NTM isolates were detected from a bovine nasal swab, soil and water, during an NTM survey in South Africa. These were all found using 16S rRNA gene sequence analysis to be closely related to *Mycobacterium moriokaense*. The isolates were further characterised by sequence analysis of the partial fragments of *hsp65*, *rpoB* and *sodA*. The genome of the type strain was also elucidated. Gene (16S rRNA, *hsp65*, *rpoB* and *sodA*) and protein sequence data analysis of 6 kDa early secretory antigenic target (ESAT 6) and 10 kDa culture filtrate protein (CFP-10) revealed that these isolates belong to a unique *Mycobacterium* species. Differences in phenotypic and biochemical traits between the isolates and closely related species further supported that these isolates belong to novel *Mycobacterium* species. We proposed the name *Mycobacterium komaniense* sp. nov. for this new species. The type strain is GPK 1020[T] (=CIP 110823T=ATCC BAA-2758).

Some species of non-tuberculous mycobacteria (NTM) have been reported to be opportunistic pathogens of animals and humans [1]. NTM species like *Mycobacterium szulgai, Mycobacterium marinum, Mycobacterium kansasii, Mycobacterium abscessus* and *Mycobacterium avium* complex are now recognised as emerging or opportunistic pathogens of humans and animals causing mycobacteriosis, such that their isolation from clinical samples is regarded as significant [2–4]. NTM can cause skin lesions, localized lymphadenitis, and pulmonary diseases resembling tuberculosis and disseminated diseases [3]. Recently, there has been an increase in the number of reported cases of NTM disease globally [4–6]. The upsurge can be associated with increased awareness among physicians and advancement in technology for diagnosis of NTM. However, this may not be the only explanation. Rapidly growing NTM have also received an increased attention because

of characteristic multiple antibiotic resistance [1, 6]. Among the rapidly growing NTM species, human infections by members of *Mycobacterium chelonae–abscessus* complex including *Mycobacterium abscessus, Mycobacterium massiliense* and *Mycobacterium bolletii* have been on the rise worldwide [6]. Cases of NTM infection in animals are still under-investigated as compared to human cases. From a veterinary point of view, the major significance of NTM is the cross-reactive immune responses induced by certain NTM that interfere with the diagnosis of bovine tuberculosis by immunoassays [7]. These specificity constraints are associated with the presence of shared antigens between certain NTM species and *Mycobacterium bovis*. The ESAT 6 and CFP-10 proteins encoded in the RD1 region of mycobacteria are the most studied virulence factors and immunogenic proteins of mycobacteria for their potential as vaccine and diagnostic candidates [8, 9]. Thus

Research paper

Standardization of natural mycolic acid antigen composition and production for use in biomarker antibody detection to diagnose active tuberculosis

F.L. Ndlandla [a,b], V. Ejoh [b], A.C. Stoltz [c], B. Naicker [a,d], A.D. Cromarty [d], S. van Wyngaardt [b], M. Khati [f], L.S. Rotherham [f], Y. Lemmer [a], J. Niebuhr [b], C.R. Baumeister [b], J.R. Al Dulayymi [e], H. Swai [a], M.S. Baird [e], J.A. Verschoor [b,*]

[a] Polymers and Composites, Council for Scientific and Industrial Research, Pretoria, South Africa
[b] Department of Biochemistry, University of Pretoria, South Africa
[c] Division of Infectious Diseases, Faculty of Health Sciences, University of Pretoria, South Africa
[d] Department of Pharmacology, Faculty of Health Sciences, University of Pretoria, South Africa
[e] School of Chemistry, Bangor University, Wales, UK
[f] Biosciences, Council for Scientific and Industrial Research, Pretoria, South Africa

ARTICLE INFO

ABSTRACT

Mycobacterium tuberculosis, the causative agent of tuberculosis, is characterized by the abundance of species specific, antigenic cell wall lipids called mycolic acids. These wax-like molecules all share an identical, amphiphilic mycolic motif, but have different functional groups in a long hydrophobic hydrocarbon mero-chain that divide them into three main classes: alpha-, keto- and methoxy-mycolic acids. Whereas alpha-mycolic acids constitutively maintain an abundance of around 50%, the ratio of methoxy- to keto-mycolic acid types may vary depending on, among other things, the growth stage of M. tuberculosis. In human patients, antibodies to mycolic acids have shown potential as diagnostic serum biomarkers for active TB. Variations in mycolic acid composition affect the antigenic properties and can potentially compromise the precision of detection of anti-mycolic acids antibodies in patient sera to natural mixtures. We demonstrate this here with combinations of synthetic mycolic acid antigens, tested against TB patient and control sera. Combinations of methoxy- and α-mycolic acids are more antigenic than combinations of keto- and α-mycolic acids, showing the former to give a more sensitive test for TB biomarker antibodies. Natural mixtures of mycolic acids isolated from mature cultures of M. tuberculosis H37Rv give the same sensitivity as that with synthetic methoxy- and α-mycolic acids in combination, in a surface plasmon resonance inhibition biosensor test. To ensure that the antigenic activity of isolates of natural mycolic acids is reproducible, we cultured M. tuberculosis H37Rv on Middlebrook 7H10 solid agar plates to stationary growth phase in a standardized, optimal way. The proportions of mycolic acid classes in various batches of the isolates prepared from these cultures were compared to a commercially available natural mycolic acid isolate. LC-MS/MS and NMR data for quantitation of mycolic acids class compositions show that the variation in batches is small, suggesting that the quality of the results for anti-mycolic acid antibody detection in the TB patients should not be affected by different batches of natural mycolic acid antigens if prepared in a standard way.

© 2016 Elsevier B.V. All rights reserved.

1. Introduction

Mycolic acids (MA) are high molecular weight (C60–C90) α-alkyl-β-hydroxy fatty acids produced by all mycobacterial species and closely related genera (Minnikin, 1982). MAs are the major components in the heterogeneous mixture of lipids that make up about 40–60% of the mycobacterial cell dry weight (Brennan and Nikaido, 1995). They exist in the cell wall either linked to the arabinogalactan layer by phosphodiester bonds, or bound to trehalose as trehalose monomycolate (TMM)

and trehalose dimycolate (TDM) (Barry et al., 1998). All the members of the Mycobacterium tuberculosis complex (Mycobacterium tuberculosis, Mycobacterium bovis, Mycobacterium africanum and Mycobacterium microti) produce three major classes of MA, alpha-, keto- and methoxy-MA. These three classes are differentiated by the presence of different chemical functional groups on the main hydrophobic chain of MA, called the mero-chain. The most abundant class of MA, alpha-MA, contains two cis cyclopropane rings and has no oxygenated functional groups on its mero-chain, compared to keto- and methoxy-MA, which contain respectively oxygenated distal keto and methoxy functional groups. The proximal cyclopropane rings of oxygenated MA can either be cis or trans. While alpha- and keto-MA are present in various

* Corresponding author at: Department of Biochemistry, University of Pretoria, Pretoria 0002, South Africa.

105

Mycobacterium malmesburyense sp. nov., a non-tuberculous species of the genus Mycobacterium revealed by multiple gene sequence characterization

Nomakorinte Goebe,[1,2,*] Victor Rutten,[2,3] Nicolaas Gey van Pittius,[4] Brendon Naicker[5] and Anita Michel[2]

Abstract

Non-tuberculous mycobacteria (NTM) are ubiquitous in the environment, and an increasing number of NTM species have been isolated and characterized from both humans and animals, highlighting the zoonotic potential of these bacteria. Host exposure to NTM may impact on cross-reactive immune responsiveness, which may affect diagnosis of bovine tuberculosis and may also play a role in the variability of the efficacy of Mycobacterium bovis BCG vaccination against tuberculosis. In this study we characterized 10 NTM isolates originating from water, soil, nasal swabs of cattle and African buffalo as well as bovine tissue samples. These isolates were previously identified during an NTM survey and were all found, using 16S rRNA gene sequence analysis to be closely related to Mycobacterium moriokaense. A polyphasic approach that included phenotypic characterization, antibiotic susceptibility profiling, mycolic acid profiling and phylogenetic analysis of four gene loci, 16S rRNA, hsp65, sodA and rpoB, was employed to characterize these isolates. Sequence data analysis of the four gene loci revealed that these isolates belong to a unique species of the genus Mycobacterium. This evidence was further supported by several differences in phenotypic characteristics between the isolates and the closely related species. We propose the name Mycobacterium malmesburyense sp. nov. for this novel species. The type strain is WCM 7299[T] (=ATCC BAA-2759[T]=CIP 110822[T]).

Currently, more than 100 non-tuberculous mycobacterial species are listed in public databases (www.bacterio.net/). An increasing number of non-tuberculous mycobacteria (NTM) species have recently been isolated and characterized from both humans and animals, highlighting the zoonotic potential of these species (for review see [1–3]). An increased interest in these organisms has developed in view of the potential impact of host exposure to NTM on cross-reactive immune responsiveness, which may affect diagnosis of bovine tuberculosis [4–6] and may also play a role in the variability of the efficacy of Mycobacterium bovis BCG vaccination against tuberculosis [7–9]. NTM are ubiquitous in the environment, and there is no evidence of animal-to-animal or human-to-human transmission [10, 11]. Characterization of NTM isolates from environmental as well as clinical samples is important as these may also lead to identification of emerging pathogens. For instance, Mycobacterium avium was essentially a rare human pathogen before

the acquired immune deficiency syndrome (AIDS) pandemic, and since then this NTM species has become a very important pathogen of AIDS patients [12]. The reference molecular method for the identification of mycobacteria is the sequencing of the 16S rRNA gene, which has contributed to the discovery of novel NTM isolates beyond possibilities offered by conventional methods such as phenotypic characterization [13]. However, this approach has its limitations as there are instances where the sequence of this gene has been found to be similar, if not identical, among species of the genus. It has been shown that multiple locus analysis provides a more detailed and accurate identification of species of the genus Mycobacterium than the use of a single locus [14]. We previously described the prevalence of NTM isolates in cattle, African buffaloes and their environments in South Africa and found a group of isolates (most closely related by analysis of the 16S rRNA gene to Mycobacterium moriokaense) that were not well described in the literature

Author affiliations: [1]Tuberculosis Laboratory, Agricultural Research Council – Onderstepoort Veterinary Institute, Onderstepoort, Gauteng 0110, South Africa; [2]Department of Veterinary Tropical Diseases, Faculty of Veterinary Science, University of Pretoria, Onderstepoort, Gauteng 0110, South Africa; [3]Department of Infectious Diseases and Immunology, Division of Immunology, Faculty of Veterinary Medicine, Utrecht University, Utrecht, The Netherlands; [4]Centre of Excellence for Biomedical Tuberculosis Research, Division of Molecular Biology and Human Genetics, Department of Biomedical Sciences, Faculty of Medicine and Health Sciences, Stellenbosch University, Tygerberg, South Africa; [5]Polymers and Composites, Materials Science and Manufacturing, Council for Scientific and Industrial Research, Brummeria, South Africa.
*Correspondence: Nomakorinte Goebe, goeben@arc.agric.za
Keywords: non-tuberculous mycobacteria; Mycobacterium malmesburyense sp. nov.; multiple gene sequence characterization.
Abbreviation: NTM, non-tuberculous mycobacteria.
One supplementary table is available with the online Supplementary Material.

Conference and Symposium presentations

- **ChromSAAMS Conference 2016**

- **Federation of Infectious Diseases South Africa (FIDSSA) 2015**

- **Council for Scientific and Industrial Research (CSIR) South Africa, Emerging Researchers Symposium 2015**

- **South African Association of Mass Spectrometry (SAAMS) Symposium 2015**

- **Analitika Conference 2014**

- **World Congress of Basic and Clinical Pharmacology (WCP) 2014**

- **International Chemistry Conference Africa (ICCA) 2013**

- **ChromSAAMS Conference 2012**

Approval Certificate

Annual Renewal

Ethics Reference No.: 88/2016

Title: Identification of mycolic acid class ratios from Mycobacterium species using liquid chromatography-mass spectrometry

Dear Mr B Naicker

The **Annual Renewal** as supported by documents received between 2019-01-29 and 2019-02-13 for your research, was approved by the Faculty of Health Sciences Research Ethics Committee on its quorate meeting of 2019-02-13.

Please note the following about your ethics approval:

- Renewal of ethics approval is valid for 1 year, subsequent annual renewal will become due on 2020-02-14.

- Please remember to use your protocol number (88/2016) on any documents or correspondence with the Research Ethics Committee regarding your research.

- Please note that the Research Ethics Committee may ask further questions, seek additional information, require further modification, monitor the conduct of your research, or suspend or withdraw ethics approval.

Ethics approval is subject to the following:

- The ethics approval is conditional on the research being conducted as stipulated by the details of all documents submitted to the Committee. In the event that a further need arises to change who the investigators are, the methods or any other aspect, such changes must be submitted as an Amendment for approval by the Committee.

We wish you the best with your research.

Yours sincerely

_____

Dr R Sommers

MBChB MMed (Int) MPharmMed PhD

Deputy Chairperson of the Faculty of Health Sciences Research Ethics Committee, University of Pretoria

The Faculty of Health Sciences Research Ethics Committee complies with the SA National Act 61 of 2003 as it pertains to health research and the United States Code of Federal Regulations Title 45 and 46. This committee abides by the ethical norms and principles for research, established by the Declaration of Helsinki, the South African Medical Research Council Guidelines as well as the Guidelines for Ethical Research: Principles Structures and Processes, Second Edition 2015 (Department of Health)